

Alma Mater Studiorum – Università di Bologna

**DOTTORATO DI RICERCA IN
SCIENZE CARDIO NEFRO TORACICHE**

Ciclo XXXIII

Settore Concorsuale: 06/D2

Settore Scientifico Disciplinare: MED/14

**ERYTHROPOIETIN REDUCES PATHOGENIC HUMORAL
IMMUNITY BY INHIBITING T FOLLICULAR HELPER CELL
DIFFERENTIATION AND FUNCTION**

Presentata da:

Sofia Bin

Coordinatore Dottorato:

Prof. Gaetano Domenico Gargiulo

Supervisore:

Prof. Gaetano La Manna

Co-supervisore:

Prof. Paolo Cravedi

Esame finale anno 2021

SUMMARY

ABSTRACT	6
1. BACKGROUND.....	8
1.1 Transplant, donor-specific antibodies and antibody-mediated rejection.....	8
1.2 Humoral immunoregulation of antibody responses	9
1.3 Germinal Center	10
1.4 B-Cell development and class switch recombination.....	12
1.5 Development and features of T _{FH} cells	13
1.6 Mechanisms of T _{FH} cell function	14
1.7 Development and features of T _{FR} cells.....	15
1.8 Mechanisms of T _{FR} cell function.....	16
1.9 T _{FH} cells in alloimmunity	17
1.10 T _{FR} cells in alloimmunity	18
1.11 Erythropoietin (EPO)	19
1.12 EPO structure	20
1.13 Tissue expression of EPO.....	22
1.14 Molecular mechanism of EPO	22
1.15 EPO and innate immune cells	23
1.16 EPO and T cells	25
1.17 EPO, Kidney, and renal injury	28
1.18 EPO in transplantation.....	29
1.19 Pharmacological use of recombinant human EPO and biosimilars	30
2. PRINCIPAL AIM	33
3. MATERIALS AND METHODS	34
3.1 Mice.....	34
3.2 NP-KLH immunization and EPO administration.....	34
3.3 TNP-AECM-FICOLL immunization and EPO administration.....	35
3.4 Sheep red blood cell immunization and EPO administration.....	35
3.5 B cells Activation	36
3.6 Heterotopic heart transplantation	36
3.7 Isolation of murine serum.....	37

3.8	Isolation of murine splenocytes and thymocytes	37
3.9	NP-Enzyme-Linked Immunosorbent Assay (ELISA).....	37
3.10	Alloantibody detection	38
3.11	Flow cytometry.....	38
3.11.1	Extracellular staining.....	38
3.11.2	Intracellular staining	39
3.11.3	Acquisition	40
3.12	T _{FH} differentiation assay.....	40
3.13	Suppression assays	41
3.14	Cell Sorting.....	42
3.15	Parent-to-F1 models	42
3.16	Renal histology.....	43
3.16.1	Light microscopy.....	43
3.16.2	Immunofluorescence	43
3.17	Urinary albumin and creatinine measurement.....	44
3.18	Statistical Analyses.....	44
4.	RESULTS AND DISCUSSION	45
4.1	EPO regulates T cell dependent antibody production.....	45
4.2	EPO regulates Germinal Center (GC) responses	48
4.3	EPO administration has no effect on T-independent antibody responses	52
4.4	EPO has no direct inhibitory effect on B cells	53
4.5	EPO inhibits T _{FH} through T cell-expressed EPOR <i>in vivo</i>	56
4.6	EPO directly prevents T _{FH} induction.....	61
4.7	EPO directly inhibits T _{FH} , without affect T _{FR}	64
4.8	EPO inhibits pre-formed DSA	69
4.9	EPO ameliorates disease severity in murine models of systemic lupus erythematosus.....	73
5.	CONCLUSION	80
6.	BIBLIOGRAPHY	82

ABSTRACT

Despite significant advances in the short-term graft survival, a large fraction of organ transplant recipients develop anti-donor antibodies (DSA) that are associated with accelerated graft loss and increased mortality. In this study, we tested the hypothesis that erythropoietin (EPO), a kidney-produced erythropoietic hormone that directly inhibits effector T cells, reduces DSA formation by inhibiting T follicular helper (T_{FH}) cells.

We measured DSA levels, splenic T_{FH} and T_{FR} cells, germinal center (GC), and class switched B cells, in murine models of allogeneic sensitization, allogeneic transplantation and in parent to F1 models of graft versus host disease (GVHD).

We quantified the same cell subsets and specific antibodies, upon EPO or vehicle treatment, in wild type mice and animals lacking EPO receptor selectively on T or B cells, immunized with T-independent or T-dependent stimuli.

In vitro, we tested the EPO effect on T_{FH} induction. Using B6.129(Cg)-FOXP3^{tm3(DTR/GFP)Air/J} strain, we isolated T_{FH} and T_{FR} cells to perform *in vitro* assay and clarify the role of these specific subsets.

EPO significantly reduced DSA levels, GC, class switched B cells, and increased the T_{FR}/T_{FH} ratio in the heart transplanted mice and in two GVHD models.

EPO did also reduce T_{FH} and GC B cells in mice immunized with SRBC (T-dependent), while had no effect in TNP-AECM-FICOLL-immunized (T-independent) animals, indicating that EPO inhibits GC B cells by targeting T_{FH} cells. EPO effects were absent in T cells EPOR conditional KO mice, supporting the concept that EPO affects T_{FH} *in vivo* through EPOR.

In vitro, EPO affected T_{FH} induction through an EPO-EPOR-STAT5-dependent pathway. Suppression assay demonstrated that the reduction of IgG antibodies was dependent on T_{FH} cells, sustaining the central role of the subset in this EPO-mediated mechanism.

In conclusion, EPO prevents DSA formation in mice through a direct suppression of T_{FH}. The fact that development of DSA is associated with high risk of graft rejection, gives to our data a strong rationale for studies testing the hypothesis that EPO administration prevents their formation in organ transplant recipients. Altogether, our findings provide a foundation for testing EPO as a treatment of antibody mediated disease processes.

1. BACKGROUND

1.1 Transplant, donor-specific antibodies and antibody-mediated rejection

Chronic kidney disease (CKD), affects about 9-10% of the population worldwide (Carney, 2020) and it may lead to end-stage kidney disease (ESKD). Kidney transplantation is the ideal therapeutic option for these patients and offers the greatest survival opportunity in selected patient populations. With more than 100,000 transplants per year, this surgical procedure has been carried out in large numbers since the 1980s with a gradual improvement of patient outcomes noted especially in the last two decades. The success of the transplant has been largely due to the antirejection treatments that allow to overcome the immunological barrier between donor and recipient. Nonetheless, forty percent of transplanted organs are still lost within 10 years leading many patients to return to the waiting list for another new organ. In the case of a failed kidney, patients return to dialysis and the risk of death increases considerably (Coemans et al., 2018). Inflammation, injury, and fibrosis of the allograft are hallmarks of the transplant rejection response. Gaining a better understanding of the pathogenic mechanisms involved in allograft rejection is instrumental to more effectively treat patients in order to modulate the immune reaction that leads to the loss of kidney function (Niu et al., 2019).

Over the past decades, the progress of new, wide-ranging immunosuppressive drugs has dramatically enhanced short-term graft survival after organ transplantation. However, long-term survival has not substantially improved (Coemans et al., 2018). Largely contributing to long-term graft failure is the formation of donor-specific antibodies (DSA) (Prémaud et al., 2017; Zhang, 2018).

Considerable progress in the field of kidney transplantation began with the recognition of anti-HLA donor-specific antibodies (DSAs). A wide-range of allograft injury is linked to DSAs. Antibody-mediated rejection (ABMR) is the most severe manifestation of DSA pathogenicity. ABMR involves C1q-binding IgG1 and IgG3 DSAs carrying complement activation and microvascular inflammation through allograft capillaries. In contrast, IgG4 DSAs are associated with tardy and chronic damage (Louis et al., 2020).

Despite the advancement in new treatments, 33% of de novo DSA positive transplant recipients still develop ABMR in the setting of kidney transplantation (Schwaiger et al., 2016). Prior sensitization, such as previous pregnancies or blood transfusions, can lead to preexisting DSA. Since preexisting DSA outcomes in earlier graft rejection, transplantation into patients with preexisting DSA is avoided if possible (Konvalinka and Tinckam, 2015).

1.2 Humoral immunoregulation of antibody responses

T and B cells interaction is crucial for the humoral immune response as they provide a protective role during infections, while they mediate graft rejection after organ transplantation. In all of these cases, the antibody responses are monitored by humoral immunoregulation in which T follicular helper (T_{FH}) cells stimulate and T follicular regulatory (T_{FR}) cells prevent Germinal Center formation and antibody responses (Qin et al., 2018). Alloantigen-activated T follicular helper cells provide help to antigen-activated B cells that produce antibodies. T_{FH} cells are essential in guiding immunoglobulin class switching, somatic hypermutation of immunoglobulin variable region genes, and secretion of high affinity antibodies (Ma et al., 2012). All of these events take place principally within Germinal Centers (GC) in secondary lymphoid tissues (Figure 1).

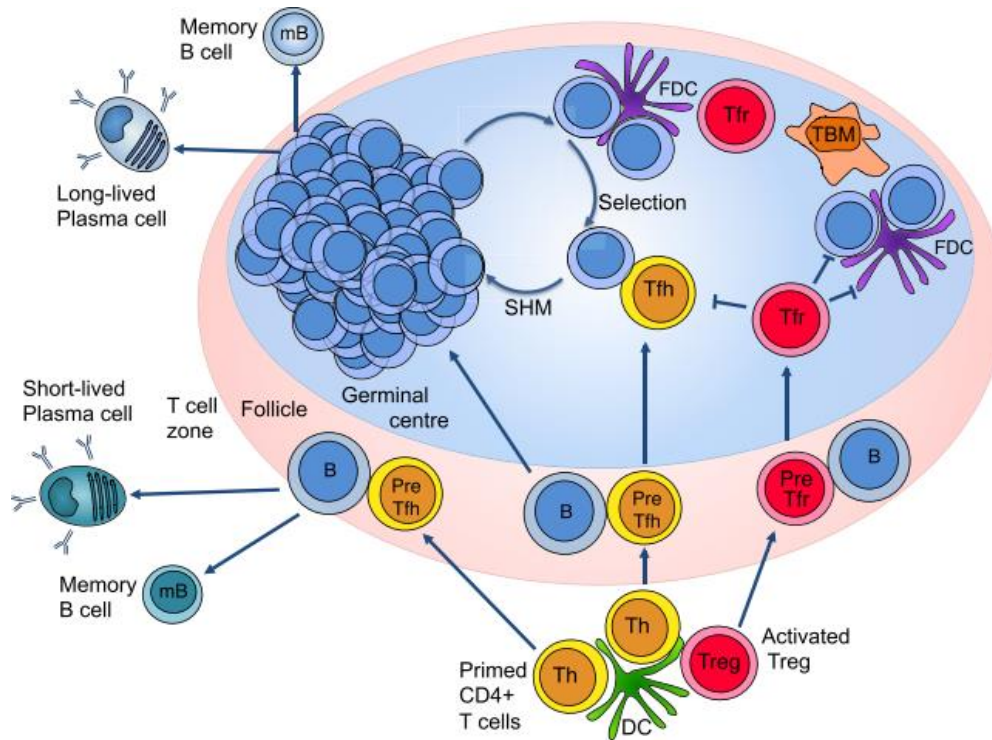


Figure 1. In the Germinal Center (GC) T Follicular helper (T_{FH}) and T follicular regulatory (T_{FR}) play their role in regulating the generation of Long-lived Plasma cells and Short- lived Plasma cells, antigen (Ag)-specific antibody-secreting cells. After activation with Ag and dendritic cell (DC) presentation, conventional $CD4^+$ T cells differentiate into T_{FH} cells. T_{FR} cells originate from conventional regulatory T cells (Tregs) and migrate into the GC(Xie and Dent, 2018)(Xie and Dent, 2018). DC, dendritic cell; FDC, follicular dendritic cell; mB, memory B cell; SHM, somatic hypermutation; TBM, tingible body macrophage; Th, T helper cell; Treg, regulatory T cell (Linterman and Hill, 2016).

1.3 Germinal Center

Germinal Centers (GC) are a temporary structures in the center of B cell follicles of peripheral lymphoid organs. Here, besides IgM^- - IgD^+ naïve B cells, a network of stromal cells, known as follicular dendritic cells (FDCs), are present (Heesters et al., 2014). After the acquisition of exogenous antigen, resting naïve B cells start the GC formation (Cyster, 2010; Gonzalez et al., 2011). Subsequently, B cells migrate to the follicle:T-zone (T:B) border where $CD4^+$ T cells deliver the B cells co-stimulatory signals through the $CD40$ - $CD40L$ interaction (Garside et al., 1998; Okada et al., 2005). A phase of strong proliferation starts after the interaction between $CD4^+$ T cells and B cells, with the responding B cells preferentially sited in the outer B cell follicle (Francis Coffey, Boris

Alabyev, 2009). An early GC starts from these cells, which can form tight clusters in the follicle center in close apposition with the follicular dendritic cells network.

The mature GC is characterized by a division into two “zones” (Figure 2). The dark zone (DZ) is the GC pole closest to the T-zone in lymph nodes and the spleen, lacking in follicular dendritic cells. The light zone (LZ) is the pole distal to the T-zone, closest to the capsule in lymph nodes or the marginal zone in the spleen (where FDCs are widely present). A tight cluster of highly proliferative B cells, within the DZ, form regions usually known as “centroblasts” where the cells highly express chemokine receptor CXCR4 (Allen et al., 2004, 2007; Victora and Nussenzweig, 2012; Victora et al., 2012). The surrounding stroma is composed of a network of Reticular Cells: the source of the CXCL12 chemokine (the ligand for CXCR4) that avoids the interaction between DZ B cells and the FDC network (Bannard et al., 2013; Rodda et al., 2015). Supporting the idea that the DZ is the site of Ig somatic hypermutation (SHM) and where clonal variants with diverse affinities for antigen are produced, DZ strongly expresses activation-induced cytidine deaminase (AID) and DNA polymerase eta (Pol η , which introduces point mutations into DNA when repairing AID-induced lesions) (Victora et al., 2010, 2012; Victora and Nussenzweig, 2012; Mcheyzer-Williams et al., 2015). The LZ has a different composition compared to the DZ. This zone contains GC B cells, FDCs, and a large amount of infiltrating naïve B cells (Schwenger et al., 2007). Furthermore, it includes a smaller but essential population of T follicular helper (T_{FH}) cells. It has been demonstrated that T_{FH} has a key part in the positive selection of higher-affinity B cells, allowing their proliferation and differentiation into plasma cells (Meyer-Hermann et al., 2006; Allen et al., 2007; Victora et al., 2010). The LZ contains another population of CD4⁺ T cells, the T follicular regulatory (T_{FR}) cells. They present similar phenotypic characteristics, such as CXCR5 expression, as T_{FH} cells but express FOXP3, a master regulator of Treg cell development (Chung et al., 2011b; Linterman et al., 2011; Wollenberg et al., 2011). B cells included in the LZ are known as “centrocytes”, and they show a high expression of CD86 and CD83 markers and genes associated with activation of the CD40, BCR, and Myc pathways. Altogether, these characteristics indicate an activated B cell phenotype (Dominguez-Sola et al., 2012; Victora and Nussenzweig, 2012; Victora et al., 2012). LZ is the site where high-affinity SHM variants are selected, as suggested by the co-localization of activated B cells, antigen, and T_{FH} cells. During the immunity reaction, a cell's migration between the DZ and the LZ is necessary due to the equally relevant events

of proliferation and hypermutation in the DZ and antigen-driven selection in the LZ (Mesin et al., 2016).

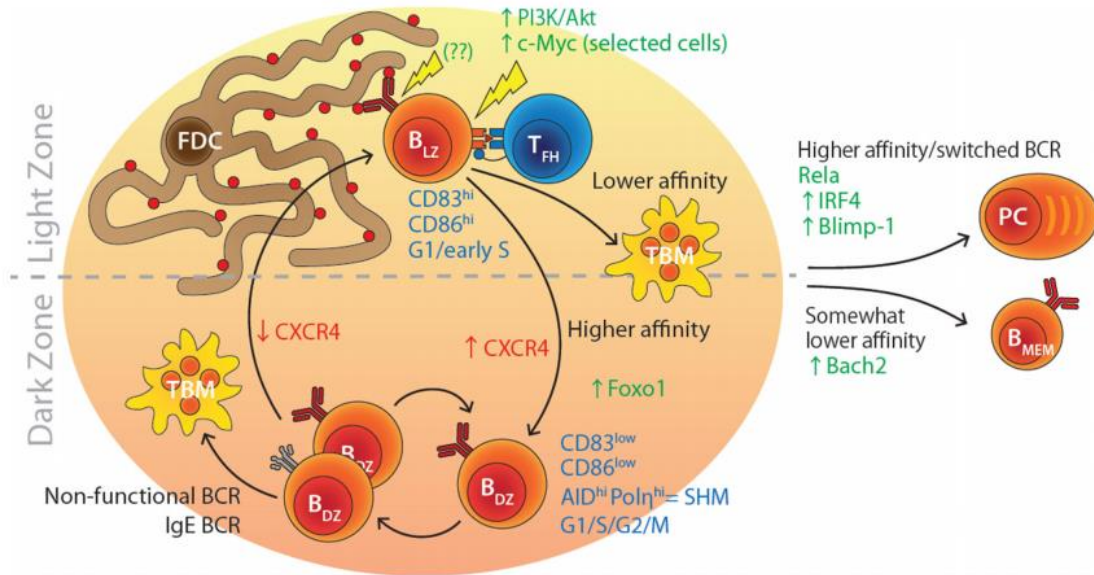


Figure 2. GC is divided into two anatomical compartments: light zone, the site of antigen-driven selection, and dark zone, the site of B cell proliferation and hypermutation. FDC, follicular dendritic cells; TBM, tingible body macrophage; PC, Plasma cells; B_{MEM} B memory cells (Mesin et al., 2016).

1.4 B-Cell development and class switch recombination

During their initial phase of development, bone marrow-derived B-cell precursors are subjected to recombination of immunoglobulin (Ig) heavy (H) and light (L) chain genes to produce a functional B-cell antigen receptor. Before antigen encounter, recombination-activating genes RAG1 and RAG2 act on the variable (V), diversity (D), and joining (J) regions of IgH, and the VJ regions of IgL, to complete this first stage of B cells maturation.

The primary immune response leads to the production of IgM subclass, low affinity antibodies.

After the antigen encounter, naïve B-cells are stimulated, through an interaction of the B cell antigen receptor and CD40, to translocate in the GC. Here, they start to proliferate and undergo clonal expansion (MacLennan et al., 1990; Rajewsky, 1996). Somatic

hypermutation (SHM) is a process that occurs within the GC (DZ), allowing the introduction of many non-random, single-base changes into the Ig V regions that encode the antigen-binding site. Thanks to this accumulation of mutations, the Ig V repertoire can achieve a high diversification. At the same time, Ig constant regions undergo a series of recombination events. This process, called class-switch recombination (CSR), promotes the production of different subclasses of antibodies (IgG, IgA or IgE).

A specific immune response is, therefore, possible thanks to SHM and CSR, which generate subclasses of high-affinity antibodies. Both, SHM and CSR, take place in the centroblast stage of B-cell maturation, in the DZ of the GC. Here, B cells differentiate into plasma cells, programmed to secrete massive amounts of specific antibodies, or become memory B cells, which are responsible for recognizing and responding to antigens on reiterate exposure.

Through CD95/Fas-mediated apoptosis, centroblasts are quickly removed in presence of low-affinity antibodies, impaired B-cell antigen receptor (caused by non-functional mutations in their Ig V regions), or in the context of autoreactivity (Lam et al., 1997; Takahashi et al., 2001).

Significantly, ongoing mutational activity, the hallmark of GC-derived B cells, promotes further diversification of Ig V region genes, enhancing intraclonal heterogeneity and the chance to produce high-affinity antibodies (Natkunam, 2007).

1.5 Development and features of T_{FH} cells

T follicular helper cells (T_{FH}) are a specialized subset of CD4⁺ T cells and have a distinctive phenotype. These cells present high expression levels of CXC chemokine receptor 5 (CXCR5), a receptor that directs T_{FH} cells to migrate to B cell follicles, where CXCL13 (the ligand for CXCR5) is expressed. Concomitantly, the loss of CCR7 allows the T_{FH} to localize to B cell follicles and GCs in the secondary lymphoid organs (SLOs). Here, they play their role as helpers in B cell proliferation and GC reactions. The CXCR5⁺ T_{FH} cells express high levels of several molecules known to be involved in T and B cell interactions and promoting antibody production. These include the co-stimulatory molecule CD40 ligand (CD40L), inducible co-stimulator (ICOS), programmed death 1

(PD-1), signaling lymphocytic activation molecule (SLAM)-associated protein (SAP), and the cytokines interleukin IL-4, IL-6, and IL-21 (van Besouw et al., 2019).

As mentioned above, B cells undergo somatic hypermutation and affinity maturation within GCs. Thanks to these events naïve B cells become memory and long-lived plasma cells, that are accountable for the production of long-term high-affinity antibody responses (Ma et al., 2012). Production of IL-21 and expression of CD40L are essential to an functional antibody response in an allograft by promoting T cell assistance of B cells (Niu et al., 2019).

A hallmark of T_{FH} cells is the expression of its distinctive master transcription factor, B cell lymphoma Bcl-6. This transcription factor regulates T_{FH} cell differentiation and phenotype acquisition by upregulating the expression of CXCR5, PD-1 and ICOS, and by inhibiting the production of interferon IL-17 and IFN- γ (Nurieva et al., 2009; Yu et al., 2009).

The Bcl-6-dependent differentiation of T_{FH} cells is a complex process that comprises several steps and requires a GC environment. Numerous surface receptors, including CD28, ICOS, CD40L, and SLAM are involved.

Antigen-presenting dendritic cells (DCs) start the T_{FH} cell differentiation process, which is sustained by subsequent interactions with B cells. The differentiation of the T_{FH} cell subset is also directed by stimuli supplied by cytokines and the signal transducer and activator of transcription (STAT) family of transcription factors (Tangye et al., 2013; Niu et al., 2019).

1.6 Mechanisms of T_{FH} cell function

To initiate class switch recombination and promote the development of activated B cells, T_{FH} -GC B cell interaction is required. Among several key molecules, the CD40-CD40L costimulatory pathway is essential. These two membrane proteins are expressed by B cells and T cells respectively (Kawabe et al., 2011).

As demonstrated in several models, T_{FH} cells produce, upon stimulation, a series of cytokines, such as IL-21, IL-10, IL-4, IFN- γ , IL-17 and IL-9, which act on a different stage of the GC responses.

IL-21 plays a direct role in B cells to control Bcl-6 expression, consequently enhancing GC formation and promoting plasma cell development (Niu et al., 2019). Blocking the IL-21 receptor (IL-21R) inhibits B cell differentiation as well as plasmablast formation and consequent IgM and IgG production (de Leur et al., 2017).

Recent studies showed that T_{FH} -derived IL-10 has an essential role in stimulating humoral immunity during persistent viral infection (Xin et al., 2018). Other data have demonstrated that IL-9 enhances memory B cell formation in GCs (Wang et al., 2017). IL-4 is produced by GC T_{FH} cells and is required by T_{FH} cells for optimal B cell help (Yusuf et al., 2010). Furthermore, class-switched B cells can generate different Ig isotypes based on the combination of different cytokines produced by T_{FH} cells. For example, IgG1 or IgE isotype are produced by class switch recombination of B cells after IL-4 exposition, while $IFN\gamma$ drives the production of IgG2a and IgG3 isotypes (Niu et al., 2019).

In sum, the T_{FH} subset are critical for germinal center formation, affinity maturation, and the production of most high affinity antibodies and memory B cells.

These cells play a key role in many protective immune responses against pathogen, and in other diseases, principally autoimmune diseases. Further studies will be necessary to learn more about T_{FH} cell biology, in the interest of applying that knowledge to biomedical needs (Crotty, 2014).

1.7 Development and features of T_{FR} cells

An overproduction of Igs may end in autoimmunity, chronic inflammation, and B cell malignancies. To avoid this issue, antibody production of plasma cells requires a monitoring system. T follicular regulatory cells (T_{FR}), a unique subset originating from Treg cells, are involved in regulating T_{FH} -mediated immune response.

The expression of specific Treg cell markers, the transcription factor FOXP3, and cytotoxic T-lymphocyte antigen (CTLA)-4 characterize T_{FR} cells. The presence of these markers allows T_{FR} cells to carry out their immunity suppressive activity.

Like T_{FH} , high expression of CXCR5 and low expression of CCR7, drive T_{FR} cells to migrate to GCs. The T_{FR} subset also expresses Bcl-6, ICOS, and PD-1, similar to T_{FH} cells, but IL-21, IL-4, and CD40L are scarcely expressed (Niu et al., 2019).

T_{FR} cells are usually defined as $CD4^+ CXCR5^+ FOXP3^+ PD-1^+ Bcl-6^+$ T cells. Their differentiation and maintenance are driven by signals from the T cell receptor (TCR) and the costimulatory molecules CD28 and ICOS. Instead, other molecules, such as PD1, CTLA-4, and the cytokine IL-2, inhibit T_{FR} development (Maceiras et al., 2017; Qin et al., 2018). By inhibiting p-AKT to down-regulate FOXP3 expression, IL21 acts as a negative regulator of T_{FR} cell numbers (Ding et al., 2014). While the transcription factors Bcl-6 and NFAT2 have an essential role in the T_{FR} differentiation and enhance the upregulation of the expression of CXCR5 (Vaeth et al., 2014), the transcription factor Blimp-1 inhibits Bcl-6. In addition, SLAM-associated protein (SAP), mediates the interactions of T_{FH} precursors and B cells to promote T_{FH} formation (Qi et al., 2008), and, at the same time, stimulates T_{FR} development and cell numbers (Qin et al., 2018).

1.8 Mechanisms of T_{FR} cell function

The T_{FR} cell subset has a crucial function acting as a regulator on GC reactions and obstructing T_{FH} and B cell responses. Several pathways and molecules are involved in these mechanisms comprising cytokine production, downregulating the expression of co-stimulatory molecules, and mediating cytolysis (Miles and Connick, 2018).

CXCR5 and Bcl-6, highly expressed by T_{FR} , have an essential functional activity in reducing the GC B cell numbers, affinity maturation, plasma cell formation, and consequently antibody production (Chung et al., 2011c, 2011a). T_{FR} cells exert their suppressive function also through Cytotoxic T-lymphocyte-associated antigen-4 (CTLA-4) present on the cell surface. This molecule decreases expression of the costimulatory ligands CD80/86 on B cells, thus inhibiting T cell CD28 engagement (Wing et al., 2008; Wang et al., 2015). Another way that this cell subset may apply its suppressing function may be through cytolysis since T_{FR} cells express granzyme B (Qin et al., 2018). With these different mechanisms, T_{FR} cells can impair T_{FH} generation and differentiation, in addition to limit B cell responses (Sage et al., 2014; Wing et al., 2014).

Transforming growth factor TGF- β or IL-10 are immune inhibitory cytokines secreted by T_{FR} cells. It is known that TGF- β signaling is another key mechanism for reducing T_{FH} and self-reactive B cell accumulation (McCarron and Marie, 2014), but the role of T_{FR} derived IL-10 is currently not completely clear.

To result in the proliferation of antigen-activated B cells, lymphocytes must have high-affinity receptors to bind antigens, whereas low-affinity B cells receive a ‘death signal’ through CD95/Fas. T_{FH} cells produce IL-21 that has a key role to increase the affinity of the B cell receptors. The last mechanism by which T_{FR} cells exert an inhibition role is by suppressing IL-21 production in T_{FH} cells, limiting the B cell selection process during affinity maturation. Only the B cells with the highest affinity B cell receptors can overcome this suppression (Wu et al., 2016).

In sum, T_{FR} subset play an essential role in regulating T_{FH} mediated B cell responses after antigenic exposure. However, these cells appear involved in controlling autoimmune disease, but further studies will be necessary to elucidate the precise role of this cell population (Sage and Sharpe, 2020).

1.9 T_{FH} cells in alloimmunity

T_{FH} cells have a central role in the humoral response. It is possible that this cell subset directly triggers B cell-dependent alloreactivity in the context of organ transplantation, leading to the production of DSA and the possible outcome of antibody-mediated rejection.

Numerous studies confirm that T_{FH} cells are involved in allogeneic immune responses after organ transplantation.

Data from an allogeneic kidney transplant model in macaque showed that these cells interact with B cells in lymph nodes to promote DSA production and ABMR (Kim et al., 2014). Others reported a co-localization of T_{FH} cells, B cells, and Igs to follicular-like structures in the transplanted kidney in the context of allograft rejection (de Graav et al., 2014), and a correlation between circulating T_{FH} numbers and anti-donor HLA sensitized transplant patients (Cano-Romero et al., 2019). Other investigations described the presence of higher frequencies of pre-transplantation donor-reactive memory IL-21⁺ circulating T_{FH} cells in patients who developed DSA post-kidney transplantation (Macedo et al., 2019). Moreover, higher levels of CD40L⁺ PD1⁺ circulating T_{FH} cells were noticed in recipients who developed de novo DSA at one-year post kidney transplantation in comparison to de novo DSA-negative patients (Iwasaki et al., 2018). Chenouard et al. confirmed that a compromised T_{FH} function (low IL-21 production and affected IgG

production *in vitro*) or reduced number of these cells was related to a low incidence of post-transplant de novo DSA production (Chenouard et al., 2017), underscoring the essential role of this cell subset in allogeneic immune responses.

In another experimental transplant model, a temporal correlation between the T_{FH} cells phenotypic differentiation into ICOS⁺ PD-1⁺ and GC alloreactivity sustained the role of T_{FH} cells in the generation of DSA (La Muraglia et al., 2019). Furthermore, indirect-pathway CD4⁺ T cell responses delivering help for GC responses, which resulted in the production of long-lasting alloantibodies, needs T_{FH} cells.

Several evidences that showed an association between the manifestation of chronic allograft rejection and the presence of functional T_{FH} cells, even though these T cells seem to be associated also with acute allograft rejection after transplantation (Conlon et al., 2012).

Besides the effector role in allograft rejection, transplant-associated autoimmunity is also affected by T_{FH} cells, which have a crucial function in the mechanisms resulting in transplant failure. For instance, Qureshi et al. described that the GC autoantibody responses independently mediated the advancement of allograft vasculopathy in experimental heart transplantation, which was dependent on recipient T_{FH} cells (Chhabra et al., 2019).

Overall, the results support the contribution of circulating T_{FH} in complex and dynamic rejection responses in organ transplant patients. Furthermore, the present knowledge and literature propose that measuring the numerical and phenotypic changes of circulating T_{FH} cells, may help to recognize transplant recipients who are predisposed to develop DSA (Schmitt et al., 2014).

To potentially improve transplant outcomes, a better knowledge of this immune mechanism could be translated into more effective drugs that target T_{FH} cells and monitor the B cell-dependent alloimmune response.

1.10 T_{FR} cells in alloimmunity

T_{FH} and T_{FR} cells have opposing effects in regulating the GC response. Various studies have demonstrated that immune responses, homeostasis, and tolerance are correctly maintained by a dynamic balance between these two populations. More and more often,

researchers are focusing on the measure of the T_{FR}/T_{FH} ratio in different patient populations due to the increased understanding of these dynamic populations (Niu et al., 2019).

In both kidney graft and peripheral blood, ABMR is associated with an augment in T_{FH} cell numbers and a reduction of T_{FR} cells. T_{FR} cells exert similar inhibitory functions in non-ABMR recipients and in transplant patients that developed ABMR. The latter show a fewer amount of T_{FR} cells, but they exercise regular function (Chen et al., 2017).

Other studies proposed by Niu et al. showed a decrease in circulating T_{FR} cell (cT_{FR}) numbers in kidney transplant patients.

They saw that lower numbers of cT_{FR} cells were detected in kidney transplant recipients with anti-HLA antibodies, including DSA, treated with immunosuppressive therapy (tacrolimus, mycophenolate mofetil and steroids), in comparison to patients without anti-HLA antibodies (Niu et al., 2019). Moreover, some mouse models of chronic graft-versus-host disease indicated that T_{FR} cells inhibited pathology. This data suggests that T_{FR} cells could regulate pathogenic antibodies during transplantation, promoting allograft tolerance (McDonald-Hyman et al., 2016).

Despite these evidences, many outstanding questions remain regarding the function of T_{FR} in regulation of humoral immune response in health and disease. A deeper understanding of the exact molecular mechanisms by which this unique subset acts it will be necessary, also with the chance to consider these cells a potential therapeutic target.

1.11 Erythropoietin (EPO)

EPO is an erythropoietic hormone crucial for survival, proliferation, and differentiation of erythrocyte progenitors in bone marrow (Lombardero et al., 2011). Tissue hypoxia is the main stimulus that increases EPO gene transcription and induces up to a 1000-fold increase in circulating serum protein levels (Ebert and Bunn, 1999).

In a hypoxic condition, hypoxia-inducible factor HIF-1 α transcription factor is stabilized. In renal peritubular interstitial cells, HIF-1 α translocates into the nucleus where it dimerizes with the constitutively expressed HIF-1 β subunit, mediating transcription of target genes, including EPO (Bunn, 2013).

EPO receptors (EPOR) are highly expressed on bone marrow erythroid progenitors, and bound EPO promotes viability, proliferation, and terminal differentiation of these cells, increasing the red blood cell mass and the oxygen-carrying capacity. This signaling completes a feedback loop that leads to an inhibition of further EPO expression (Martinez and Pallet, 2014) (Figure 3).

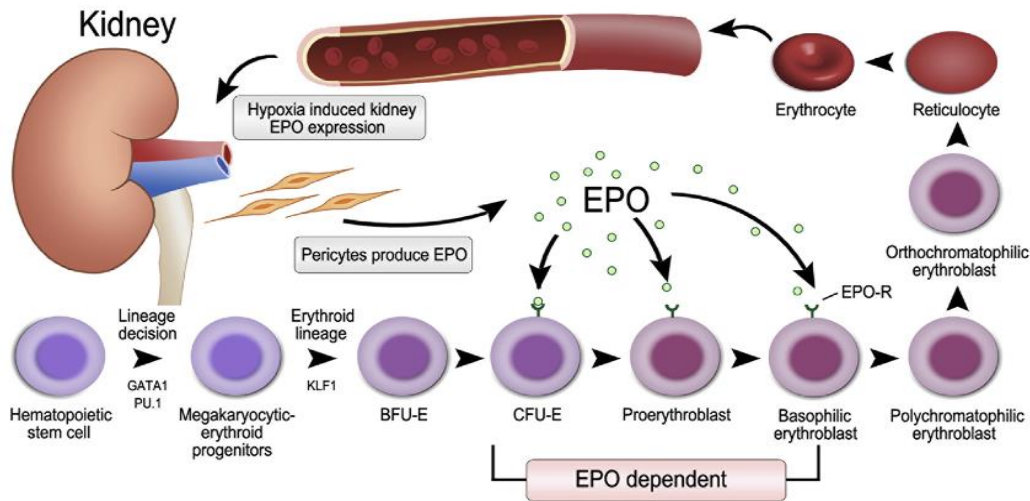


Figure 3. In hypoxic condition, with low hemoglobin concentration, renal pericytes (stromal cells that support vasculature) are stimulated to produce EPO. EPO binds to EPOR which is expressed on erythrocyte progenitors, preventing them from apoptosis. Increased erythrocytes in circulation lead to improvement of tissue oxygenation, diminishing EPO production. EPO, erythropoietin; EPOR, erythropoietin receptor; KLF1, Krüppel-like factor 1; BFU-E, burst-forming unit-erythroid; CFU-E, colony-forming unit-erythroid (Shih et al., 2018).

1.12 EPO structure

The EPO human gene localizes on chromosome 7 and is composed of five exons and four introns (Jelkmann, 1992). EPO messenger RNA (mRNA) encodes an amino acid chain of 193 bases. During translation, a canonical leader sequence of 27 amino acid, mostly of hydrophobic residues, is cleaved in the endoplasmic reticulum. Glycosylation occurs in the Golgi, and a 166-residue polypeptide is released (Jacobs et al., 1985; Lin et al., 1985). The EPO protein reaches the final length of 165 amino acids, and the weight of 30.4 kDa, losing its final arginine residue at the C-terminus (Erslev and Caro, 1986) (Figure 4A).

Glycosylation of EPO marginally inhibits its biological activity but is indispensable for guaranteeing protracted circulation in the plasma (Goldwasser et al., 1974). As other hematopoietic cytokines, EPO folds into a globular three-dimensional structure comprising a bundle of four amphipathic helices linked by loops lacking secondary structure, and stabilized by a disulfide bridge between the amino-terminal and carboxy-terminal helices (Bazan, 1990; Boissel et al., 1993) (Figure 4B). The structure was proven by X-ray crystallographic analysis of EPO in a complex with two extracellular domains of the EPO receptor (Syed et al., 1998), and using nuclear magnetic resonance spectroscopy of EPO in solution (Cheetham et al., 1998).

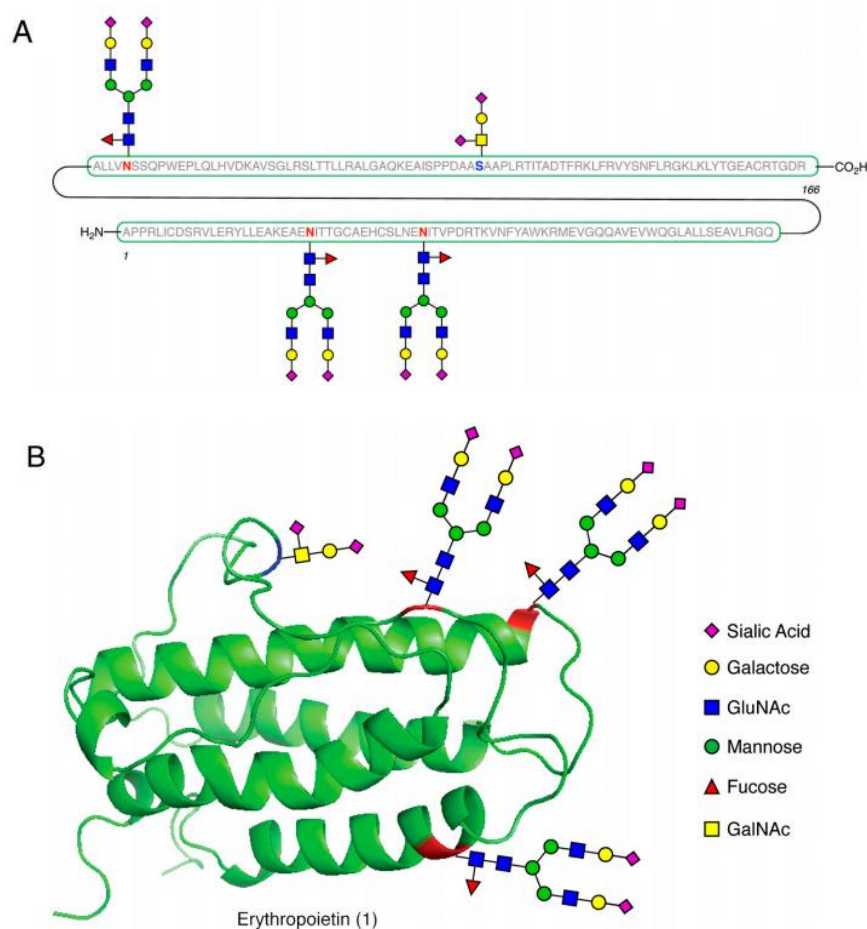


Figure 4. EPO structure. (A) Amino acidic sequence of EPO; (B) Ribbon diagram that shows the four major α -helices and selected oligosaccharides. (Brailsford and Danishefsky, 2012).

1.13 Tissue expression of EPO

Experiments in murine models provide evidence that, during mammalian development, EPO is first expressed transiently in neural crest cells during mid-gestation. The presence of this hormone promotes yolk sac primitive erythropoiesis for oxygen transport in mid-stage embryos (Malik et al., 2013; Suzuki et al., 2013; Hirano and Suzuki, 2019).

Afterward, the liver begins to produce EPO which becomes the site of erythropoiesis (Palis, 2014; Palis and Koniski, 2018).

It has been demonstrated that EPO is essential for erythropoiesis. Due to the interference of erythropoiesis in the fetal liver, EPO or EPOR knockout mice die in utero around day 13.5 (Wu et al., 1995; Lin et al., 1996). In mammals, by the last third gestation, the site of EPO production progressively shifts to the kidney, an organ that becomes and remains the main source of EPO production (Zanjani et al., 1981; Dame et al., 1998).

The site of hematopoiesis switches as well, and bone marrow becomes the site of red blood cell production (Ho et al., 2015).

Several *in situ* hybridization, immunohistochemistry, and *in vivo* studies have shown that EPO mRNA expression in the kidney is localized to a subset of cortical peritubular fibroblasts close to the boundary of the medulla (Souma et al., 2015).

Although EPO expression is detected in other tissues such as the brain, neural cells, spleen, lung, and bone marrow (Blanchard et al., 1993; Masuda et al., 1994; Marti et al., 1996; Dame et al., 1998; Juul et al., 1998), EPO production provided by the kidney is necessary for erythropoietic regulation (Suresh et al., 2020).

1.14 Molecular mechanism of EPO

Stimulating EPOR on erythroid precursor cells in the bone marrow, EPO induces erythropoiesis.

The EPOR is activated by direct binding of a single EPO molecule. This event triggers the formation of an EPOR homodimer, and its conformational change initiates a signaling pathway through phosphorylation of Janus kinase 2 (JAK2). The activation of JAK2 results in the phosphorylation of mitogen activated protein kinases (MAP kinases),

phosphatidylinositol 3 kinase (PI3K γ /AKT), and signal transducer and activator of transcription 5 (STAT5) phosphorylation (Sinclair and Elliott, 2012) (Figure 5).

In non-hematopoietic tissue such as the brain and heart, EPO also binds an alternative EPOR, a heterodimer complex composed of one chain of the EPOR and the ubiquitous β -common receptor (β cR, CD131, colony-stimulating factor 2 receptor- β) (Brines and Cerami, 2006a). The activation of this alternative heterodimeric EPOR needs much higher concentrations of EPO compared with the homodimeric receptor form. It does not have erythropoietic effects, but, similarly to the homodimer, it activates PI3K γ /AKT, MAP kinases, and STAT5 phosphorylation mediated pathways. Furthermore, EPOR/CD131 mediates the binding activity of nuclear factor κ light chain enhancer of activated B cells (NF- κ B) family members (Broxmeyer, 2013; Cantarelli et al., 2019) (Figure 5).

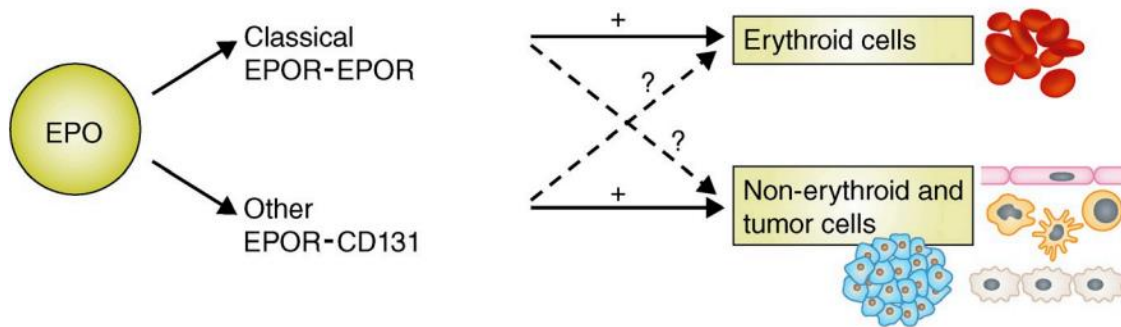


Figure 5. EPO signals in erythroid cells via EPOR-EPOR homodimers and in nonerythroid cells via EPOR-CD131 heterodimers. (Broxmeyer, 2013)

1.15 EPO and innate immune cells

Beside its erythropoietic role, growing evidences indicate that EPO has also important effects in tissue protection and immune regulation (Peng et al., 2020).

Monocytes, T cells and B cells, express functional EPO receptors on the cell surface (Lisowska et al., 2010; Purroy et al., 2017). Several studies show that a pharmacologic dose of EPO administration in mice leads to a better experimental condition of arthritis, colitis, and autoimmune encephalomyelitis (Cuzzocrea et al., 2005; Yuan et al., 2008; Nairz et al., 2011). Both innate (macrophages) and adaptive (T lymphocytes) immune

cells are involved in this mechanisms (Yuan et al., 2008; Nairz et al., 2011; Cravedi et al., 2014; Luo et al., 2016).

As demonstrated in different *in vitro* experiments, the production of murine macrophage-derived inflammatory mediators (IL-6, tumor necrosis factor α (TNF α), and inducible nitric oxide synthase (iNOS)) is reduced after EPO treatment compared to vehicle-treated controls. Furthermore, this study proved that EPO acts by inhibiting NF- κ B-inducible pathways. Salmonella typhimurium–infected mice treated with EPO confirmed the *in vitro* data conclusions, supporting the idea that EPO has a direct anti-inflammatory role on murine monocytes (Nairz et al., 2011).

Upon toll-like receptor (TLR) ligation, human monocytes exposed to EPO *in vitro* presented a decrease in IL-6 and IL-8 production (Cantarelli et al., 2019).

EPO demonstrates further anti-inflammatory function through its involvement in improving the clearance of apoptotic cells. Dying cells start a “find-me” signal sphingosine 1-phosphate (S1P) which stimulates macrophages to produce and release EPO.

EPO acts, through an autocrine signaling loop, inducing macrophages to increase peroxisome proliferator-activated receptor γ (PPAR γ). Impaired apoptotic cell phagocytosis is detectable in EPOR-deficient macrophages confirming that the EPO-EPOR pathway is involved. Consistently, macrophages specific EPOR knockout mice develop lupus-like symptoms, while EPO administration ameliorates disease progression in these lupus-prone mice (Luo et al., 2016).

However, other studies indicate that, in several contexts, EPO may have an opposite effect and strengthen immune responses.

In vitro experiments show that EPO promotes the expression of costimulatory molecules CD80 and CD86. Similarly, the expression of HLA-DR in peripheral blood dendritic cells (DCs) and monocyte-derived DCs (MoDCs) is augmented after EPO exposition. EPO treatment leads to an increase of antigen uptake and IL-12 secretion by MoDCs, and induces the maturation of these cells (Sagiv et al., 2008). Avneon et al. noticed an increase of neutrophil numbers related to augmented EPO levels in EPO transgenic mice after treatment with recombinant EPO. However, these experiments do not provide evidences supporting a direct effect of EPO on neutrophil function (Avneon et al., 2009).

In an experimental colitis model, Cuzzocrea et al. showed that EPO was associated with reduced disease severity and fewer neutrophil infiltrations in the colon mucosa, probably arbitrated by a diminished integrin expression (Cuzzocrea et al., 2004).

Altogether, these studies evidence that EPO plays a significant role as immune-modulator, making this hormone and its derivatives promising drugs in immune and autoimmune disorders.

1.16 EPO and T cells

Several recent studies have shown that EPO has an immune-regulatory effect by acting on T cells (Peng et al., 2020).

The EPOR is sparsely expressed on the murine and human T cells surface in a resting condition. However, when antigens on major histocompatibility complex molecules are recognized by T cell receptor (TCR), and T cells are activated, a rapid upregulation of EPOR occurs (Cantarelli et al., 2019).

EPO treatment leads to a reduction in the amount of T_H17 cells and an increase of Tregs in the T helper 17 (T_H17) mouse model of autoimmune encephalomyelitis, with a significant amelioration of the disease (Yuan et al., 2008).

In previous studies, Cravedi's group showed that through the homodimeric form of the EPOR, EPO acts directly by inhibiting naïve and memory conventional T cell (T_{conv}) proliferation (Cravedi et al., 2014). EPO treatment inhibits the strong human anti-mouse T cell xeno-response resulting from the transfer of human T cells into NOD scid γ c^{null} mice (lacking T and B cells and functional NK cells). This data indicates that EPO inhibits human T cells in this *in vivo* system.

EPO impedes T_{conv} cell activation by binding the homodimeric form of EPOR and inducing STAT5 phosphorylation, but this obstruction only occurs in the presence of TCR engagement with co-stimulation molecules (Lisowska et al., 2011). Usually, IL-2 is produced by T cells and, through an autocrine loop, this interleukin improves their expansion. However, when EPO binds the homodimeric EPOR, the receptor mediates SH-2 containing inositol-5- phosphatase 1 (SHIP-1) activation. SHIP-1 cross-talks with the β chain of the IL-2 receptor (IL-2R) and impedes IL-2-dependent signals transmitted,

inhibiting AKT and extracellular signal-regulated kinase phosphorylation. These events prevent conventional T cell activation and proliferation (Figures 6).

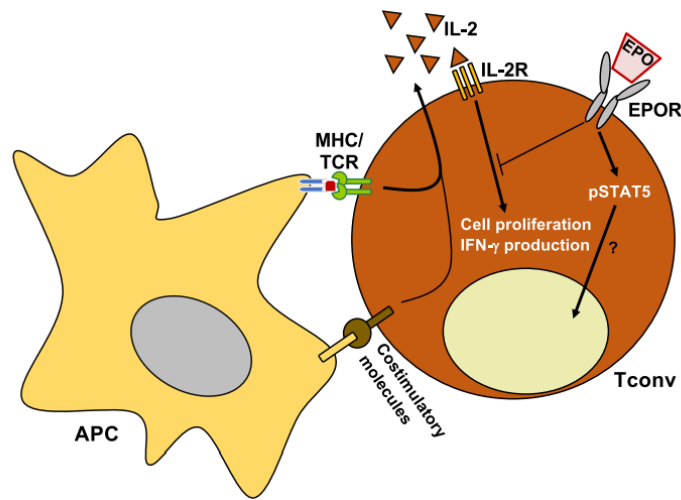


Figure 6. The homodimer EPO receptor (EPOR) activations inhibits IL-2 receptor (IL-2R) and, consequently, Conventional T cells (Tconv) expansion and $\text{INF}\gamma$ production. When activated, homodimer EPOR promotes STAT5 phosphorylation, but the effect of this pathway on Tconv is unclear. APC, antigen presenting cells; MHC, Major histocompatibility complex; TCR, T cell receptor. (Cantarelli et al., 2019).

Although never formally confirmed, signaling downstream the TCR could be prevented by SHIP-1 phosphatase (Hebeisen et al., 2013). This provides another potential mechanism accountable for EPOR-induced T cell inhibition.

Tolerance toward self and alloantigens is preserved by Treg subsets whose survival and proliferation is dependent on IL-2 signaling. Like Tconv cells, EPOR is expressed on the surface of Treg cells, but their function is not affected by EPO even if the hormone inhibits signaling downstream the IL-2R.

Collazzo et al. showed that *in vitro* EPO-mediated SHIP-1–dependent inhibition of IL-2R β signaling does not impair Treg survival and proliferation. Indeed, EPO does not affect IL-2R γ /STAT5 signaling necessary for IL-2-induced Treg proliferation, and AKT signaling is constitutively inhibited by endogenous phosphatases peculiarly expressed in Treg (Collazzo et al., 2009, 2012).

Although SHIP-1 has been shown to impair Treg function and expansion (Collazzo et al., 2009, 2012), EPO does not affect Treg proliferation or suppressive capacity, EPO/ EPOR signaling in Treg activates SHIP-1, and, at the same time, increases STAT5

phosphorylation, required to complete the differentiation of this cell subset (Cantarelli et al., 2019).

Through transforming growth factor β (TGF β)-dependent induction and stabilization of FOXP3, the Treg cell subset can originate from the thymus or from naïve CD4⁺ T cells (induced or iTreg) in the periphery.

Knowing that EPO plays a role in inhibiting Tconv but not Treg, and since there is evidence that EPO induces TGF β synthesis by monocytes (Mausberg et al., 2011) and tubular cells (Gobe et al., 2014), Cravedi's group tested the effect of EPO on Tregs, Both *in vitro* and *in vivo* experiments confirm that, by enhancing local production of TGF β by antigen-presenting cells (APCs), EPO helps the naïve CD4⁺ T cells maturation into functional iTreg. Cravedi's group established that this maturation is mediated through EPO ligating the heterodimeric form of the EPOR, demonstrating that EPO-induced TGF β production requires CD131 on APCs (Figure 7). Cravedi's group also showed that EPO treatment, using dosages comparable to those used to manage anemic alteration, increased frequencies of circulating Tregs in patients with chronic kidney disease in a prospective cohort study. This evidence supports the conclusion that EPO effects detected *in vitro* and *in vivo* in animal models are also applicable to humans *in vivo* (Purroy et al., 2017).

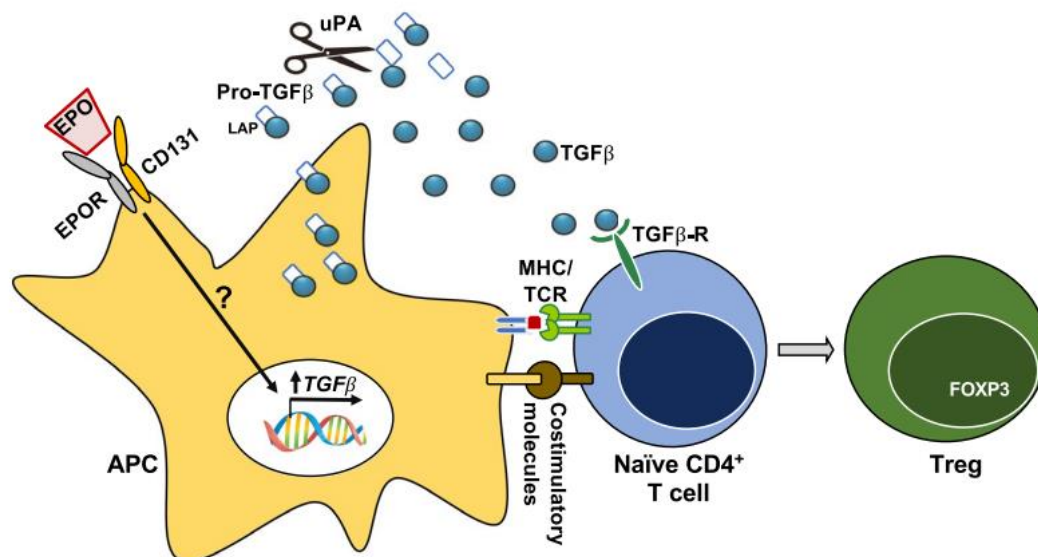


Figure 7. EPO binds heterodimer receptor on APCs, inducing an increase of TGF β and urokinase-type plasminogen activator (uPA) production. uPA cleaves the latency-associated peptide (LAP) from pro-TGF β , and the mature cytokine acts on naïve CD4⁺ T cells, promoting the conversion into functional regulatory T cells (Treg). MHC, Major histocompatibility complex; TCR, T cell receptor (Cantarelli et al., 2019).

1.17 EPO, Kidney, and renal injury

Abundant evidence documents the wide range of EPOR-expressing cells and the many erythropoietic-independent functions of EPO in the body. Several studies of injury in the nervous system and heart show that EPO is an anti-apoptotic hormone analogous to its endocrine effects in the bone marrow. In the context of inflammatory processes enhanced by injury, EPO has a clear role (Brines and Cerami, 2005), as seen with its reduction capabilities of pro-inflammatory cytokine production (Luo et al., 2015). Based on each specific tissue, EPO demonstrates different interactions and actions in several unique pathways.

To consider a possible role for the local non-hematopoietic effects of EPO, the identification of EPOR protein expressed throughout the kidney, comprising both proximal and distal tubular cells, was crucial. Nevertheless, these receptors show lower affinity than normal plasmatic EPO concentration, sustaining the idea that in some tissue EPO acts with a paracrine signaling (Westenfelder et al., 1999; Brines and Cerami, 2006a).

Although some studies show that EPO levels in the kidney are reduced in the context of Ischemia/Reperfusion Injury (IRI), EPO/EPOR pathway activation inhibits tubular cells apoptosis and helps recovery after injury. (Rankin et al., 2012).

Analogous to action in nervous tissue, EPO strongly inhibits the inflammatory response to ischemia-reperfusion in the kidney. EPO inhibits pro-inflammatory cytokine production, reducing leukocyte recruitment, and amplifying damage (Chatterjee, 2005). Acting on the EPOR heterodimer, recombinant EPO and non-erythropoietic EPO derivative, can reduce tubular apoptosis and interstitial fibrosis in rats with unilateral ureteral obstruction (Kitamura et al., 2008).

No increases in hemoglobin concentration were observed in these acute experiments, indicating that EPO acts directly on the kidney, and without hematopoietic effects.

Several clinical trials have also demonstrated EPO's non-hematopoietic effects. In pre-dialysis patients early treated with EPO, kidney disease has a slower progression (Brines and Cerami, 2006a).

Another study showed that EPO administration in healthy control subjects augmented renal vascular resistance and diminished renal plasma flow (Aachmann-Andersen et al., 2018). Despite regenerative properties on tubular cells, this could partially explain the

absence of nephroprotective effects of EPO in humans (Cantarelli et al., 2019). A complication of chronic administration of EPO ultimately resides with its hematopoietic function by increasing hemoglobin levels, complicating the assignment of cause and effect (Brines and Cerami, 2006a).

1.18 EPO in transplantation

During the first week after transplantation, the onset of anemia is a common event, increasing the risk for cardiovascular morbidity and mortality. Among the therapeutic options, EPO is an attractive possibility to ameliorate patient and graft outcomes in the context of organ transplantation, considering its pleiotropic effects constituting erythropoietic, tissue-protective, and immune-modulating effects.

Cravedi's group showed that treating heart transplant recipient mice with a short-term course of EPO or vehicle control significantly extended graft survival. Moreover, EPO administration diminishes alloreactive conventional T cells (Tconv) and increases regulatory T cell (Treg) frequencies (Purroy et al., 2017).

In murine models, heart transplants are quickly rejected, but kidney grafts are naturally tolerated across certain strain combinations. A hypothesis is that EPO plays a protolerogenic role, according to the fact that this hormone is mainly produced by the kidney. It has been demonstrated that, in rat transplant models, ischemic injury of kidney graft is prevented with EPO administration, supporting the protective role of this hormone (Zhang et al., 2018b).

In a rat model of chronic kidney transplant rejection, EPO completely adjusted post-transplant anemia and reduced the risk of progressive graft dysfunction and fibrosis. Furthermore, the EPO effect on graft protection is independent of anemia correction, since the normalization of post-transplant hemoglobin levels by blood transfusions does not affect chronic allograft injury (Cassis et al., 2012).

Cravedi's group also showed that, in mice, acriflavine downregulates EPO, inhibiting Treg-mediated spontaneous acceptance of allogeneic kidney transplants. These effects induced by acriflavine administration were rescued by supplying recombinant EPO. All together, these data sustain the idea that kidney-derived EPO is an essential regulator of T cell alloimmunity after kidney transplantation (Purroy et al., 2017).

Aside from the immune-modulating effects, considering the reduction of inflammatory cell infiltrates, EPO prevents graft chronic injury through its nephroprotective action, as suggested by the upregulation of the anti-apoptotic factor Bcl-2 in the graft (Cantarelli et al., 2019).

Heart and lungs produce marginal amounts of EPO, while the kidney is the major source (Jelkmann, 2011). This difference could explain the lower rates of acute rejection in the kidney when compared to heart or lung transplant recipients (Matas et al., 2013). In humans, more successful outcomes have been revealed combining kidney/heart transplants from the same donor vs recipients of hearts alone (Gill et al., 2009). Although infrequent, spontaneous kidney transplant acceptance/tolerance occurs in human as well, supporting the hypothesis of EPO-dependent immune-regulation (Newell et al., 2010). Additionally, protolerogenic properties have been demonstrated in the liver, the second major source of EPO (Travis D. Hulla, Gilles Benichoub, 2019), providing further evidence that EPO production reduces organ immunogenicity (Cantarelli et al., 2019).

From different clinical trials, conflicting data were obtained about the consequence of EPO administration on delayed graft function, acute rejection, or graft function in kidney transplant recipients (Martinez et al., 2010).

Incongruities across studies testing the EPO-immune-modulating activity and its nephroprotective effects could depend on patient characteristics, dosage, or treatment timing. For this reason, additional studies will be needed to clarify the ideal therapeutic strategies.

In conclusion, these data report that EPO has immune-modulating effects, with a positive impact on the graft outcomes, and a potential role in the unique tolerogenic properties of kidney grafts (Cantarelli et al., 2019).

1.19 Pharmacological use of recombinant human EPO and biosimilars

As previously mentioned, human EPO is a hematopoietic growth factor, produced principally in the kidneys, with a role in red blood cell production. In 1985, EPO gene was isolated and characterized (Lin et al., 1985). The first technique utilized, recombinant DNA technology, was used in mammalian cells to produce exogenous EPO, also called recombinant human erythropoietin (rhEPO) (Brines and Cerami, 2006b).

In 1989, U. S. Food & Drug Administration (FDA) approved Epoetin alfa (Epogen, Amgen) as the first agent in the class of erythropoiesis-stimulating agents (ESAs) for clinical use. Later, other biosimilar erythropoietins have been developed and approved. These are complex proteins with substantial micro-heterogeneity, obtained by genetically modified living cells, and challenging to produce and purify. Manufacturing procedures affect the biological parameters, purity, and clinical activity, which in turn affects the safety and efficacy of the final product (Abraham and Macdonald, 2012).

In this study, we used Retacrit (Epoetin alfa-epbx, Pfizer, Lake Forest, IL), which was approved by the European Medicines Agency (EMA) in December 2007, and by FDA in May 2018 as a biosimilar of epoetin alfa (Amgen Inc., Thousand Oaks, CA). Retacrit is equivalent in amino acid sequence and similar in carbohydrate composition to the reference product, Epoetin alfa (Fishbane et al., 2018).

These approved biosimilars bind with a high affinity the homodimeric EPOR on erythroid precursor cells in the bone marrow, promoting erythropoiesis. Instead, on non-erythroid cells, the heterodimeric form EPOR/ β c (CD131), which mediates non-hematopoietic tissue-protective effects, has a low affinity, and its activation requires a high concentration of these drugs (Cantarelli et al., 2019).

However, the administration of these ESAs can result in adverse events such as cardiac, vascular, blood, lymphatic, and nervous system disorders (Abraham and Macdonald, 2012).

To avoid the side effects of erythropoiesis, several non-erythropoietic derivatives of EPO, that bind the only alternative heterodimeric EPOR, have been developed (Peng et al., 2020). These comprise ARA 290 [cibinetide; helix B surface peptide (11 amino acid peptide derived from the EPO sequence)], carbamylated EPO, and recombinant EV-3 (an EPO derived a spliced variant with exon 3 deleted) (Erbayraktar et al., 2003; Brines et al., 2004; Fiordaliso et al., 2004; Robertson and Sadrameli, 2013; Bonnas et al., 2017).

A new study in a rat model of fully MHC-mismatched kidney transplantation showed that carbamylated EPO controls adaptive and innate immune cells through the phosphoinositide 3-kinase (PI3K)/protein kinase B (AKT) signaling pathway. Moreover, activating the same signaling pathway prolongs the survival time of kidney allografts in an EPOR-dependent manner (Na et al., 2020).

In several animal models, ARA290 has been shown to have a cytoprotective role in renal ischemia/reperfusion, e.g. by reducing inflammation, apoptosis and structural damage.

Mechanistically, ARA290 acts through the heterodimeric receptor, activating PI3/AKT pathway and mediating the increase of eNOS phosphorylation (van Rijt, 2014; Zhang et al., 2018a).

Zhang et al. demonstrated that, in rats, ARA290 plays a protective role against early renal allograft injury by reducing macrophage infiltration, improving renal morphology, preventing mRNA expression of inflammatory mediators, and diminishing the binding affinity of NF- κ B to DNA (Zhang et al., 2018a).

Other studies reported a neuroprotective role for recombinant EV-3, without any influence on hematopoiesis (Bonnas et al., 2017).

Constant exposure of precursor red blood cells to EPO is necessary for stimulation of erythropoiesis, whereas cytoprotection can be achieved by short-term exposure. An exception among the EPO derivatives is asialoerythropoietin, which maintains a high affinity for the homodimeric receptor. However, it has a half-life of several minutes, inducing cytoprotection but not erythropoiesis (van Rijt, 2014).

Altogether, these pieces of evidences open up the possibility to use EPO derivatives as a therapeutic approach. Further studies will be necessary to optimize the activation of tissue-protective activity, but reducing the risk ascribed to increases in erythropoiesis and hematocrit (Suresh et al., 2020).

2. PRINCIPAL AIM

EPO promotes erythrocyte maturation, but it also has immune modulatory effects, including inhibition of conventional T cell and induction of regulatory T cells (Treg) (Cravedi et al., 2014; Purroy et al., 2017; Cantarelli et al., 2019; Donadei et al., 2019). In a model of systemic lupus erythematosus, EPO treatment was associated with reduced levels of anti-dsDNA autoantibodies (Donadei et al., 2019).

Building logically on this evidence, the principal aim of this project is to test the hypothesis that EPO reduces alloantibody formation by inhibiting T_{FH}/B cell activation.

3. MATERIALS AND METHODS

3.1 Mice

C57BL/6 (B6, H-2^b), BALB/c (H-2^d), (B6 x BALB/c) F1 [(bxd) F1], (B6 x DBA) F1 [(bxd) F1], B6.129(Cg)-FOXP3^{tm3(DTR/GFP)Ayr/J} mice, were bought from Jackson Laboratory (Bar Harbor, ME) or bred from Jackson-derived animals at Mount Sinai.

C57BL/6J EPO-Rfl/fl mice were obtained from Embryonic Stem cells from the Knockout Mouse Project (Davis, California, USA). We produced and screened founders at Mount Sinai core facility, and then we crossed them with CD19-Cre^{+/-} or CD4-Cre^{+/-} mice (The Jackson Laboratory) to obtain C57BL/6J EPOR^{fl/fl} CD4-Cre or C57BL/6J EPOR^{fl/fl} CD19-Cre mice.

All animals were accommodated in the Center for Comparative Medicine and Surgery at the Icahn School of Medicine at Mount Sinai under Institutional Animal Care in agreement with guidelines of the Association for Assessment and Accreditation of Laboratory Animal Care International.

In all our experiments we tested animals of 6-8 weeks of age, using age- and sex-matched mice. Tests were performed with mice that were littermates or were maintained in the same room. Within the same experiment, animals were co-housed within the same cages for at least 2 weeks to prevent potential effects of microbiome differences.

3.2 NP-KLH immunization and EPO administration

Groups of B6 wild type animals were immunized with NP-KLH (Biosearch Technologies). We precipitated 100ug of NP-KLH 1:1 vol/vol in Alum (Immject Alum, Thermofischer) and injected mice intraperitoneally in a final volume of 200 μ l.

The animals were treated with 10,000 IU/Kg of EPO (Retacrittm Epoetin Alfa-epbx recombinant, Pfizer, 10,000 Units/mL) or vehicle (PBS) with intraperitoneal injections daily, starting on the day of immunization. At 10 days after immunization, mice were euthanized by carbon dioxide (CO₂)-induced asphyxia and cervical dislocation.

Serum samples were collected to perform Enzyme-Linked Immunosorbent Assay (ELISA) and measure high affinity and total anti-NP antibodies.

Splenic cells were collected and analyzed for NP⁺-specific and total Germinal Center B cells, class switched B cells, T_{FH}, and T_{FR} cells.

3.3 TNP-AECM-FICOLL immunization and EPO administration

B6 wild type mice were immunized with 50 µg of 2,4,6-trinitrophenyl-AminoEthylCarboxyMethyl-FICOLL (TNP-AECM-FICOLL, Bioresearch Technologies) resuspended in PBS, in a final volume of 200 µl. The immunization was performed by intraperitoneal injection.

The animals were treated with 10,000 IU/Kg of EPO (Retacrittm Epoetin Alfa-epbx recombinant, Pfizer, 10,000 Units/mL) or vehicle (PBS) with intraperitoneal injections daily, starting on the day of immunization.

At 10 days after immunization, mice were euthanized by carbon dioxide (CO₂)-induced asphyxia and cervical dislocation.

Splenocytes were collected to quantify total TNP⁺-specific B cells. Serum samples were collected to perform ELISA and measure anti-TNP IgM and anti-TNP IgG antibodies.

3.4 Sheep red blood cell immunization and EPO administration

Two ml of sheep red blood cells, supplied as a 100% suspension (SRBC; Innovative Research), were washed three times with 15 ml of PBS and resuspended 1:10 in PBS. At day 0, groups of B6 EPOR^{fl/fl} CD4-Cre^{POS/NEG} or B6 EPOR^{fl/fl} CD19-Cre^{POS/NEG} animals were immunized with 200 µl of the SRBC suspension through intraperitoneal injection. At day 6, the same mice were immunized a second time with washed SRBC not diluted. The animals were treated with 10,000 IU/Kg of EPO (Retacrittm Epoetin Alfa-epbx recombinant, Pfizer, 10,000 IU/mL) or vehicle (PBS) daily, with intraperitoneal injections, starting one day before the immunization. After 12 days, mice were euthanized by carbon dioxide (CO₂)-induced asphyxia and cervical dislocation. Spleens were collected, class switched, and GC B cells, T_{FH}, and T_{FR} cells were quantified.

3.5 B cells Activation

B cells were enriched from total splenocytes by magnetic negative selection with EasySep™ Mouse B Cell Isolation Kit (STEMCELL Technologies Inc.), according with the manufacturer's instructions. Subsequently, B cells were stimulated with LPS (Sigma-Aldrich) at different concentrations (0.1, 1, 10 µg/ml) and incubated in R10 medium [RPMI 1640 1X (Corning), 10% Fetal Bovine Serum (Corning), 100 IU/ml Penicillin-Streptomycin, 10 mM HEPES, 2mM L-glutamine, Sodium Pyruvate (100mM) (Gibco)] with vehicle (PBS) or EPO (1,000 IU/ml) (Retacrit™ Epoetin Alfa-epbx recombinant, Pfizer, 10,000 Units/mL) for 3 days at 37°C, in a 5% CO₂ humidified atmosphere, in 96-well round bottom plates. Cells were collected for flow cytometric analyses.

3.6 Heterotopic heart transplantation

Murine heterotopic heart transplantation was performed by the microsurgery core in the Icahn School of Medicine at Mount Sinai, using a standard methods as previously reported by our laboratory (Valujskikh et al., 2002; Raedler et al., 2011; Chun et al., 2017). Vascularized heterotopic cardiac grafts obtained from 8- to 10-week-old BALB/c donors were placed in the recipients' abdomen. Heart graft function was checked every day by palpation. Rejection was defined as the day on which a palpable heartbeat was absent.

In selected experiments, recipient mice were sensitized by allogeneic spleen cell intraperitoneal injections (20×10^6 cells). After 2 weeks, animals with DSA MFI >1,500 at 1:50 dilution received heart transplant.

Recipients were treated with EPO (Retacrit™ Epoetin Alfa-epbx recombinant, Pfizer, 10,000 Units/mL) or PBS with intraperitoneal injections daily, starting on the day of surgery for 10, 12 or 14 days. After 2 weeks, animals were euthanized by carbon dioxide (CO₂)-induced asphyxia and cervical dislocation. Splenic cells were collected to measure T_{FH}, T_{FR}, class switched, and Germinal Center B cells. Serum samples were collected to perform DSA analysis.

3.7 Isolation of murine serum

Blood samples were collected from mice via facial vein bleeds or by cardiac puncture. Blood was collected in BD Microtainer® containing an inert gel to allow to separate the serum and the blood clot. The samples were centrifuged 10 minutes, at 12000 rpm, at room temperature.

3.8 Isolation of murine splenocytes and thymocytes

Once harvested, spleens or thymes were smashed with a plunger, filter through a 40 µm strainer, and wash extensively with PBS. Cells were spun down (1,300 rpm, 5 min at room temperature). The supernatant were dumped off and ACK Lysing Buffer (Life Technologies) were added. The cells were incubate at room temperature for 5 minutes. PBS was added to stop the lysis reaction. Cells were anew spun down, resuspended in PBS, and counted.

3.9 NP-Enzyme-Linked Immunosorbent Assay (ELISA)

ELISA were performed on serum samples to assess high affinity and total anti-NP antibodies, using BSA with different degrees of NP conjugation. We used a standard approach as published (Le et al., 2008).

Plates were coated overnight at 4°C with 50 µg/ml NP(27)-BSA (Biosearch Technologies) to measures total antibody or 50 µg/ml NP(2)-BSA (Biosearch Technologies) to measures high affinity antibody. Plates were blocked with PBS and 5% skim milk, and incubated 2 hours at room temperature, out of light.

Anti-TNP (clone 107.3) (BD Pharmingen) was used as standard to quantify the titers. Serum samples (dilution from 1:10³ to 1:10⁸) and standard were diluted in Diluent Buffer (PBS/0.1% Tween /1% BSA). Plates were incubated overnight at 4°C, out of light.

Bound antibodies were detected using anti-mouse IgG-HRP (Southern Biotech). IgG-HRP were diluted (1:2000) in Diluent Buffer and added to each wells. Plates were then incubated 2 hours at room temperature, out of light.

TMB solution was added and plates were incubated 5-10 minutes at room temperature, out of light. Stop solution (H₂SO₄ or HCl 1M) was added. The absorbance was read at 450 nm.

3.10 Alloantibody detection

Serum samples from recipient mice were serially diluted in PBS. As target cells, thymocytes from donor mice were isolated and plated (200,000 cells per well). Serum samples were added to the thymocytes and the cells were incubated one hour at 4°C. Following a wash step with PBS 1% albumin, the cells were incubated with fluorescein isothiocyanate (FITC)-conjugated rat anti-mouse IgG (eBioscience) for one hour at 4°C. The bound antibody was detected and quantified by flow cytometry.

3.11 Flow cytometry

We used standard approaches for surface and intracellular staining (Purroy et al., 2017). For both, extracellular and intracellular, we stained 1×10^6 cells for each sample. PBS was used to wash the cells. Appropriate dilutions of antibodies were prepared and combined to obtain dedicate antibody cocktails. For every staining, cells were incubate for 30 minutes, at 4°C, and out of light. Before acquisition, cells were washed and resuspended in PBS.

3.11.1 Extracellular staining

For surface staining, we used the following antibodies:

APC-anti-CD4 - clone RM4-5 (Biolegend)

BV510-anti-CD4 - clone GK1.5 (BD Pharmingen)

APC-Cy7-anti-CD4 - clone GK1.5 (BioLegend)

PE-Cy7-anti-CD4 - clone RM4-5 (BD Pharmingen)

Biotinylated anti-CXCR5 (BD Pharmingen)

Pacific Blue streptavidin (Thermo Fisher Scientific)
PerCP-Cy5.5-anti-TCRb - clone H57-597 (Biolegend)
PE-anti-ICOS - clone 15F9 (BD Pharmingen)
PE-anti-ICOS - clone 7E.17G9 (BD Pharmingen)
PE-Cy7-anti-PD-1 - clone RMP1-30 (Biolegend)
PerCP-Cy5.5-anti-B220 - clone RA 3-6 B2 (BD Pharmingen)
Pacific Blue-anti-B220 - clone RA 3-6 B2 (BD Pharmingen)
APC-Cy7-anti-IgD - clone 11-26c (Thermo Fisher Scientific)
PE-Cy7-anti-IgM - clone eB121-15F9 (Thermo Fisher Scientific)
APC and PE-anti-FAS - clone Jo2 (BD Pharmingen)
FITC-anti-GL7 - clone Ly-77 (BD Pharmingen)
FITC-anti-GL7 - clone GL7 (BD Pharmingen)
PE-Cy7-anti-CD38 (clone 90) (eBioscience)
PE-Cy7-anti-CD73 (clone TY/11.8) (Biolegend)
PE-anti-CD45.1 (clone A20) (BD Pharmingen)
TNP-BSA (Bovine Serum Albumin)-Fluorescein (Biosearch Technologies)
Fixable Viability Dye eFluor™ 506 (Thermo Fisher Scientific)
Fixable Viability Dye eFluor™ 780 (Thermo Fisher Scientific)

To preserve the cells, we performed a cells fixation. Cells were washed in PBS, resuspended in Paraformaldehyde 4% solution (Elettron Microscopy Sciences), and incubated 10 minutes at 37°C, out of light. PBS was added to stop the reaction, and the cells were newly washed and resuspended in PBS before to be acquired.

3.11.2 Intracellular staining

For the intracellular staining we perform the permeabilization and fixation using FOXP3 Transcription Factor Staining Buffer Set (Invitrogen), according with the manufacturer's instructions.

We used the following antibodies:

FITC-anti-FOXP3 - clone FJK-16S (Thermo Fisher Scientific)
PerCP-Cy5.5-anti-IgG - clone Poly45053 (Biolegend)

PE-anti-IL17A - clone eBio17B7 (eBioscience)
PE-Cy7-anti-IL4 - clone 11B11 (BD Pharmigen)
FITC-anti-INF γ (BD Pharmigen)
IL-21R subunit/Fc chimera (R&D Systems)
AffiniPure F(ab')₂ Fragment Goat Anti- Human IgG, Fc γ (Jackson Immunoresearch).

3.11.3 Acquisition

Cytofluorimetric acquisitions were performed on a three-laser Canto II flow cytometer (BD Biosciences). For each sample 10,000 to 100,000 events were acquired and analyzed using FlowJo (<https://www.flowjo.com>) software.

3.12 T_{FH} differentiation assay

Murine anti-CD3 and anti-CD28 antibodies (8 μ g/ml each, clones 145-2c11 and 37.51 respectively, Invitrogen) were resuspended in PBS and plated to coat 48-well plates. The coating was performed overnight at 4° C. The following day, wild type B6 mice were sacrificed and splenic cells were collected. CD4⁺ cells were enriched by magnetic negative selection with EasySep™ Mouse CD4⁺ Cell Isolation Kit (STEMCELL Technologies Inc.), according with the manufacturer's instructions.

Enriched cells were resuspended in supplemented RPMI [RPMI 1640 1X (Corning), 10% Fetal Bovine Serum (Corning), 100 IU/ml Penicillin-Streptomycin, 2mM L-glutamine, β -mercaptoethanol (50 μ M) (Thermo Fischer Scientific)], and plated (125,000 cells/well) in pre-coated plates. Murine IL-6 (30 ng/ml, PeproTech), anti-TGF- β (20 μ g/ml, clone 11D.11.15.8 BioXCell), anti-IFN- γ (10 μ g/ml, clone XMG1.2, BioXCell), and anti-IL-4 (10 μ g/ml, clone 11B11, BioXCell) were added.

Cells were treated with EPO (1,000 UI/ml) (Retacrit™ Epoetin Alfa-epbx recombinant, Pfizer, 10,000 Units/mL) or PBS, and cultured at 37 °C in a 5% CO₂ humidified atmosphere for 5 days.

The same experiment was performed adding STAT5 Inhibitor (CAS 285986-31-4, Millipore Sigma) at different concentrations (50 μ M, 250 μ M, 500 μ M).

For intracellular cytokine staining, cells were stimulated for 4 hours with Golgiplug (1 µg/ml; BD Biosciences). PMA (50 ng/ml; MilliporeSigma) and Ionomycin (500 ng/ml; MilliporeSigma) were added to control wells.

We performed a surface staining (CD4⁺, viable cells), and then cells were fixed, permeabilized, and stained for intracellular cytokines (IL-4, IL-17, INF γ , IL-21). For IL-21, IL-21R subunit/Fc chimera (R&D Systems) was used as primary antibody, and AffiniPure F(ab')₂ Fragment Goat Anti- Human IgG, Fc γ (Jackson ImmunoResearch) as secondary antibody. Analysis was performed on a FACSCanto II flow cytometer (BD Biosciences).

3.13 Suppression assays

Splenic cells were collected from BALB/c mice. B6 wild type or EPOR^{fl/fl} CD4-Cre^{POS/NEG} animals were immunized with BALB/c splenocytes, by allogeneic spleen cell intraperitoneal injections (20×10^6 cells). Seven days after immunization, B6 or EPOR^{fl/fl} CD4-Cre^{POS/NEG} mice were sacrificed and CD4⁺ cells were enriched from total splenocytes by magnetic negative selection with EasySepTM Mouse CD4⁺ Cell Isolation Kit (STEMCELL Technologies Inc.), according with the manufacturer's instructions. T_{FH} and T_{FR} cell subsets (CD4⁺TCR β ⁺ICOS⁺CXCR5⁺PD-1⁺) were sorted (see par. 3.14 Cell Sorting). Splenic B cells from BALB/c mice were enriched by magnetic negative selection with EasySepTM Mouse B Cell Isolation Kit (STEMCELL Technologies Inc.), according with the manufacturer's instructions. Sorted pre-immunized B6 T_{FH} and T_{FR} (3×10^4 cells) and BALB/c enriched B cells (5×10^4 cells) were cultured in R10 medium [RPMI 1640 1X (Corning), 10% Fetal Bovine Serum (Corning), 100 IU/ml Penicillin-Streptomycin, 10 mM HEPES, 2mM L-glutamine, Sodium Pyruvate (100mM) (Gibco)] with 2 µg/ml anti-CD3 (clone 145-2C11, Thermo Fisher Scientific), 10 µg/ml anti-IgM (Jackson ImmunoResearch) and with vehicle (PBS) or EPO (1,000 UI/ml) (Retacrittm Epoetin Alfa-epbx recombinant, Pfizer, 10,000 Units/mL) for 2 days at 37°C, in a 5% CO₂ humidified atmosphere, in 96-well plates. Cells were collected for flow cytometric analyses.

Similarly, enriched CD4⁺ splenic cells were collected from pre-immunized [by allogeneic spleen cell intraperitoneal injections (20×10^6 cells)] B6.129(Cg)-FOXP3^{tm3(DTR/GFP)Ayr/J}.

This strain allowed us to sort CD4⁺TCRβ⁺ICOS⁺CXCR5⁺PD-1⁺ FOXP3-GFP positive (T_{FR}) and FOXP3-GFP negative (T_{FH}) cells separately. BALB/c enriched B cells (5×10⁴ cells) were differentially cultured with 3×10⁴ of T_{FR} or T_{FH} cells at the same conditions previously reported. Cells were collected for flow cytometric analyses.

3.14 Cell Sorting

CD4⁺ cells were enriched from total splenocytes by magnetic negative selection with EasySep™ Mouse CD4⁺ Cell Isolation Kit (STEMCELL Technologies Inc.), according with the manufacturer's instructions (See par. 3.13 Suppression assay). CD4⁺ enriched cells were stained for CD4, TCRβ, ICOS, CXCR5, and PD-1.

From B6 wild type or EPOR^{fl/fl} CD4-Cre^{POS/NEG} pre-immunized animals, CD4⁺TCRβ⁺ICOS⁺CXCR5⁺PD-1⁺ (T_{FR} and T_{FH}) cells were sorted on SH800Z Cell Sorter Sony Biotechnology Inc. (70-μm Sorting Chip) using optimal purity settings.

Using the same conditions, from pre-immunized B6.129(Cg)-FOXP3^{tm3(DTR/GFP)Ayr/J} animals, CD4⁺TCRβ⁺ICOS⁺CXCR5⁺PD-1⁺ FOXP3-GFP positive (T_{FR}) and FOXP3-GFP negative (T_{FH}) cells were sorted. Cells were collected in R10 medium [RPMI 1640 1X (Corning), 10% Fetal Bovine Serum (Corning), 100 IU/ml Penicillin-Streptomycin, 10 mM HEPES, 2mM L-glutamine, Sodium Pyruvate (100mM) (Gibco)].

3.15 Parent-to-F1 models

B6 splenocytes were CD8⁺ T cells depleted (Dynabeads Flow Comp Mouse CD8 kit, Invitrogen). Resultant B6 spleen cells containing 10 to 15 × 10⁶ CD4⁺ T cells were injected intravenously into non-irradiated (bxd) F1 recipients (BALB/c x B6). Flow cytometric analysis verified <1% CD8⁺ T cells with equal numbers of CD4⁺ T cell transfers between groups within an experiment.

F1 recipients were treated with EPO (Retacrit™ Epoetin Alfa-epbx recombinant, Pfizer, 10,000 Units/mL) or PBS with intraperitoneal injections daily. After 6 weeks, animals were euthanized by carbon dioxide (CO₂)-induced asphyxia and cervical dislocation. Splenic cells were collected to measure T_{FH}, Germinal Center B cells. Serum samples

were collected to quantify Anti-dsDNA autoantibodies, using an Autoimmune ELISA kit (Signosis, Inc) according with the manufacturer's instructions.

Analogous experiments were performed on B6xDBA F1 (H-2^{b/d}) recipients of DBA/2J (DBA) splenocytes (H-2^d) CD8⁺ T cells depleted, treated for 6 weeks with EPO or vehicle.

3.16 Renal histology

Mice were deeply anesthetized injecting a solution of sterile ketamine (200-300 mg/kg) and xylazine (20-30 mg/kg) in PBS and trans-cardially perfused with 4% paraformaldehyde fixate in PBS at a rate of 8-10cc. Kidneys were paraffin-embedded (10%) or frozen in Optimal Cutting Temperature compound (Tissue-Tek O.C.T., Sakura) after soaking overnight in 18% sucrose in PBS.

3.16.1 Light microscopy

Paraffin-embedded kidney sections (3 μ m) were stained with Periodic-Acid Schiff (PAS). Images were acquired at random for at least 20 glomeruli per section. Imaging brightfield was performed on the widefield microscope (Zeiss AxioImager Z2M).

3.16.2 Immunofluorescence

Cryosections (5- μ m thick) were washed three times with PBS for 5 minutes and then incubated with a blocking solution containing 5% bovine serum albumin for 30 minutes at room temperature. Cryosections were stained for 1 hour at room temperature for IgG (anti-mouse IgG antibody conjugated with Alexa Fluor 488, 1:500; Jackson ImmunoResearch) or C3b (anti-mouse goat FITC-conjugated C3b, 1:100; Cappel). Nuclei were counterstained with DAPI (Invitrogen). 20 glomeruli or more per section for each animal were randomly acquired using a fluorescence non-confocal laser scanning microscope (Zeiss AxioImager Z2M with ApoTome.2). IgG and C3b expression were

estimated by constructing a contour mask on the monochrome image. Software ImageJ (NIH) was used to quantify antibodies intensity.

3.17 Urinary albumin and creatinine measurement

Urine spot samples were collected from individual mice through gentle restrain and accrual of urine in a collection device. Urine creatinine was quantified using Creatinine Colorimetric Assay Kit (Cayman Chemical), according with the manufacturer's instructions. Urine albumin was determined using a commercial assay (Mouse Albumin ELISA Kit, Bethyl Laboratory Inc.), according with the manufacturer's instructions. Albuminuria was expressed as the ratio of urine albumin to creatinine.

3.18 Statistical Analyses

GraphPad Prism (version 8 for Windows, GraphPad Software, Inc.) was used to perform all statistical analyses. Group comparisons of paired data were analyzed by *t* tests. Wilcoxon test was employed for histological score comparisons. For multiple comparisons among treatment groups we used two-way repeated measures ANOVA test. *P* values < 0.05 were considered significant.

4. RESULTS AND DISCUSSION

4.1 EPO regulates T cell dependent antibody production

The first goal was to evaluate the role of EPO on the donor specific antibodies production. Murine models were used to perform T cell dependent immunization and allogeneic heart transplant, to test the effect of administering recombinant EPO on T cell dependent antibody formation.

Wild type B6 males mice were immunized with nitrophenol (NP), a hapten linked to keyhole limpet hemocyanin (KLH), a model antigen that promote a T-cell-dependent antibody response (Barrio et al., 2020). Starting from day 0 (day of transplant) to day 10, a group of these mice was treated daily with recombinant EPO, and another with Phosphate-buffered saline (PBS) as a vehicle control. Ten day after immunization, the animals were euthanized (Figure 8).

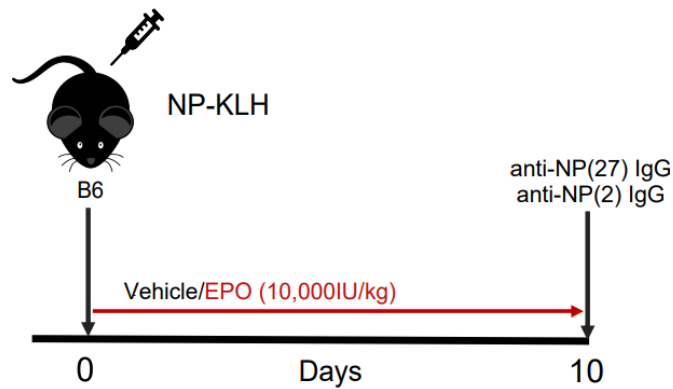


Figure 8. B6 mice were immunized with NP-KLH Hydroxy-3-nitrophenylacetyl-Keyhole Limpet Hemocyanin (NP-KLH) on day 0 and treated with EPO (10,000 IU/Kg,) or vehicle control by intraperitoneal injections starting from day 0 to day 10 when the animals were euthanized. Total and high affinity anti-NP antibodies were quantified.

On serum samples, we performed an NP-ELISA (Le et al., 2008) to detect total NP-reactive IgG [anti NP (27), Figure 9A], and, by limiting the quantity of NP on the ELISA plate, high affinity NP-reactive IgG [anti NP (2), Figure 9B].

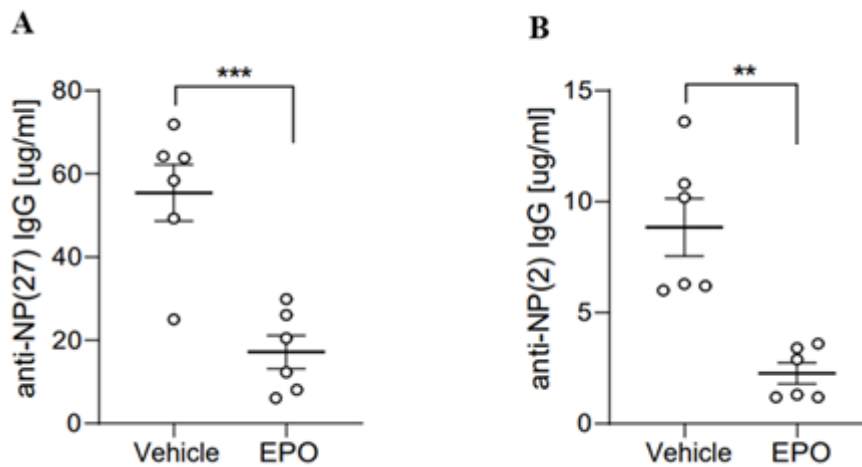


Figure 9. Sera were collected from B6 mice 10 days after immunization with NP-KLH and treatment with EPO (10,000 IU/Kg) or vehicle control by intraperitoneal injections starting from day 0. **(A)** Total and **(B)** high affinity anti-NP antibodies were quantified by ELISA using BSA with different degrees of NP conjugation. Data represent means \pm SE. Empty circles represent male animals. ** $P < 0.01$; *** $P < 0.001$.

Mice subjected to recombinant EPO administration reduced total and high affinity NP-reactive IgG by about 3-fold compared with the control group. High affinity IgG antibodies reactive to exogenous pathogens as well as pathogenic auto- and alloantibodies develop when activated B cells undergo isotype switch recombination and affinity maturation (Natkunam, 2007). Our assay may suggest that an EPO treatment could reduce these two events.

Mouse allogeneic heart transplantation was used to test whether EPO similarly affects a more potent polyclonal antibody response. We transplanted wild type B6 recipients (males and females) with MHC-disparate BALB/c heart allografts. From the day of transplant, and for fourteen days, we treated a group of animals with recombinant EPO, and another with PBS as a control. The fourteenth day, the mice were euthanized (Figure 10).

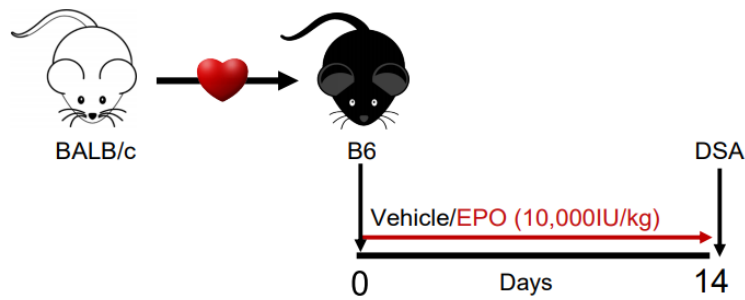


Figure 10. B6 recipients of an allogeneic heterotopic transplantation from BALB/c mice were treated with EPO (10,000 IU/kg) or vehicle control by intraperitoneal injection from the day of transplant up to day 14, when the animals were euthanized. After this time, Donor Specific Antibodies (DSA) levels were measured.

We performed flow cytometry analysis to quantify serum anti-class-I MHC alloantibodies namely Donor Specific Antibodies (DSA). A representative histograms of DSA IgG (Figure 11A) and the Mean Fluorescence Intensity (MFI) levels (Figure 11B), showed a reduction of DSA in sera from EPO-treated mice compared to the vehicle. These assays similarly showed that EPO treatment reduced the alloantibody titer by about 3-fold (Figure 11C), with significantly less IgG binding to the allogeneic target cells as all serum concentrations, the latter suggestive of reduced affinity maturation.

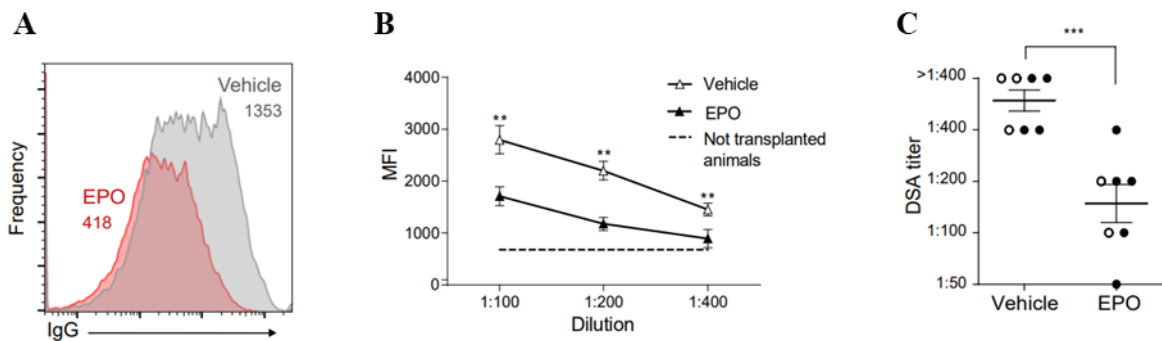


Figure 11. DSA levels were measured on serum samples by flow cytometry. Representative histograms of DSA IgG (A), MFI levels (B), and titers (C) in EPO- and vehicle treated mice. Data represent means \pm SE. Empty circles represent male animals, full circles females. ** $P < 0.01$; *** $P < 0.001$.

Although they not elucidate the mechanism, these first experiments indicate a clear EPO effect on the reduction of donor specific antibodies in both NP-KLH immunized and transplanted murine models.

4.2 EPO regulates Germinal Center (GC) responses

Germinal center is an essential site for antibody diversification and affinity maturation (Mesin et al., 2016).

To explain the effects of EPO on serum antibodies, we performed flow cytometry analysis to quantify splenic B220⁺Fas⁺GL7⁺ GC B cells and NP⁺ GC B cells on post-immunization day 10 in groups of EPO-treated and control animals immunized with NP-KLH (Figure 8).

In the group of mice subjected to EPO administration, we detected a significant reduction in percentages and absolute numbers of total Germinal Center (GC) B cells (Figure 12A-C), as well as we observed a decrease of NP-specific GC B cells (Figure 12D-F).

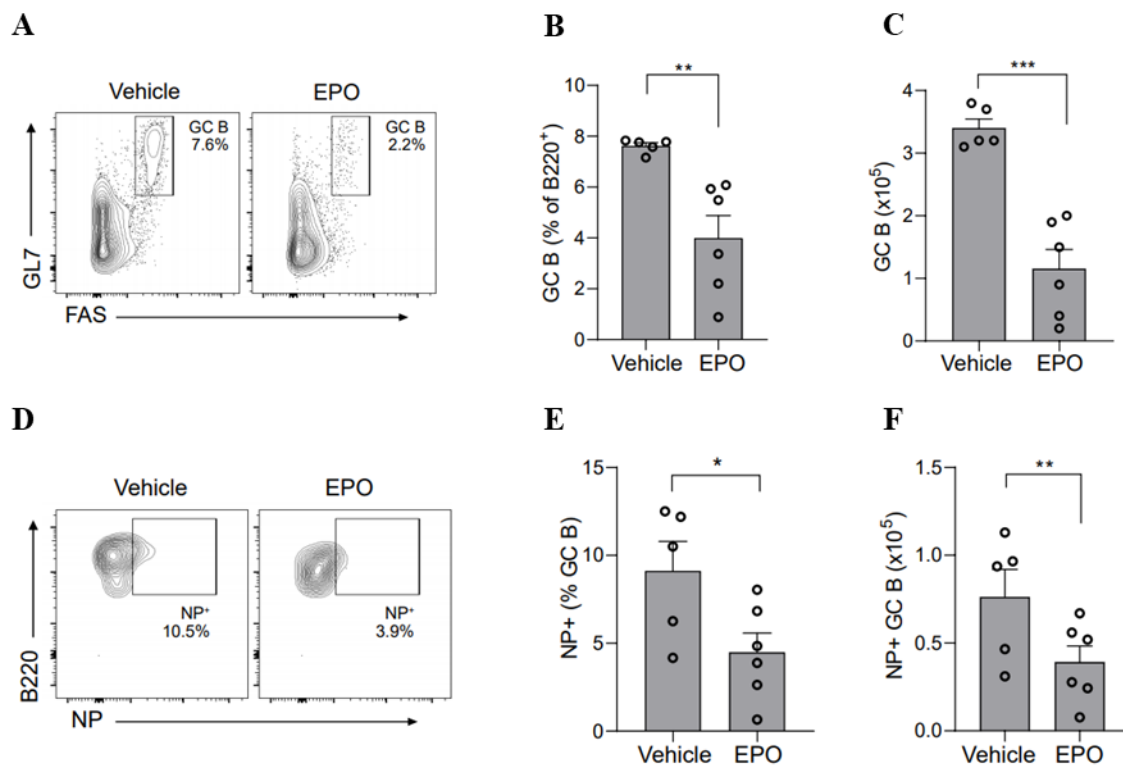


Figure 12. B6 mice were immunized with NP-KLH on day 0 and treated with EPO (10,000 IU/Kg) or vehicle control by intraperitoneal injection starting from day 0 to day 10 when the animals were euthanized. Representative plots depicting percentages of GC (A) and B220⁺ NP⁺ GC (D) B cells in the same mice. Quantified percentages (B, E) and total numbers (C, F) of B220⁺ Fas⁺ GL7⁺ GC (B, C) and B220⁺ NP⁺ GC (E, F) B cells. Data represent means \pm SE. Empty circles represent male animals. * $P < 0.05$; ** $P < 0.01$; *** $P < 0.001$.

Moreover we quantified B220⁺Fas⁺GL7⁺ GC B cells and B220⁺IgD⁺IgM⁻ Class Switched B cells in B6 recipients of allogeneic heterotopic transplantation (Figure 10).

Analogously, we observed a significant reduction in percentages and absolute number of GC B cells in the EPO-treated recipient group compared with the controls (Figure 13A-C). Likewise, Class Switched B cells were significantly fewer in percentage and absolute number after EPO administration (Figure 13D-F). These results indicate a clear effect of EPO on GC and Class Switched B cells in heterotopic murine model of heart transplantation.

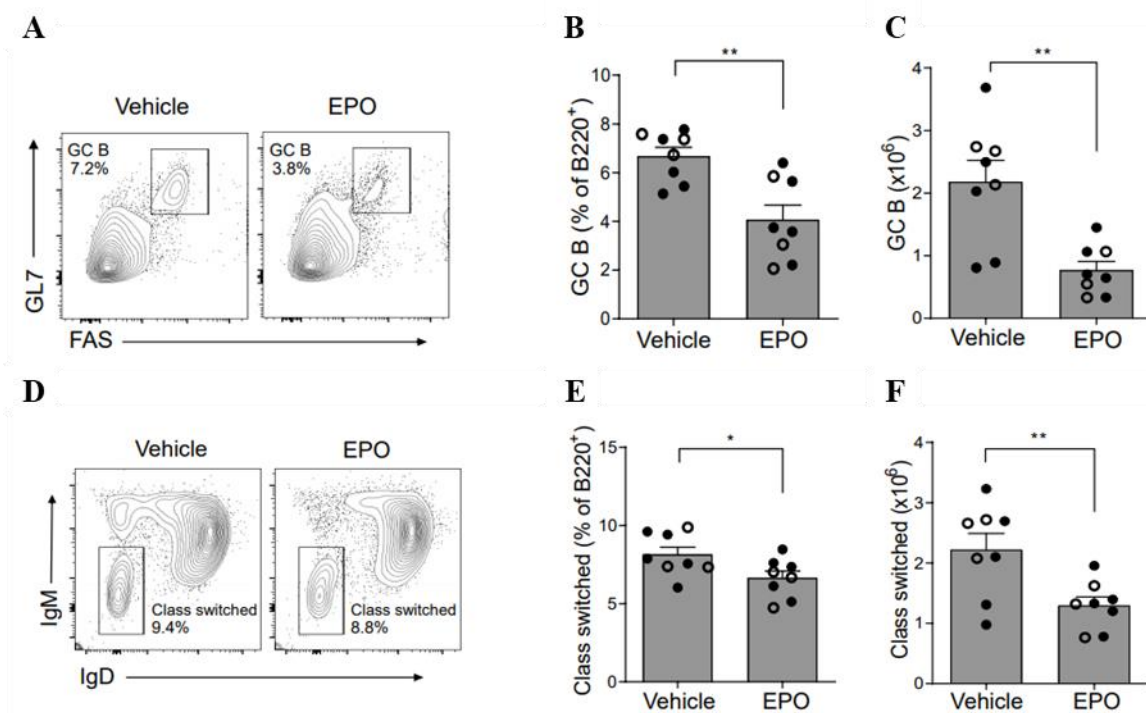


Figure 13. B6 recipients of an allogeneic heterotopic transplantation from BALB/c mice were treated with EPO (10,000 IU/kg) or vehicle control by intraperitoneal injection from the day of transplant up to day 14 post-transplant, when the animals were euthanized. Representative plots depicting percentages of B220⁺Fas⁺GL7⁺ Germinal Center (GC) (A) and B220⁺IgM⁻IgD⁺ class-switched (D) B cells in the same mice. Quantified percentages (B, E) and total numbers (C, F) of GC (B, C) and Class Switched (E, F) B cells. Data represent means \pm SE. Empty circles represent male animals, full circles females. * $P < 0.05$; ** $P < 0.01$.

Isotype switch recombination and affinity maturation are T cell dependent processes. More precisely, two T cells subsets, T_{FH} and T_{FR}, are involved in this essential B cells development (Aloulou and Fazilleau, 2019).

In an effort to delineate the role of these two cells subsets, by flow cytometry, we quantified splenic CD4⁺CXCR5⁺PD1⁺FOXP3⁻ T_{FH} and CD4⁺CXCR5⁺PD1⁺FOXP3⁺ T_{FR} cells in the same two groups of transplanted animals (with or without EPO administration) (Figure 10).

A significantly lower percentages and absolute numbers of T_{FH} were detected in EPO-treated mice (Figure 14A-C). At the same time, our analyses showed significant increases in percentages and absolute numbers of T_{FR} in the EPO-treated animals (Figure 14A, D, E). As result, in this group of mice the T_{FR}/T_{FH} ratios were higher than the control animals (Figure 14F).

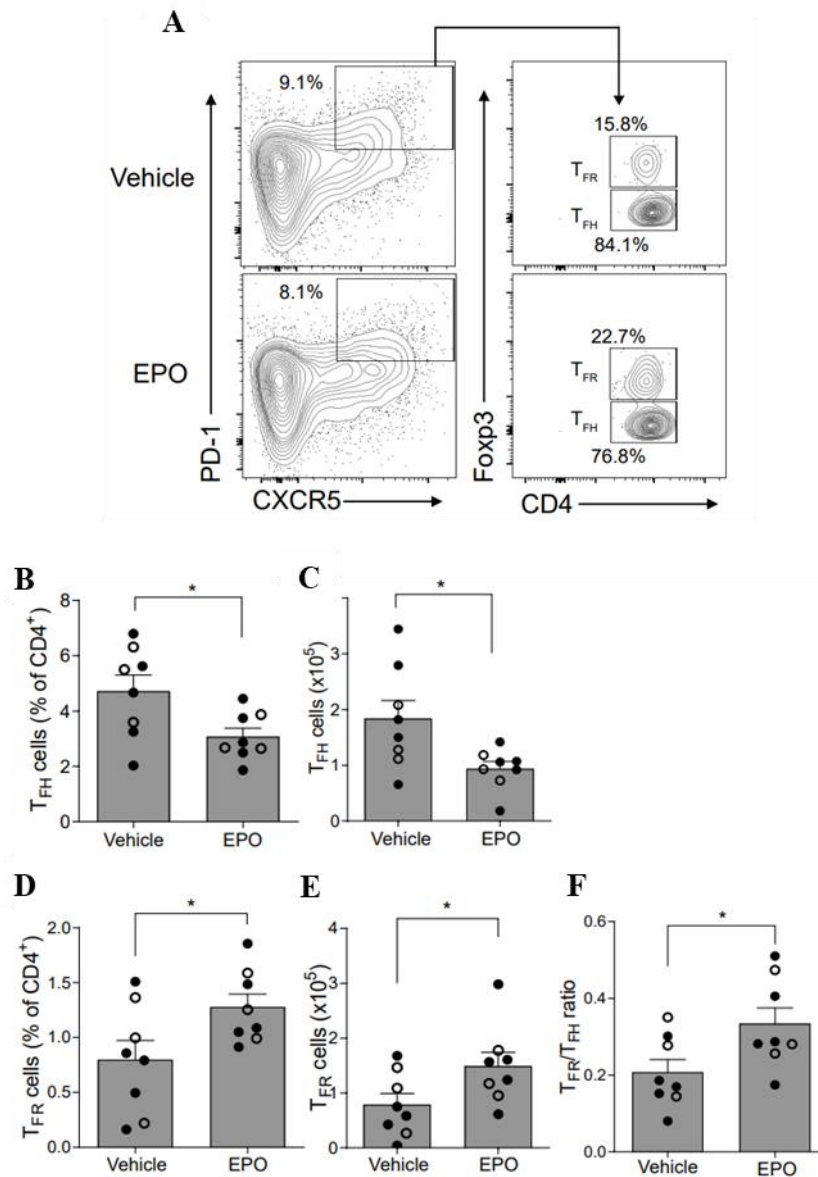


Figure 14. B6 recipients of an allogeneic heterotopic transplantation from BALB/c mice were treated with EPO (10,000 IU/kg) or vehicle control by intraperitoneal injection from the day of transplant up to day 14 post-transplant, when the animals were euthanized. Representative plots depicting percentages of CD4+PD1+CXCR5+FOXP3- T_{FH} and CD4+PD1+CXCR5+FOXP3+ T_{FR} in mice treated with EPO or vehicle control (A). Quantified percentages (B, D) and absolute numbers (C, E) of T_{FH} (B, C), T_{FR} (D, E), and T_{FH}/T_{FR} ratios (F). Data represent means \pm SE. Empty circles represent male animals, full circles females. * $P < 0.05$.

Beside the DSA reduction, our data showed that in recipient mice, EPO administration led to a reduction of GC, Class Switched B cells, but also the T_{FH} and T_{FR} amounts were altered. This suggest that EPO could act through either B or T cells to inhibit the DSA formation.

4.3 EPO administration has no effect on T-independent antibody responses

To test whether EPO inhibits T cell-independent antibody production we performed *in vitro* and *in vivo* assays. In the first case, we enriched B cells from total splenocytes of B6 wild type. Then B cells were stimulated with Lipopolysaccharides (LPS), the best-studied T-independent antigen (Parekh et al., 2003), at different concentrations and cultured with an EPO treatment or vehicle control. Cells were collected for flow cytometric analyses. We observed that LPS increased the IgD⁺ B cells fraction in a dose dependent manner but that EPO had no effect (Figure 15A). As well as, LPS stimulation augmented the percentage of viable B cells, but with no difference with or without EPO (Figure 15B).

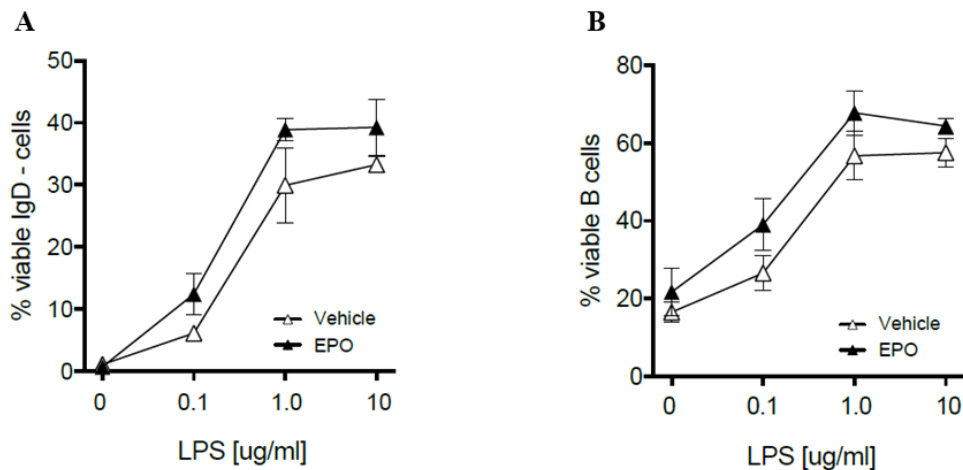


Figure 15. (A, B) B6 enriched splenic B cells were stimulated with LPS (0.1, 1.0, or 10 µg/ml) and incubated for 48 hours at 37°C with EPO (1,000 IU/ml) or vehicle control. Quantified percentage of IgD⁺ B cells (A) and total viable B cells (B). Data represent means ± SE.

In further verification of this notion, we immunized wild type B6 mice (males and females) with 2,4,6-trinitrophenyl (TNP) hapten conjugated to aminoethyl-carboxymethyl-FICOLL (AECM-FICOLL), a high molecular weight polysaccharide that promotes T-independent antibody production (Brodeur and Wortis, 1980). We treated half of them with recombinant EPO, and the other half with saline control (Figure 16).

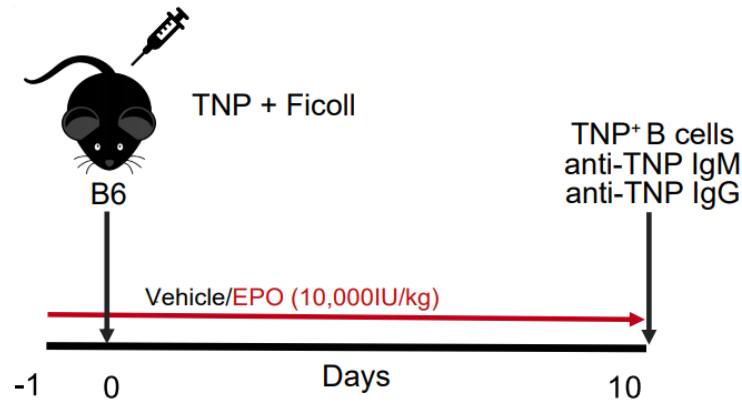


Figure 16. B6 mice were immunized with TNP-AECM-FICOLL (day 0) and treated with EPO (10,000 IU/kg) or vehicle control by peritoneal injection from day -1 to day 10. At day 10, we euthanized the mice to measure TNP-specific B cells and anti-TNP IgM and IgG.

Cytofluorimetric analyses on day 10 post TNP-FICOLL immunization showed no differences in TNP-specific B cells percentages between EPO-treated and control mice (Figure 17A, B), nor did we observe an effect of EPO in serum TNP-reactive IgM or IgG compared with the control group (Figure 17C, D). All together the *in vitro* and *in vivo* data support the conclusion that EPO does not directly inhibit B cells in the absence of T cells.

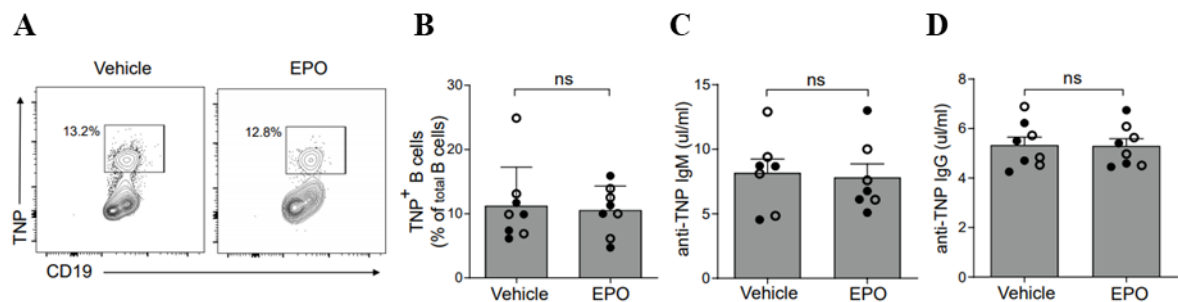


Figure 17. Representative plots (A) and data quantification (B) for TNP⁺CD19⁺ B cells. Anti-TNP IgM (C) and IgG (D) in sera collected from the same mice at sacrifice. Data represent means \pm SE. Empty circles represent male animals, full circles represent females. ns; not significant.

4.4 EPO has no direct inhibitory effect on B cells

To formally prove that EPO inhibitory effects on germinal cell formation *in vivo* are independent from a direct EPO effect on B cells, we generated EPOR^{fl/fl} CD19-Cre^{POS}

mice (in B6 background), selectively lacking EPOR expression on CD19⁺ B cells. We immunized B6 EPOR^{fl/fl}CD19-Cre^{NEG} and Cre^{POS} mice with sheep red blood cells (SRBC), a potent polyclonal T cell dependent stimulus (Ladics, 2018). We selected both females and males animals. Since the day before the immunization, and for twelve days after, we treated B6 EPOR^{fl/fl}CD19-Cre^{NEG} and Cre^{POS} mice with EPO or vehicle control. A second immunization with SRBC was repeated at day 6. Twelve days after the first immunization, the animals were euthanized, and we analyzed T and B cell responses by flow cytometry (Figure 18).

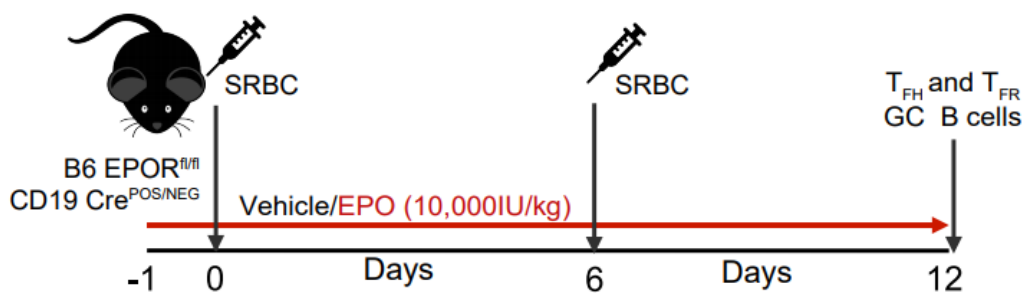


Figure 18. B6 EPOR^{fl/fl} CD19-Cre^{POS} and CD19-Cre^{NEG} mice were immunized with sheep red blood cells (SRBC) on day 0 and 6 and treated with EPO (10,000 IU/kg) or vehicle control by peritoneal injection starting from day -1 to day 12. At day 12, we euthanized the mice to measure GC B cells, T_{FH}, and T_{FR} cells.

As showed in figure 19, we found that, compared to vehicle treated controls, percentage of splenic GC B (Figure 19A-B), and T_{FH} cells (Figure 20A, B) were reduced in both CD19-Cre^{POS} and Cre^{NEG} mice treated with EPO. As well as these mice showed a significant increase in the T_{FR} percentage (Figure 20C). As result, the EPO groups showed a higher T_{FR}/T_{FH} ratios than the control animals (Figure 20D).

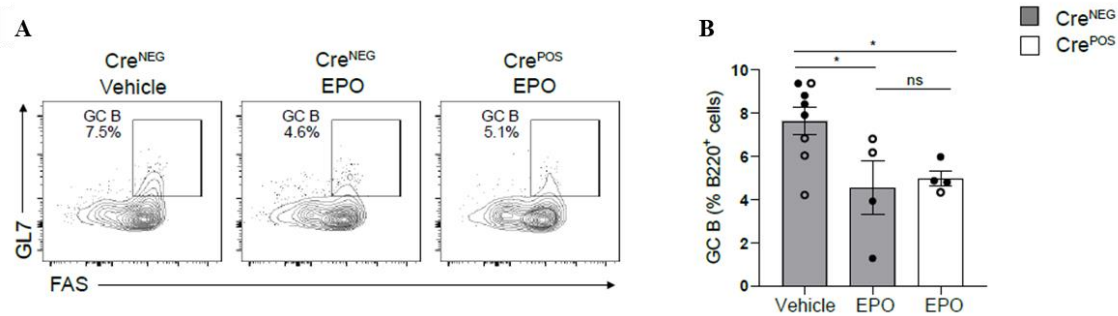


Figure 19. B6 EPOR^{fl/fl} CD19-Cre^{POS} and CD19-Cre^{NEG} mice were immunized with sheep red blood cells (SRBC) on day 0 and 6 and treated with EPO (10,000 IU/kg) or vehicle control by peritoneal injection starting from day -1 to day 12. At day 12. Representative plots (A) and data quantification for GC B cells (B). Data represent means ± SE. Empty circles represent male animals, full circles represent females. **P* < 0.05; ns; not significant.

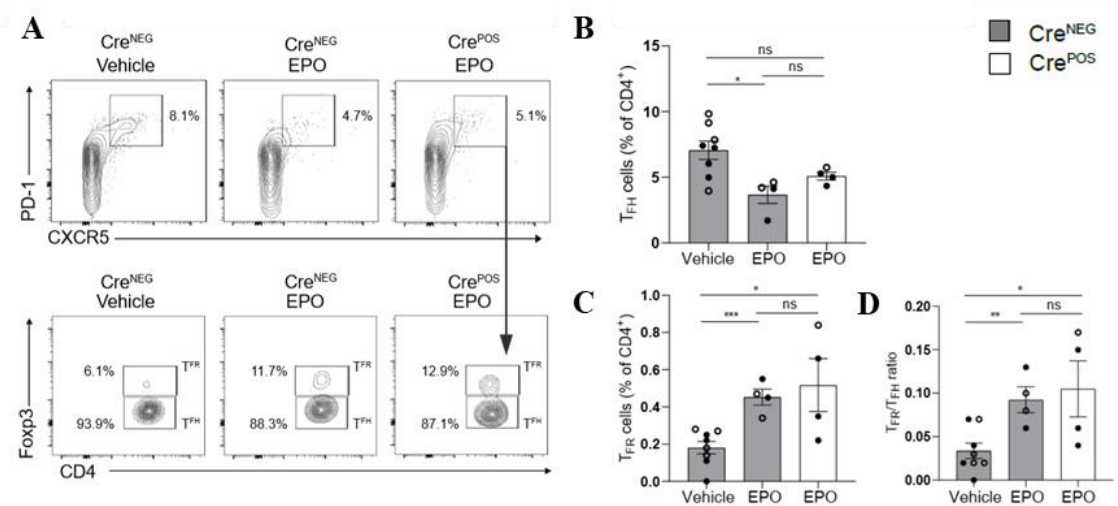


Figure 20. B6 EPOR^{fl/fl} CD19-Cre^{POS} and CD19-Cre^{NEG} mice were immunized with sheep red blood cells (SRBC) on day 0 and 6 and treated with EPO (10,000 IU/kg) or vehicle control by peritoneal injection starting from day -1 to day 12. Representative plots (A) and data quantification for CD4⁺PD1⁺CXCR5⁺FOXP3⁻ T_{FH} (B), CD4⁺PD1⁺CXCR5⁺FOXP3⁺ T_{FR} (C), and T_{FH}/T_{FR} ratio (D). Data represent means ± SE. Empty circles represent male animals, full circles represent females. **P* < 0.05; ***P* < 0.01; ****P* < 0.001; ns; not significant.

Coherently with the previous data, this experiment allowed us to provide a further *in vivo* evidence that the observed inhibitory effects on B cells are independent from a direct effect of EPO on B cells.

4.5 EPO inhibits T_{FH} through T cell-expressed EPOR *in vivo*

As mentioned before, isotype switch recombination and affinity maturation are T cell dependent processes (Aloulou and Fazilleau, 2019). With the previous experiments, we excluded that EPO acts on the direct inhibition of B cells. Our observations that EPO inhibits T dependent but not T-independent antibody formation and reduces GC B cell and T_{FH} frequencies, raised the hypothesis that EPO limits antibody formation via preventing T_{FH} differentiation/expansion.

To verify this, we employed conditional EPOR knockout mice (EPOR^{fl/fl}) crossed to a CD4-Cre transgenic to produce mice that lack EPOR specifically on all T cells (heretofore referred to as B6 EPOR^{fl/fl}CD4Cre^{POS} or B6 EPOR^{fl/fl}CD4Cre^{NEG}), previously verified to lack functional EPOR on their T cells (Donadei et al., 2019).

We immunized B6 EPOR^{fl/fl}CD4Cre^{POS} and control B6 EPOR^{fl/fl}CD4Cre^{NEG} mice with SRBC, as T dependent cells stimulus. Each group was composed of both females and males. B6 EPOR^{fl/fl}CD4Cre^{POS} and control B6 EPOR^{fl/fl}CD4Cre^{NEG} mice were split in two group and treated with EPO or saline as control (Figure 21).

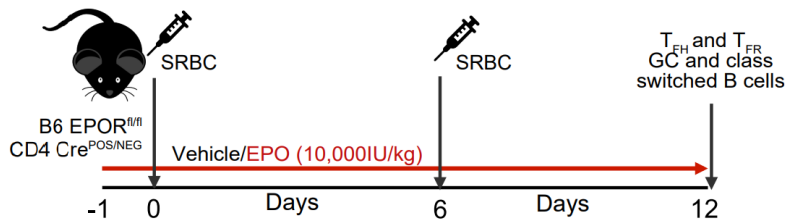


Figure 21. B6 EPOR^{fl/fl} CD4-Cre^{POS} and CD4-Cre^{NEG} mice were immunized with sheep red blood cells (SRBC) on day 0 and 6 and treated with EPO (10,000 IU/kg) or vehicle control by peritoneal injection starting from day -1 to day 12. At day 12, we euthanized the mice to measure T_{FH}, T_{FR}, GC, and Class Switched B cells.

Twelve days after immunization, we analyzed T and B cell responses by flow cytometry. As expected, in B6 EPOR^{fl/fl}CD4Cre^{NEG} control mice, EPO contributed to significantly reduce percentage and absolute numbers of Germinal Center (Figure 22A-C) and Class Switched B cells (Figure 22D-E).

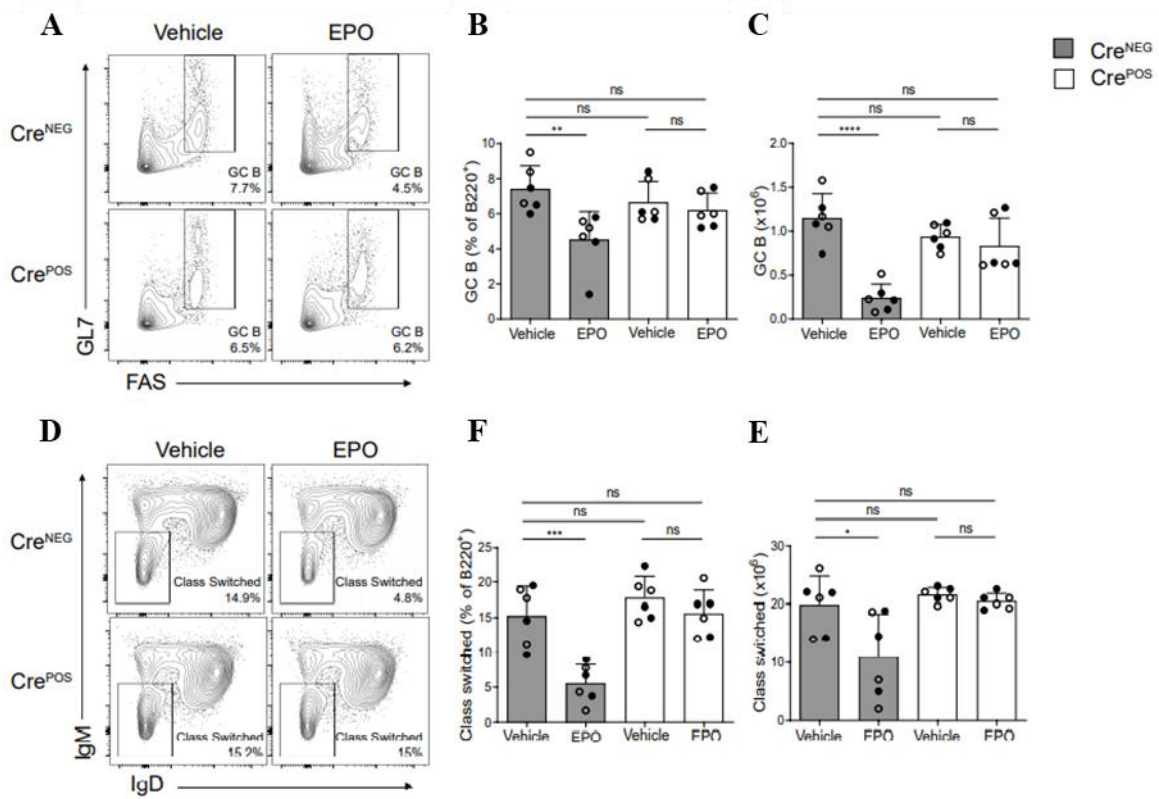


Figure 22. B6 EPOR^{fl/fl} CD4-Cre^{POS} and CD4-Cre^{NEG} mice were immunized with sheep red blood cells (SRBC) on day 0 and 6 and treated with EPO (10,000 IU/kg) or vehicle control by peritoneal injection starting from day -1 to day 12. At day 12. Representative plots (**A**, **D**) and data quantification for GC (**B**, **C**) and Class Switched (**E**, **F**) B cells. Data represent means \pm SE. Empty circles represent male animals, full circles represent females. * $P < 0.05$; ** $P < 0.01$; *** $P < 0.001$; **** $P < 0.0001$; ns; not significant.

Moreover, in EPOR^{fl/fl}CD4Cre^{NEG} control mice we founded a reduction in percentage and absolute number of T_{FH} after treatment with EPO (Figure 23A-C). As well as we saw an increase of T_{FR} cells after EPO administration (Figure 23A, D, E), and the ratio T_{FR}/T_{FH} was higher in this group of mice, although the difference was not significant (Figure 23F).

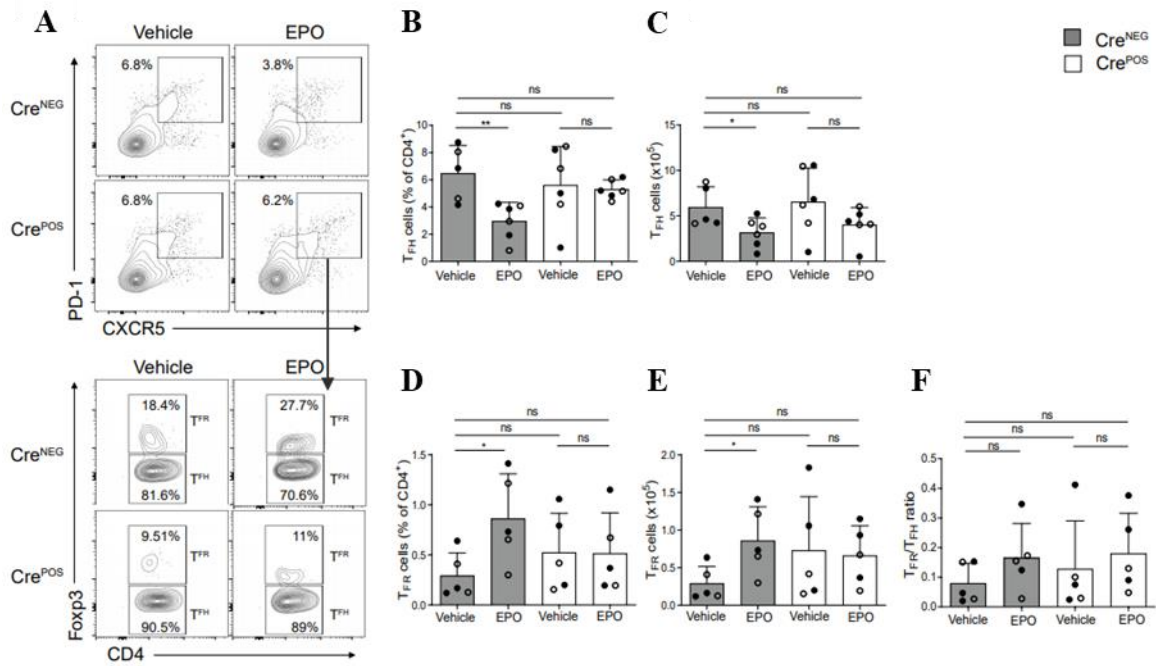


Figure 23. B6 EPOR^{fl/fl} CD4-Cre^{POS} and CD4-Cre^{NEG} mice were immunized with sheep red blood cells (SRBC) on day 0 and 6 and treated with EPO (10,000 IU/kg) or vehicle control by peritoneal injection starting from day -1 to day 12. Representative plots (A) and data quantification for CD4⁺PD1⁺CXCR5⁺FOXP3⁻ T_{FH} (B, C), CD4⁺PD1⁺CXCR5⁺FOXP3⁺ T_{FR} (D, E), and T_{FR}/T_{FH} ratio (F). Data represent means ± SE. Empty circles represent male animals, full circles represent females. **P* < 0.05; ***P* < 0.01; ns; not significant.

However, these assays showed that the absence of T cell-expressed EPOR fully prevented EPO’s inhibitory effects on GC B cells, Class Switched B cells (Figure 22) and T_{FH} (figure 23A-C), and limited the EPO-induced increase in T_{FR} compared to controls (Figure 23A, D, E). Therefore, also the T_{FR}/T_{FH} ratio was more similar among the treated and untreated B6 EPOR^{fl/fl}CD4Cre^{POS} mice (Figure 23F). All together, these results suggest that EPO acts through T cells, and the presence of EPO receptor is required to allow the inhibition of T_{FH}, GC and Class Switched B cells.

To further investigate this mechanism, we performed the same assays in B6 EPOR^{fl/fl}CD4Cre^{POS} and control B6 EPOR^{fl/fl}CD4Cre^{NEG} recipients of allogeneic heart transplant from BALB/c mice. Each group was composed of both females and males. We treated half mice for each group with EPO and the others with saline as control for fourteen days after transplant; then the mice were euthanized. We measure the DSA levels, and we quantified T_{FH} and T_{FR}, GC B cells and Class Switched B cells (Figure 24).

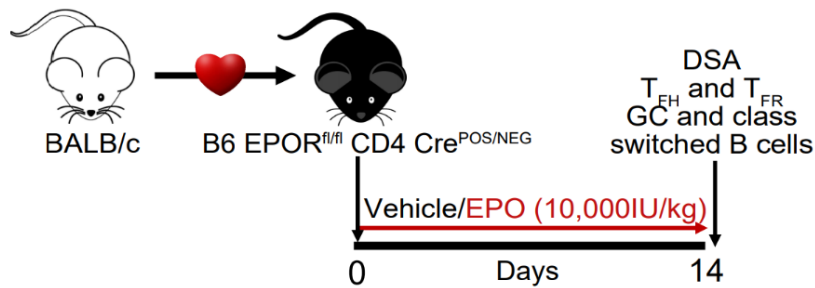


Figure 24. B6 EPOR^{fl/fl} CD4-Cre^{POS} and CD4-Cre^{NEG} recipients of an allogeneic heterotopic transplantation from BALB/c mice were treated with EPO (10,000 IU/kg) or vehicle control by intraperitoneal injection from the day of transplant up to day 14 post-transplant, when the animals were euthanized to measure T_{FH}, T_{FR}, GC, and Class Switched B cells.

B6 EPOR^{fl/fl}CD4Cre^{NEG} recipients injected with EPO showed DSA levels significantly lower compared with the vehicle-treated animals. However, consistently with the previous data, we did not see significant differences among the two group of B6 EPOR^{fl/fl}CD4Cre^{POS} (Figure 25).

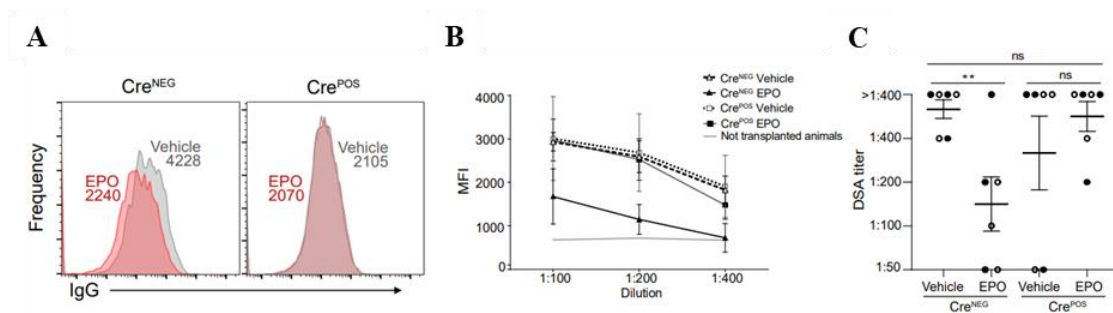


Figure 25. Representative histograms of DSA IgG (A) MFI levels (B), and titers (C) in EPO- and vehicle treated mice. Data represent means \pm SE. Empty circles represent male animals, full circles females. ** $P < 0.01$; ns; not significant.

Coherently with the preceding experiments, control B6 EPOR^{fl/fl}CD4Cre^{NEG} recipients recorded the same trend for GC B cells (Figure 26A-C) and Class Switched B cells (Figure 26D-E), with a reduction of percentages and absolute numbers in EPO-treated mice.

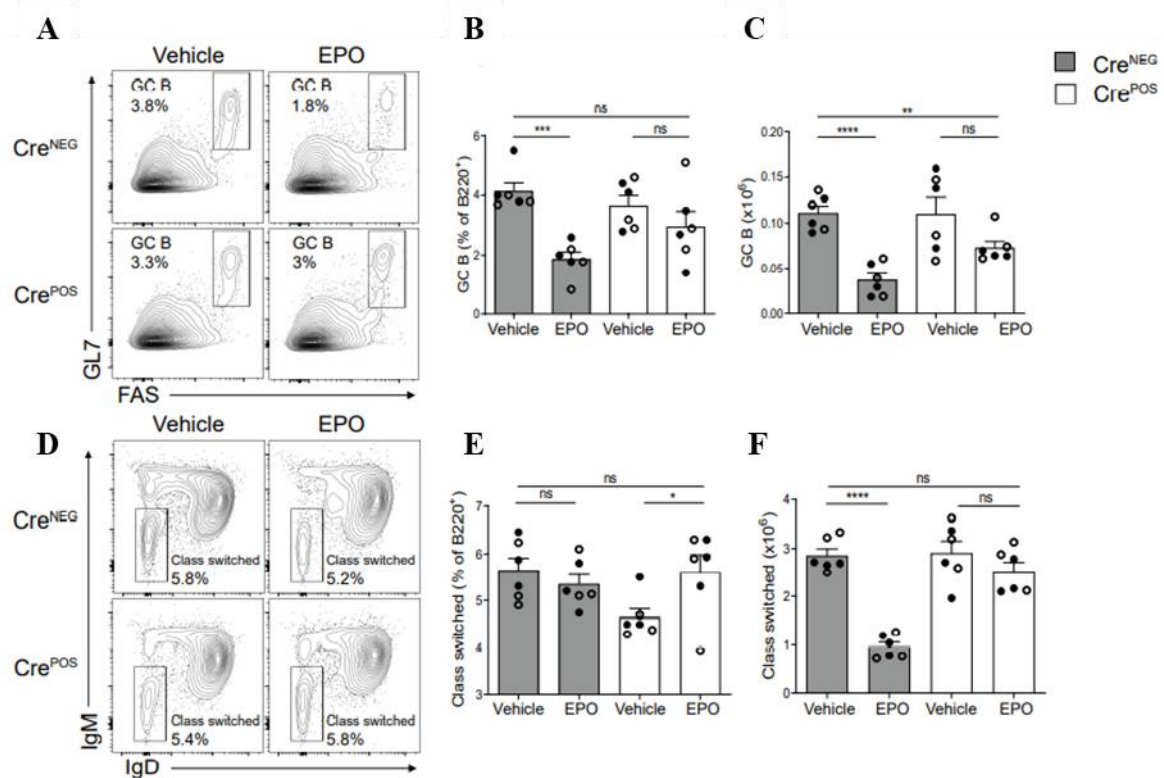


Figure 26. B6 EPOR^{fl/fl} CD4-Cre^{POS} and CD4-Cre^{NEG} recipients of an allogeneic heterotopic transplantation from BALB/c mice were treated with EPO (10,000 IU/kg) or vehicle control by intraperitoneal injection from the day of transplant up to day 14 post-transplant, when the animals were euthanized. Representative plots depicting percentages of B220⁺Fas⁺GL7⁺ Germinal Center (GC) (A) and B220⁺IgM⁻IgD⁻ class-switched (D) B cells in the same mice. Quantified percentages (B, E) and total numbers (C, F) of GC (B, C) and Class Switched (E, F) B cells. Data represent means ± SE. Empty circles represent male animals, full circles females. **P* < 0.05; ***P* < 0.01; ****P* < 0.001; *****P* < 0.0001; ns; not significant.

Likewise, after EPO administration in B6 EPOR^{fl/fl}CD4Cre^{NEG} recipients, we saw a reduction of T_{FH} (Figure 27A-C) and an increase of T_{FR} cells (Figure 27A, D, E), with a higher ratio T_{FR}/T_{FH} (Figure 27F) compared to vehicle-treated mice.

We similarly observed no effect of EPO on GC, and Class Switched B cells, T_{FH}, and T_{FR} cells in B6 EPOR^{fl/fl}CD4Cre^{POS} (Figure 26 and 27).

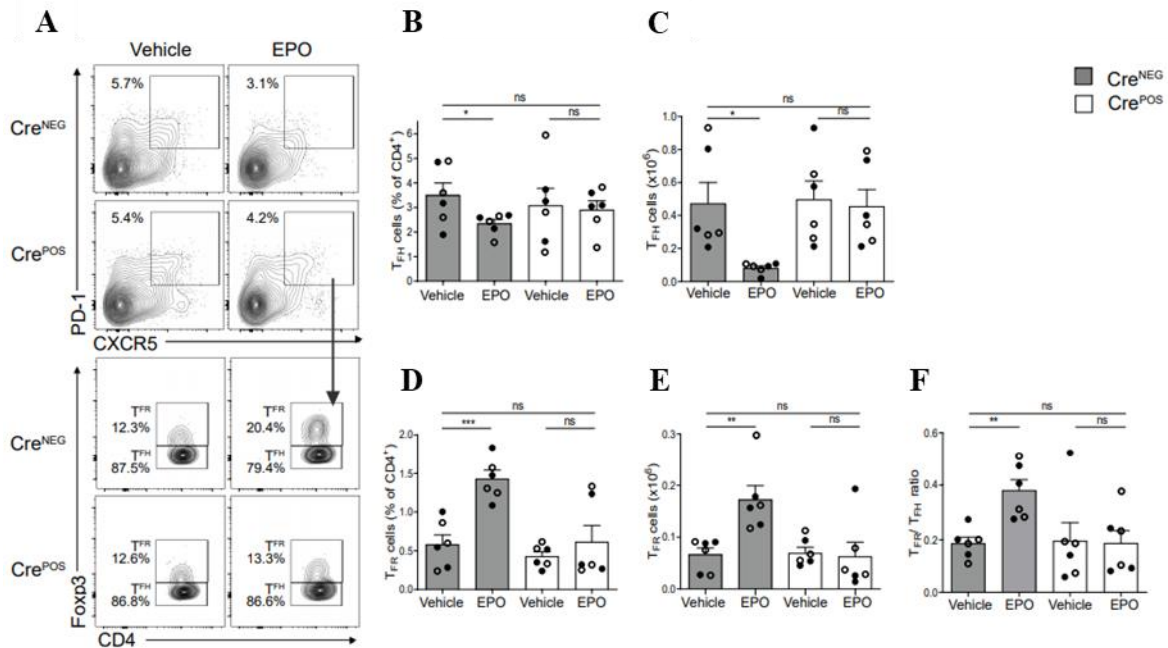


Figure 27. B6 EPOR^{fl/fl} CD4-Cre^{POS} and CD4-Cre^{NEG} recipients of an allogeneic heterotopic transplantation from BALB/c mice were treated with EPO (10,000 IU/kg) or vehicle control by intraperitoneal injection from the day of transplant up to day 14 post-transplant, when the animals were euthanized. Representative plots depicting percentages of CD4⁺PD1⁺CXCR5⁺FOXP3⁻ T_{FH} and CD4⁺PD1⁺CXCR5⁺FOXP3⁺ T_{FR} in mice treated with EPO or vehicle control (A). Quantified percentages (B, D) and absolute numbers (C, E) of T_{FH} (B, C), T_{FR} (D, E), and T_{FR}/T_{FR} ratios (F). Data represent means ± SE. Empty circles represent male animals, full circles females. **P* < 0.05; ***P* < 0.01; ****P* < 0.001; ns; not significant.

Even in allogeneic heart transplant murine model, these data confirm that EPO acts reducing T_{FH} cells, Germinal Center, and Class Switched B cells through a T cell-dependent mechanism that requires the presence of EPO receptor on CD4⁺ cells.

4.6 EPO directly prevents T_{FH} induction

In an attempt to more definitively delineate mechanistic links between EPO/EPOR and T_{FH} cells, we used an *in vitro* culture system, observing that T_{FH} cell differentiation is a multistep process involving IL-6 (in the absence of Th1, Th2, or Th17 cytokines) that is only partially replicated *in vitro* (Nurieva et al., 2008). IL-6 binds IL-6 receptor, and its

activation induces STAT3 phosphorylation. Phosphorylated STAT3 translocates into the nucleus and promotes Bcl-6 transcription, a master regulator of T_{FH}.

Our hypothesis is that EPO binds EPOR, and activates STAT5 through phosphorylation. Phosphorylated STAT5 downregulate Bcl-6 transcription, competing for the binding site of phosphorylated STAT3.

In our assay, splenic naïve CD4⁺ T cells were isolated from B6 wild type mice and induced to produce IL-21, hallmark of T_{FH}, upon stimulation with anti-CD3, anti-CD28, and via their T-cell receptor with IL-6, while simultaneously blocking TGF- β , IL-4, and IFN- γ . We induced T_{FH} in presence or absence of EPO, and five days post-incubation we quantified IL-21⁺ T_{FH} cells using cytofluorimetric analysis. As showed in figure 28, we found a significant reduction of IL-21⁺ T_{FH} cells in EPO treated mice, indicating that EPO inhibits T_{FH} induction.

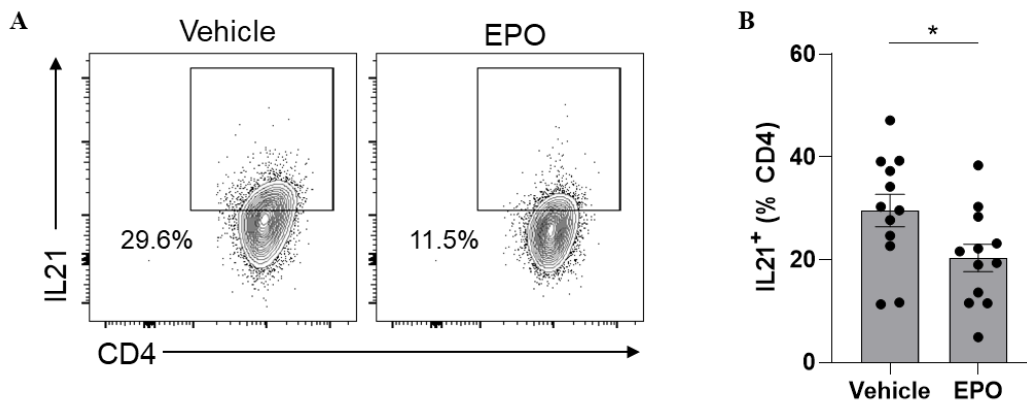


Figure 28. Representative plots (A) and quantified percentages (B) of CD4⁺ IL-21⁺ cells. Splenic CD4 naïve cells were enriched from wild type B6 animals, and plated in a pre-coated plate with anti-CD3 and anti-CD28 (8 μ g/ml). Murine IL-6 (30 ng/ml), anti-TGF- β (20 μ g/ml), anti-IFN- γ (10 μ g/ml), and anti-IL-4 (10 μ g/ml) were added. Cells were incubated at 37°C for five days in presence of EPO (1,000 IU/ml) or vehicle. Dots represent the number of replicate. Data represent means \pm SE. * P < 0.05.

To test the hypothesis that EPO-EPOR induced T_{FH} inhibition is mediated by STAT5 that inhibits Bcl-6 gene transcription, Cravedi's group previously showed that EPO promotes STAT5 phosphorylation (Figure 29, data not published and previously generated). Next, they also previously documented that EPO significantly reduced Bcl-6 mRNA increase

in naïve CD4⁺ T cells cultured under T_{FH} polarizing conditions, significantly increased (Figure 30, data not published and previously generated).

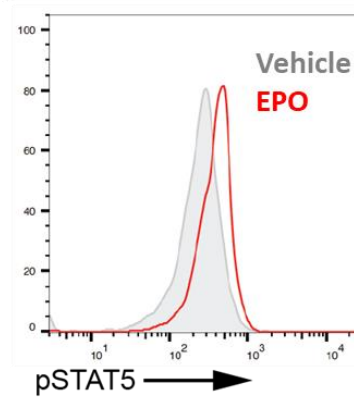


Figure 29. Representative phospho-flow. Enriched CD4⁺ cells were treated with vehicle or EPO (1,000 IU/ml) for 60 minutes at 37°C, and stained for 2 hours at room temperature for Alexa Fluor 647 conjugated anti-pSTAT5 (pY694) 10 mg/ml (clone 47/Stat5; BD Bioscience). Data previously generated.

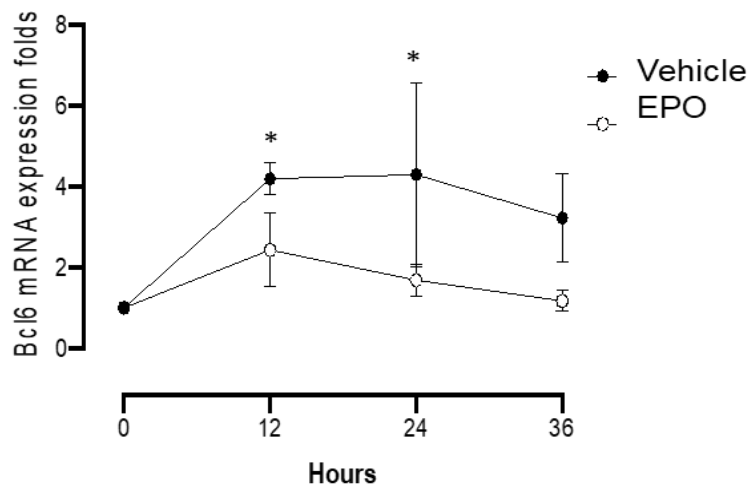


Figure 30. Bcl-6 expression. RNA was extracted (RNeasy Mini Kit, Qiagen) from enriched naïve CD4⁺ treated with vehicle or EPO. After cDNA retro-transcription (High-Capacity cDNA Reverse Transcription kit, Applied Biosystems), RT-PCR (TaqMan probes, Applied Biosystems) was performed using the CFX384 Real-Time PCR Detection System (Bio-Rad Laboratories). Primer Mm00477633_m1 (Thermo Fisher Scientific). * $P < 0.05$. Data previously generated.

Finally, to formally prove the mechanistic link between EPO/EPOR activation and Bcl-6 mRNA transcription, we cultured naïve CD4⁺ T cells under T_{FH} polarizing conditions treated with or without EPO in the presence of a selective STAT5 inhibitor, a cell-permeable compound that selectively targets the SH2 domain of STAT5 (Müller et al., 2008). In this setting, we found that the EPO effect was completely rescued in presence of STAT5 inhibitor, indicating that the involvement of EPO-EPOR-STAT5 signaling in EPO-mediated T_{FH} induction (Figure 31). This is a novel mechanism responsible for the immune modulating effects of EPO, different from the inhibition of IL-2-induced (Purroy et al., 2017) or RORC (Donadei et al., 2019) signaling in Th1 and Th17 cells, respectively.

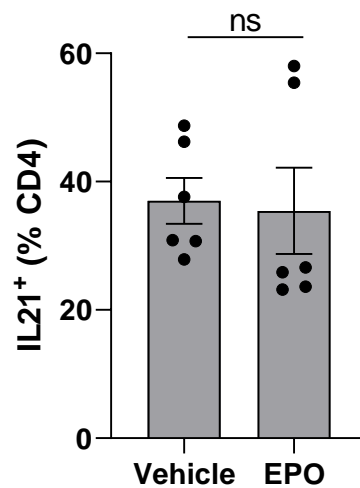


Figure 31. Quantified percentages of CD4⁺ IL-21⁺ cells. Splenic CD4 naïve cells were enriched from wild type B6 animals, and plated in a pre-coated plate with anti-CD3 and anti-CD28 (8µg/ml). Murine IL-6 (30 ng/ml), anti-TGF-β (20 µg/ml), anti-IFN-γ (10 µg/ml), and anti-IL-4 (10 µg/ml) were added. Cells were incubated at 37°C for five days in presence of STAT5 inhibitor (250 µM), and EPO (1,000 IU/ml) or vehicle. Dots represent the number of replicate. Data represent means ± SE. ns; not significant.

4.7 EPO directly inhibits T_{FH}, without affect T_{FR}

Our data indicate that EPO reduces frequencies of T_{FH} and augments frequencies of T_{FR}, both of which could potentially limit GC B cell differentiation and reduce affinity maturation. In an effort to decipher the relative importance of these two effects, we performed additional *in vitro* assays.

We immunized B6 mice (males and females) with BALB/c splenocytes; seven days later, we isolated B6 splenocytes and CD4⁺ cells were enriched. These cells were stained for CD4⁺CXCR5⁺PD1⁺, including both T_{FH} and T_{FR}. From the stained samples we flow-sorted all together T_{FH} and T_{FR} cells population. At the same time, we collected splenocytes from BALB/c mice, and B cells were enriched. We cultured together sorted T_{FH} and T_{FR} cells from pre-immunized B6, and BALB/c B cells, adding anti-CD3 for T cells stimulation and expansion (Trickett and Kwan, 2003) and anti-IgM as antigen that *in vitro* induces T cell-independent B cell activation (Patterson et al., 2006). We treated the cells with EPO or vehicle control. After two day of incubation, we quantified the percentages of B220⁺IgM⁻IgD⁻GL7⁺IgG⁺ B cells to estimate the EPO effect on the antibodies production (Figure 32).

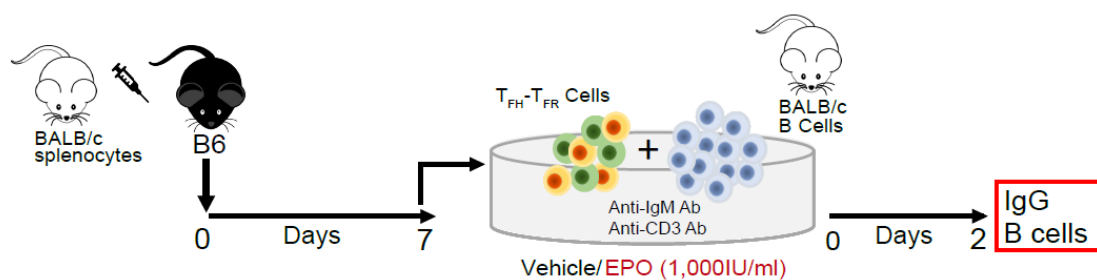


Figure 32. EPO inhibitory effects of T_{FH} through EPOR and independent of T_{FR} *in vitro*. B6 mice received allogeneic immunization with BALB/c splenocytes (20×10^6 , by intraperitoneal injection), and after 7 days the animals were euthanized. A culture of BALB/c enriched splenic B cells and pre-immunized B6 enriched splenic T_{FH}-T_{FR} were stimulated with anti-IgM (10 μ g/ml) and anti-CD3 (2 μ g/ml). Cells were treated with EPO (1,000 IU/ml) or vehicle control, incubated for two days at 37°C, and collected to measure IgG⁺ B cells.

In this assay, we saw that the percentage of IgG⁺ B cells was significantly lower in cultures treated with EPO in comparison to vehicle. As internal control, in absence of T cells, B cells alone did not show positivity for IgG (Figure 33).

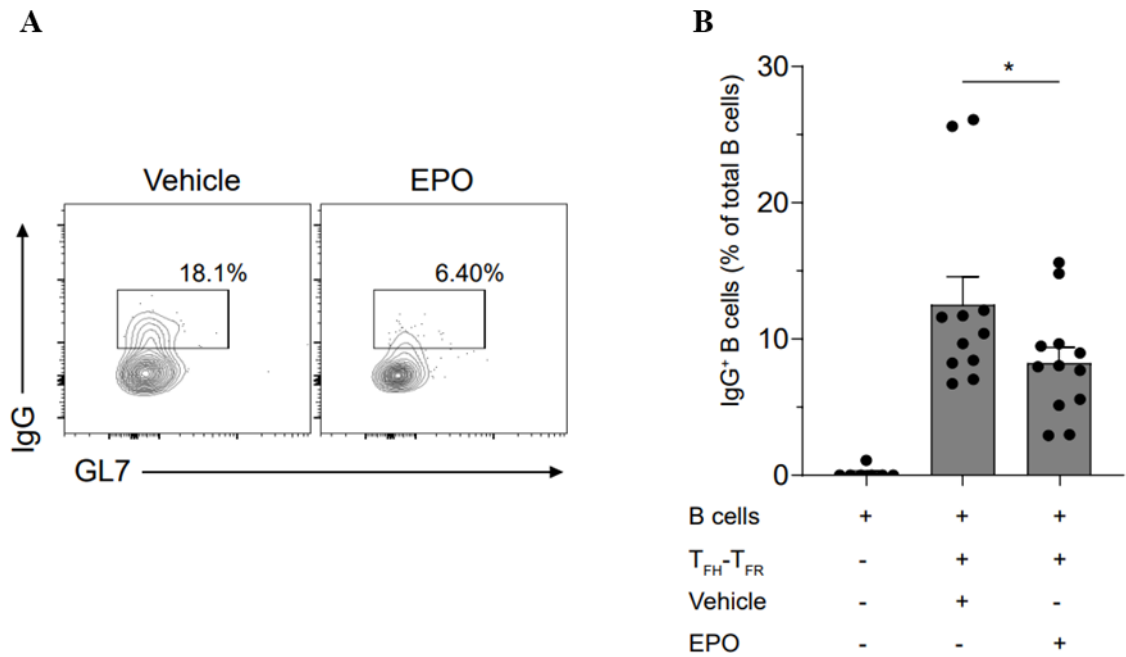


Figure 33. Representative plots (A) and quantified percentages (B) of B220⁺ IgM⁻IgD⁻ IgG⁺ B cells from BALB/c B cells cultured alone or with T_{FH} and T_{FR} from pre-immunized B6, in the presence of EPO or vehicle. Dots represent the number of replicate. Data represent means ± SE. **P* < 0.05.

We repeated the same experiment using pre-immunized B6 EPOR^{fl/fl}CD4Cre^{NEG} or EPOR^{fl/fl}CD4Cre^{POS} mice (males and females). As expected, culture cells from B6 EPOR^{fl/fl}CD4Cre^{NEG} mice had the same trend of pre-immunized wild type animals, with a significantly reduction in the percentage of B220⁺IgM⁻IgD⁻GL7⁺IgG⁺ B cells when EPO was added. However, in cell culture with T_{FH} and T_{FR} from mice that lacked EPO receptor on CD4⁺ cells (EPOR^{fl/fl}CD4Cre^{POS}), we did not see a reduction in IgG⁺ B cells after EPO administration (Figure 34), further supporting the concept that EPO inhibits B cell activation by activating EPOR on T cells.

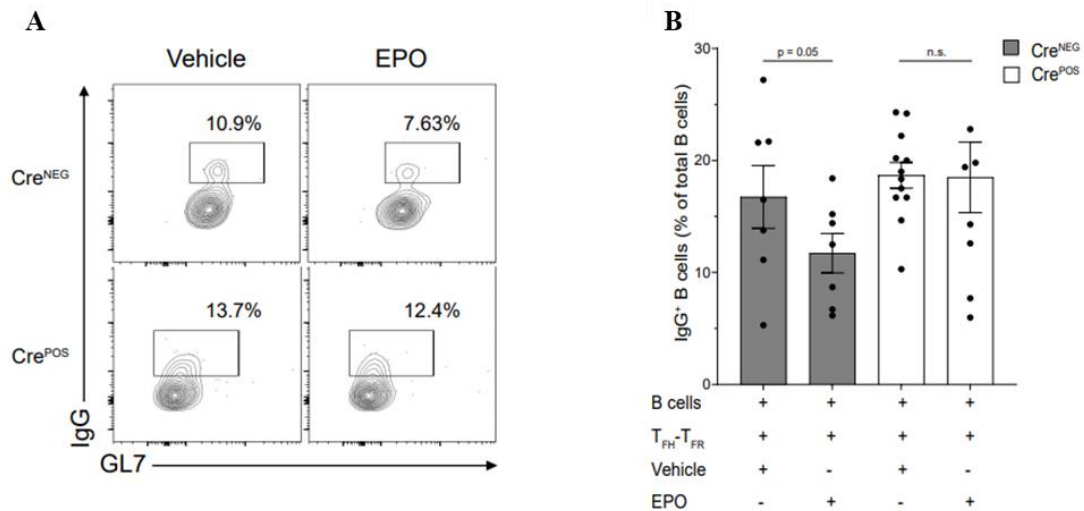


Figure 34. B6 EPOR^{fl/fl}CD4Cre^{NEG} and EPOR^{fl/fl}CD4Cre^{POS} mice received allogeneic immunization with BALB/c splenocytes (20×10^6 , by intraperitoneal injection), and after 7 days the animals were euthanized. A culture of BALB/c enriched splenic B cells and pre-immunized B6 EPOR^{fl/fl}CD4Cre^{NEG} and EPOR^{fl/fl}CD4Cre^{POS} enriched splenic T_{FH}-T_{FR} were stimulated with anti-IgM (10 μ g/ml) and anti-CD3 (2 μ g/ml). Cells were treated with EPO (1,000 IU/ml) or vehicle control, incubated for two days at 37°C, and collected to measure IgG⁺ B cells. Representative plots (A) and quantified percentages (B) of B220⁺ IgM-IgD⁻ IgG⁺ B cells from BALB/c B cells cultured alone or with T_{FH} and T_{FR} from pre-immunized B6 EPOR^{fl/fl}CD4Cre^{NEG} and EPOR^{fl/fl}CD4Cre^{POS}, in the presence of EPO or vehicle. Dots represent the number of replicate. Data represent means \pm SE. * $P < 0.05$; ns; not significant.

Based on previous results, we performed another experiment to test whether EPO directly inhibits T_{FH} in the absence of T_{FR}. We immunized B6.129(Cg)-FOXP3^{tm3(DTR/GFP)Ayr/J} mice, a genetically modified strain that allowed us to distinguish T_{FH} (FOXP3⁻/GFP⁻ cells) and T_{FR} (FOXP3⁺/GFP⁺ cells) by flow sorting. Seven days after immunization, we collected B6.129(Cg)-FOXP3^{tm3(DTR/GFP)Ayr/J} splenocytes and stained the enriched CD4⁺ for CD4, CXCR5, and PD1. We flow sorted CD4⁺CXCR5⁺PD1⁺FOXP3⁻GFP⁻ T_{FH} and CD4⁺CXCR5⁺PD1⁺FOXP3⁺GFP⁺ T_{FR} as two separate populations. Then we culture enriched BALB/c B cells with T_{FH} cells only, using the previous experimental conditions (Figure 35).

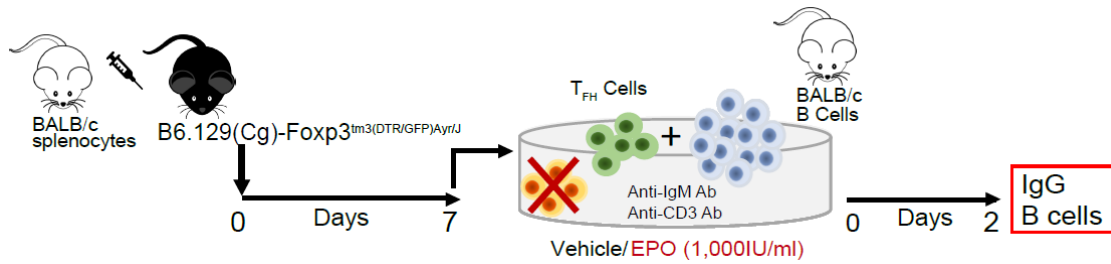


Figure 35. B6.129(Cg)-FOXP3^{tm3(DTR/GFP)}Ayr/J mice received allogeneic immunization with BALB/c splenocytes (20×10^6 , by intraperitoneal injection); after 7 days the animals were euthanized, and T_{FH} cells were sorted. A culture of BALB/c enriched splenic B cells and pre-immunized B6.129(Cg)-FOXP3^{tm3(DTR/GFP)}Ayr/J T_{FH} were stimulated with anti-IgM (10 μ g/ml) and anti-CD3 (2 μ g/ml). Cells were treated with EPO (1,000 IU/ml) or vehicle control, incubated for two days at 37°C, and collected to measure IgG⁺ B cells.

The flow cytometry analysis showed that EPO significantly reduced the *in vitro* induction of IgG⁺ B cells in culture wells containing only T_{FH} (without T_{FR}), indicating that EPO's inhibitory effect on T_{FH} is independent from T_{FR} (Figure 36).

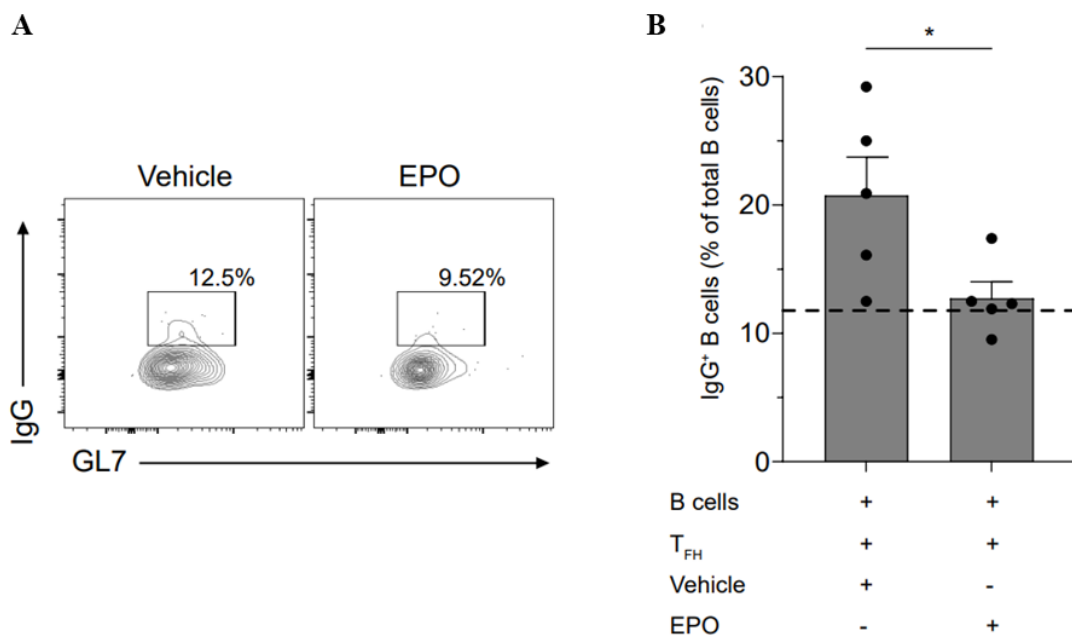


Figure 36. Representative plots (A) and quantified percentages (B) of B220⁺ IgM-IgD- IgG⁺ B cells from BALB/c B cells cultured with pre-immunized B6.129(Cg)-FOXP3^{tm3(DTR/GFP)}Ayr/J T_{FH} in the presence of EPO (1,000 IU/ml) or vehicle control. Dashed line represents the percentage value of B220⁺ IgM-IgD- IgG⁺ B cells in a culture with BALB/c B cells and B6.129(Cg)-FOXP3^{tm3(DTR/GFP)}Ayr/J T_{FH}-T_{FR} treated with vehicle control as reference value. Dots represent the number of replicate. Data represent means \pm SE. * $P < 0.05$; ns; not significant.

4.8 EPO inhibits pre-formed DSA

In an effort to assess clinical significance of our findings, we tested the effects of EPO in allosensitized heart transplant recipients and in two models of graft versus host disease (GVHD).

The presence of pre-formed DSA is a major obstacle against successful organ transplantation and therapeutic options are limited. We showed above that EPO prevents formation of newly developed DSA. Herein, we tested the hypothesis that EPO reduces also pre-formed DSA. To resemble the situation of hyperimmune patients on a waiting list for organ transplantation, we sensitized B6 mice, both males and females, with allogeneic BALB/c splenocytes and after two weeks, we measured donor-specific antibodies. We allocated mice with similar DSA levels into two groups. The following day we transplanted the sensitized mice with BALB/c hearts, and for fourteen days, we treated differently (with EPO or vehicle administration) the two groups (Figure 37).

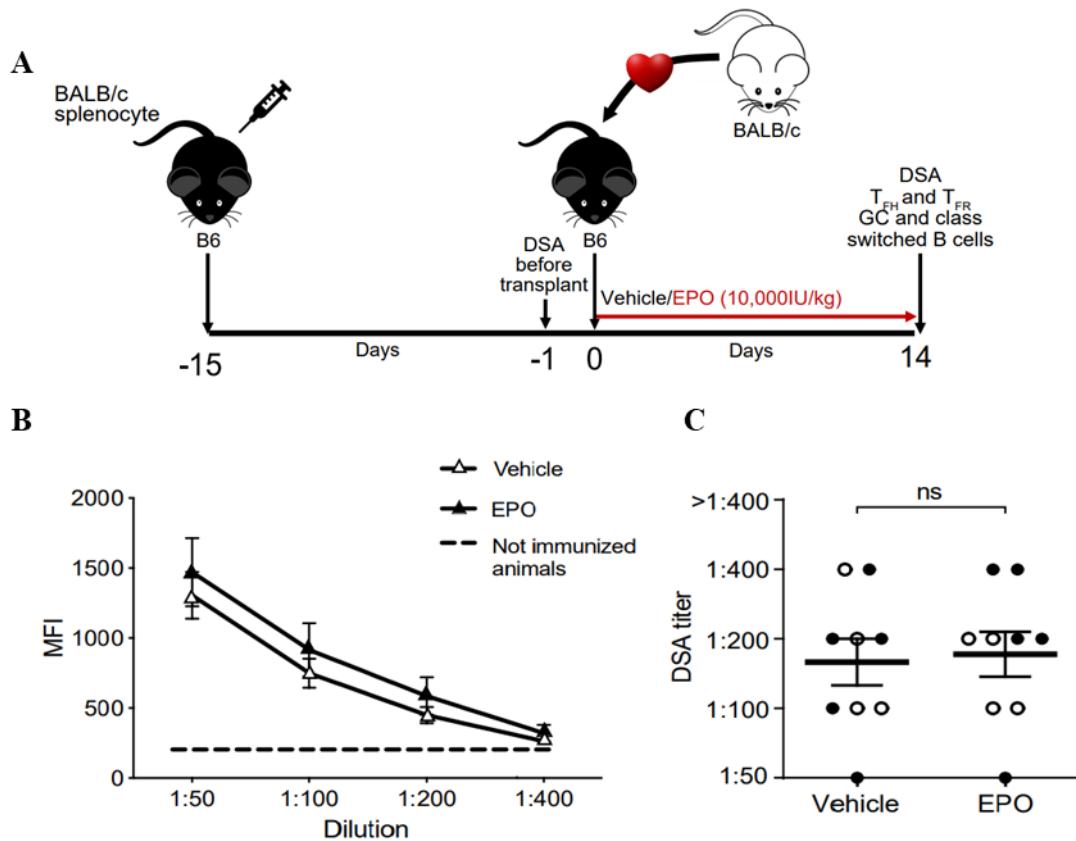


Figure 37. B6 mice received allogeneic immunization with BALB/c splenocytes (20×10^6 , by intraperitoneal injection), and after 14 days we measured DSA. On day 15 after immunization, B6 mice received an allogeneic heterotopic transplantation from BALB/c mice. We treated the recipient animals with EPO (10,000 IU/kg) or vehicle control by intraperitoneal injection from the day of transplant up to day 14 post-transplant, when the animals were euthanized (A). At day -1 before transplant we measured DSA and we allocated mice with similar DSA levels to EPO or vehicle treatment. Representative quantification MFI levels (B), and titers (C) within the two groups. Data represent means \pm SE. Empty circles represent male animals, full circles females. ns; not significant.

Fourteen days after transplant, we quantified donor specific anti class I MHC serum antibodies. These analyses showed EPO induced significant diminutions in antibody binding to target cells and in serum antibody titers compared to controls (Figure 38).

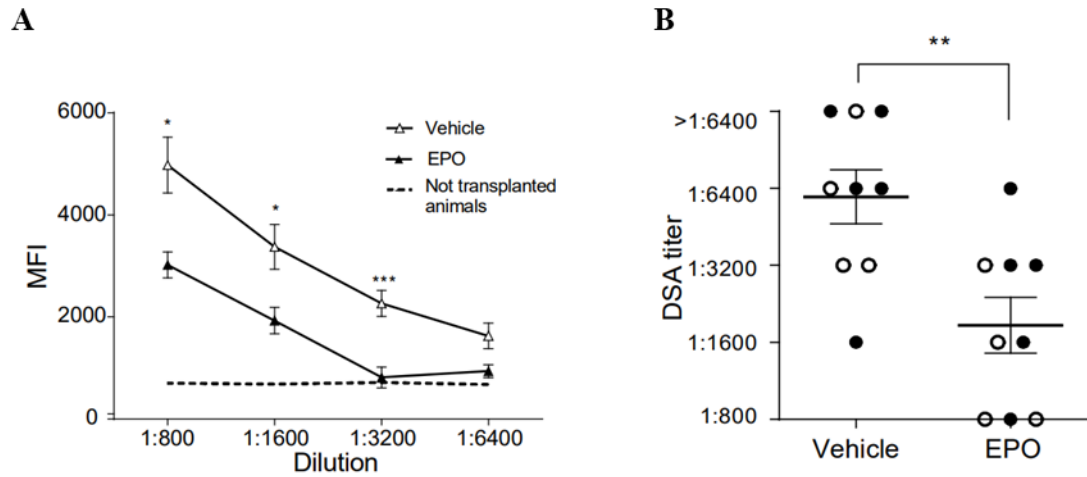


Figure 38. DSA levels were detected 14 days after transplants. Representative histograms of MFI levels (A), and titers (B) in EPO- and vehicle treated mice. Data represent means \pm SE. Empty circles represent male animals, full circles females. ** $P < 0.01$.

Splenic cells were collected to perform cytofluorimetric analysis. EPO-treated recipients showed significantly fewer GC B cells (Figure 39A-C), Class Switched (Figure 39D-F) B cells, and T_{FH} (Figure 40A-C), along with increases in T_{FR} (Figure 40A, D, E). Consequently, the ratio T_{FR}/T_{FH} in EPO-treated animals was higher too (Figure 40F).

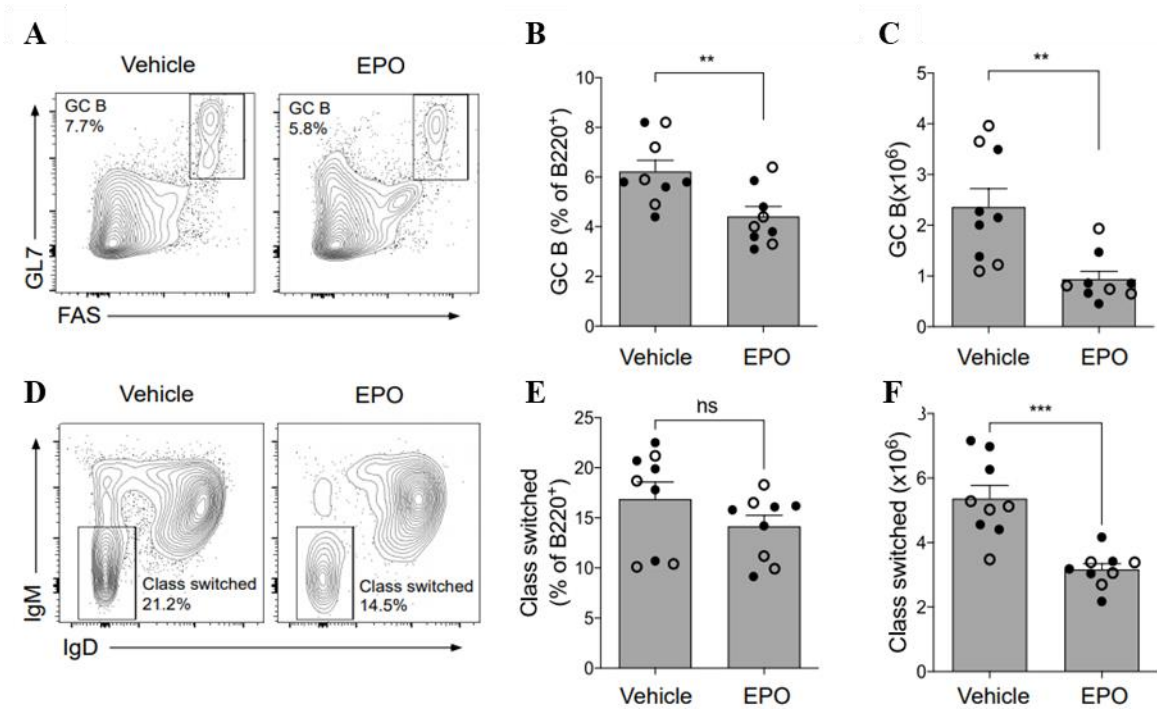


Figure 39. B6 mice received allogeneic immunization with BALB/c splenocytes (20×10^6 , by intraperitoneal injection), and after 14 days we measured DSA. On day 15 after immunization, B6 mice received an allogeneic heterotopic transplantation from BALB/c mice. We treated the recipient animals with EPO (10,000 IU/kg) or vehicle control by intraperitoneal injection from the day of transplant up to day 14 post-transplant, when the animals were euthanized. Representative plots depicting percentages of B220⁺Fas⁺GL7⁺ Germinal Center (GC) (A) and B220⁺IgM⁻IgD⁻ class-switched (D) B cells in the same mice. Quantified percentages (B, E) and total numbers (C, F) of GC (B, C) and Class Switched (E, F) B cells. Data represent means \pm SE. Empty circles represent male animals, full circles females. ** $P < 0.01$; *** $P < 0.001$; ns; not significant.

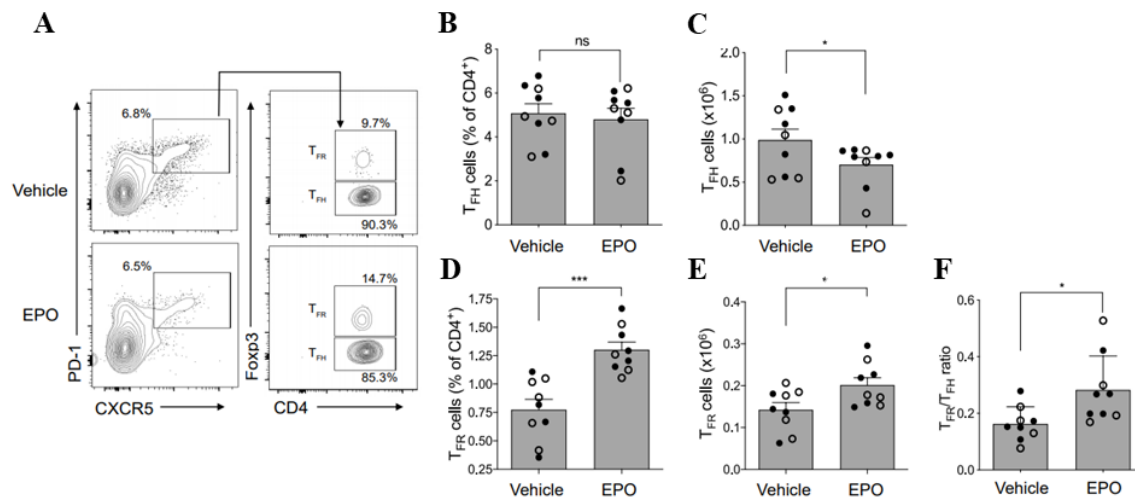


Figure 40. B6 mice received allogeneic immunization with BALB/c splenocytes (20×10^6 , by intraperitoneal injection), and after 14 days we measured DSA. On day 15 after immunization, B6 mice received an allogeneic heterotopic transplantation from BALB/c mice. We treated the recipient animals with EPO (10,000 IU/kg) or vehicle control by intraperitoneal injection from the day of transplant up to day 14 post-transplant, when the animals were euthanized. Representative plots depicting percentages of $CD4^+PD1^+CXCR5^+FOXP3^-$ T_{HF} and $CD4^+PD1^+CXCR5^+FOXP3^+$ T_{FR} in mice treated with EPO or vehicle control (A). Quantified percentages (B, D) and absolute numbers (C, E) of T_{HF} (B, C), T_{FR} (D, E), and T_{HF}/T_{FR} ratios (F). Data represent means \pm SE. Empty circles represent male animals, full circles females. * $P < 0.05$; *** $P < 0.001$; ns; not significant.

As in the other experiments, here we observed similar results in male and female recipients, suggesting a non sex-related event.

In accordance with previous results, these data support our hypothesis that EPO contributes to reduce DSA, and it has inhibitory effects on T_{HF} and GC B cells also in allosensitized heart transplant recipients.

4.9 EPO ameliorates disease severity in murine models of systemic lupus erythematosus

Systemic lupus erythematosus (SLE) is a multiorgan autoimmune disease characterized by the formation of autoantibodies, including anti double stranded DNA (ds-DNA) antibodies that promote end-organ damage. To test whether EPO ameliorates disease severity in a SLE model by inhibiting T_{HF}, we used a parent-to-F1 model of GVHD that resembles features of SLE (Cutler et al., 2017; Deng et al., 2017; MacDonald et al., 2017;

Zeiser and Blazar, 2017). We injected CD8-depleted B6 spleen cells into non-irradiated semi-allogeneic (bx_d) F1 recipients (Nguyen et al., 2012). In this murine model, alloreactive donor CD4⁺ T cells expand and differentiate into T_{FH} cells, with associated induction of GC B cells and production of autoantibodies, including anti-ds-DNA antibodies (Nguyen et al., 2012). Using this established system, we treated for six weeks a group of recipients with EPO and another group of recipients with vehicle control. Each group was composed of both females and males. We quantified frequencies of T_{FH} cells within the H-2^{b-} (donor cell) gate (Figure 41).

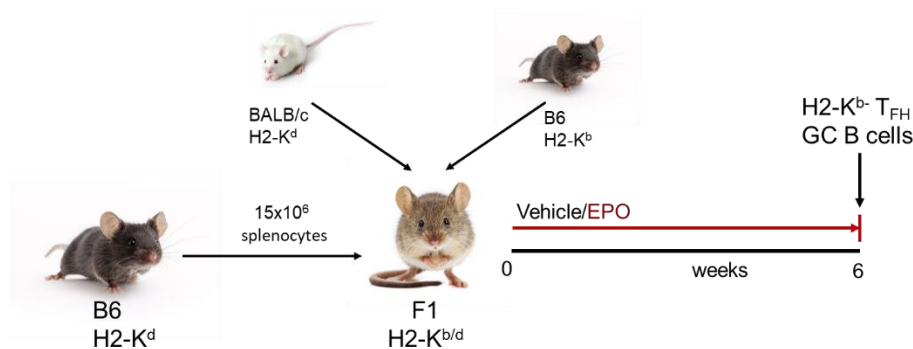


Figure 41. CD8-depleted B6 spleen cells (H2-K^d) were injected into B6 x BALB/c (bx_d) F1 recipients (H2-K^{b/d}) that were treated daily with EPO (10,000 IU/kg) or vehicle control by intraperitoneal injection until euthanasia on week 6. H2-K^{b-} T_{FH} and GC B cells were quantified.

We detected significantly fewer T_{FH} in EPO-treated animals compared with the control group (Figure 42A-C). As well as, CG B cells were significantly reduced after EPO administration (Figure 42D-F). Non-injected (bx_d) F1 animals were used as internal control (Figure 42).

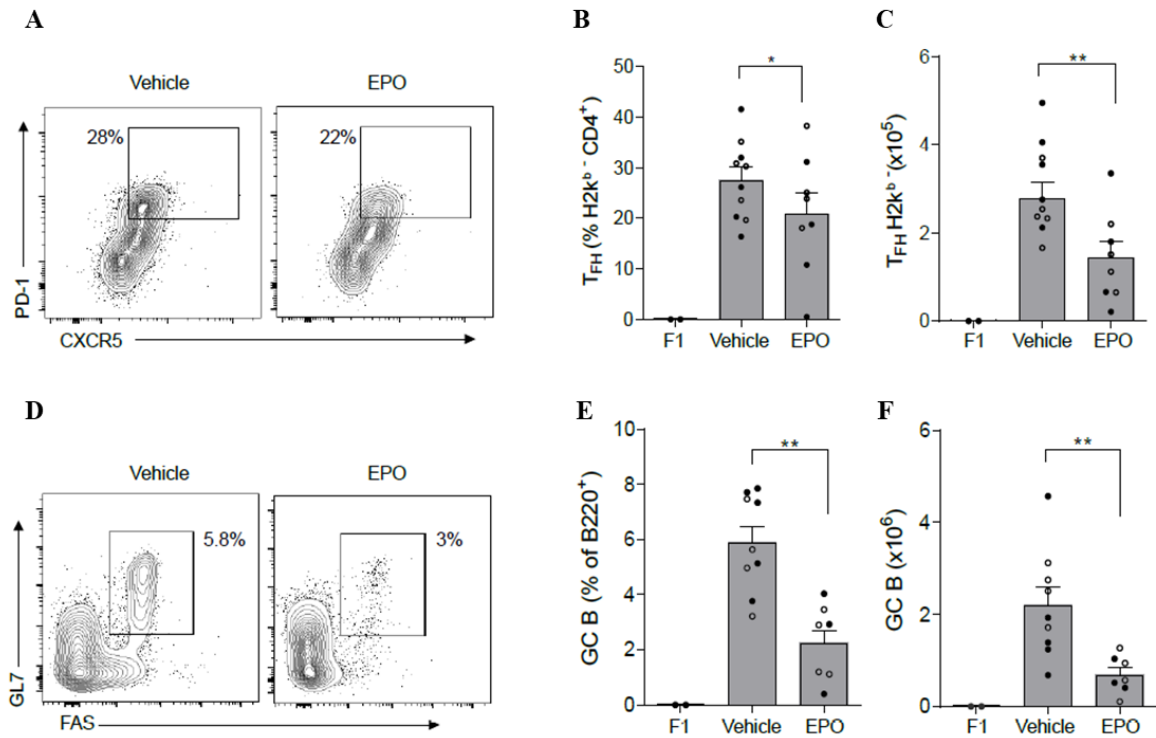


Figure 42. CD8-depleted B6 spleen cells were injected into B6xBALB/c (bx) recipients that were treated daily with EPO (10,000 IU/kg) or vehicle control by intraperitoneal injection until euthanasia on week 6. Representative plots (A, D) and data quantification (B, C, E, F) for T_{FH} (A-C) and GC B cells (D-F). Data represent means ± SE. Empty circles represent male animals, full circles represent females. F1; non injected (bx) F1 animals. *P < 0.05 **P < 0.01.

We performed serum ELISAs that revealed significantly lower anti-dsDNA autoantibody levels in EPO-treated animals (Figure 43). Altogether, these data support the conclusion that EPO inhibits T_{FH} dependent B cell activation in this GVHD model.

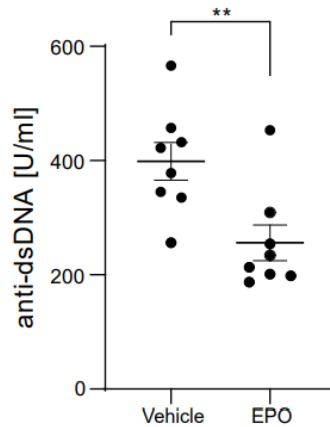


Figure 43. CD8-depleted B6 spleen cells were injected into B6xBALB/c (bx) recipients that were treated daily with EPO (10,000 IU/kg) or vehicle control by intraperitoneal injection until euthanasia on week 6. Anti-dsDNA autoantibodies in sera collected from the same mice at sacrifice. Data represent means \pm SE. **P < 0.01.

The B6 into (bx) F1 model is not associated with a clinical phenotype. To enhance the clinical significance, we performed analogous studies using B6xDBA F1 (H-2^{b/d}) recipients of DBA/2J (DBA) splenocytes (H-2^d). This system is particularly informative because GVHD results in autoantibody formation and glomerulonephritis. For six weeks, we treated recipients with EPO or vehicle as control (Figure 44).

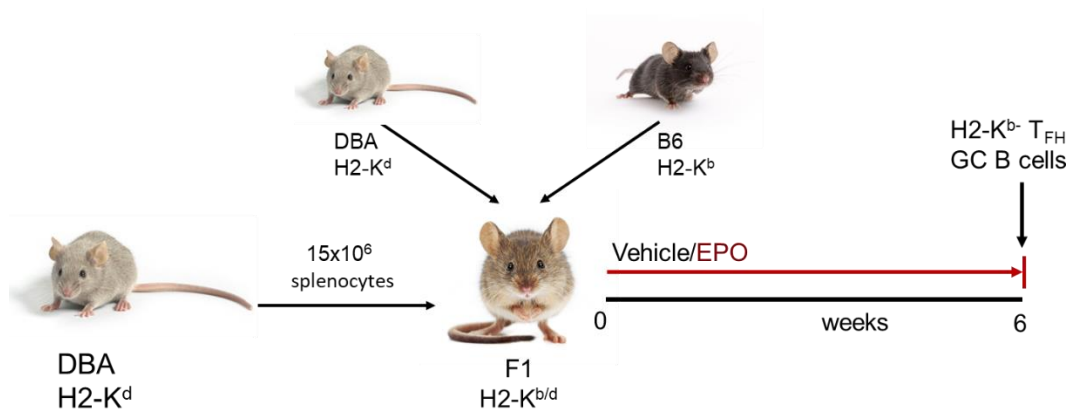


Figure 44. CD8-depleted DBA spleen cells (H-2^d) were injected into DBA x B6 F1 recipients (H-2^{b/d}) that were treated daily with EPO (10,000 IU/kg) or vehicle control by intraperitoneal injection until euthanasia on week 6. H-2^b- T_{FH} and GC B cells were quantified.

At 6 weeks, EPO-treated mice contained fewer donor-derived T_{FH} (Figure 45A) and recipient GC B cells (Figure 45B), as well as lower levels of anti-dsDNA autoantibodies compared with the control group (Figure 45C).

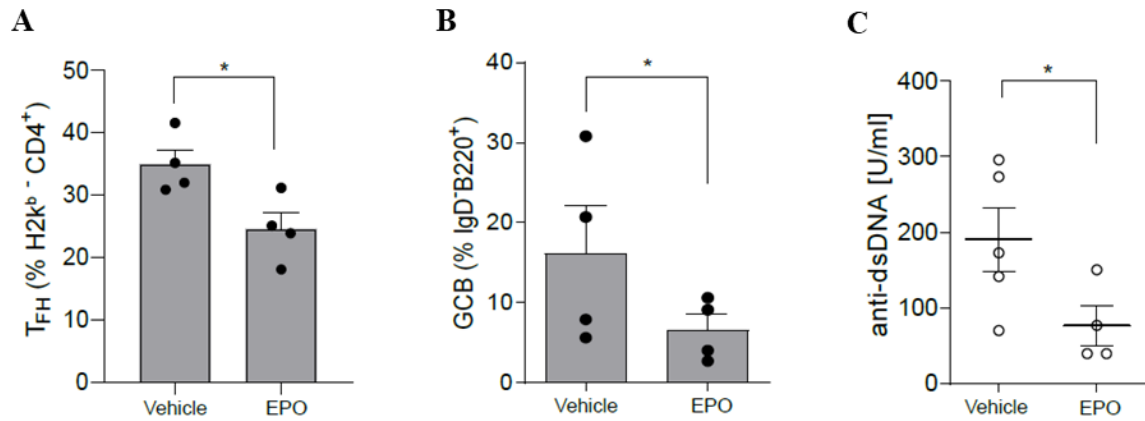


Figure 45. CD8-depleted DBA spleen cells (H2-K^d) were injected into DBA x B6 F1 recipients (H2-K^{b/d}) that were treated daily with EPO (10,000 IU/kg) or vehicle control by intraperitoneal injection until euthanasia on week 6. Data quantification for T_{FH} (A) and GC B cells (B). Anti-dsDNA autoantibodies in sera collected from the same mice at sacrifice (C). Data represent means ± SE. **P < 0.01.

At the same time, animals administrated with EPO showed significantly diminished kidney disease severity, the latter documented by fewer intrarenal infiltrates (Figure 46), lower albuminuria (Figure 47), and diminished glomerular deposition of IgG (Figure 48A, B) and C3b (Figure 48C, D). Therefore, our data converge to indicate that EPO reduces severity of diseases mediated by allo- or auto-antibodies.

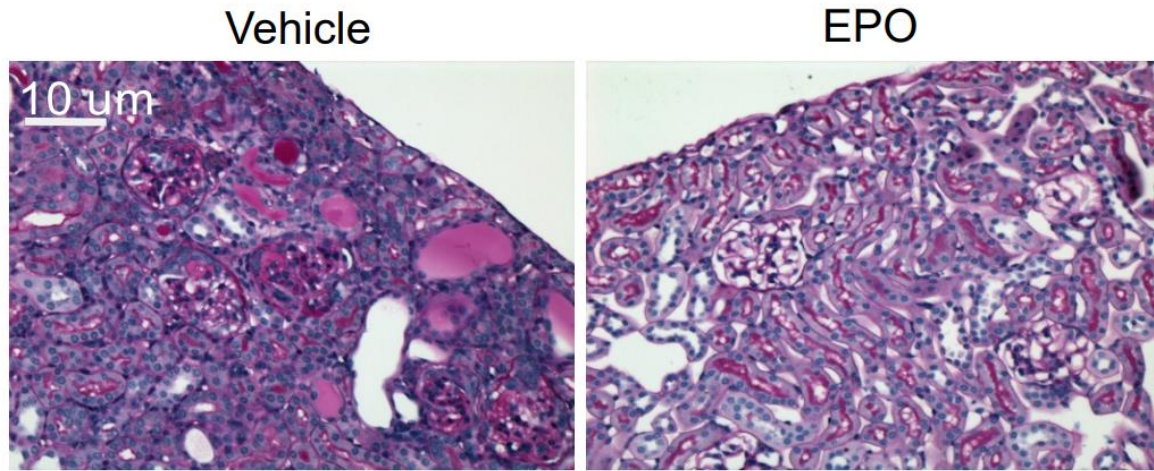


Figure 46. CD8-depleted DBA spleen cells (H2-K^d) were injected into DBA x B6 F1 recipients (H2-K^{b/d}) that were treated daily with EPO (10,000 IU/kg) or vehicle control by intraperitoneal injection until euthanasia on week 6. Representative images of PAS staining of kidney tissue. Scale bars: 10 μm.

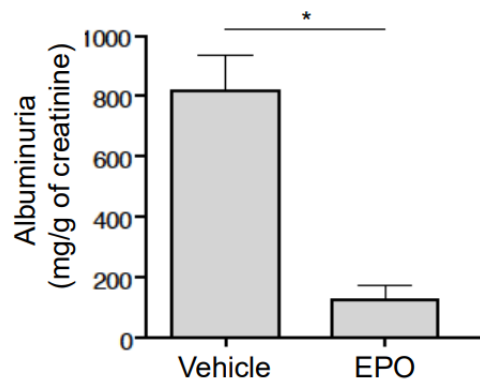


Figure 47. CD8-depleted DBA spleen cells (H2-K^d) were injected into DBA x B6 F1 recipients (H2-K^{b/d}) that were treated daily with EPO (10,000 IU/kg) or vehicle control by intraperitoneal injection until euthanasia on week 6. Albuminuria quantification expressed as the ratio of urine albumin to creatinine. Data represent means ± SE. *P<0.05.

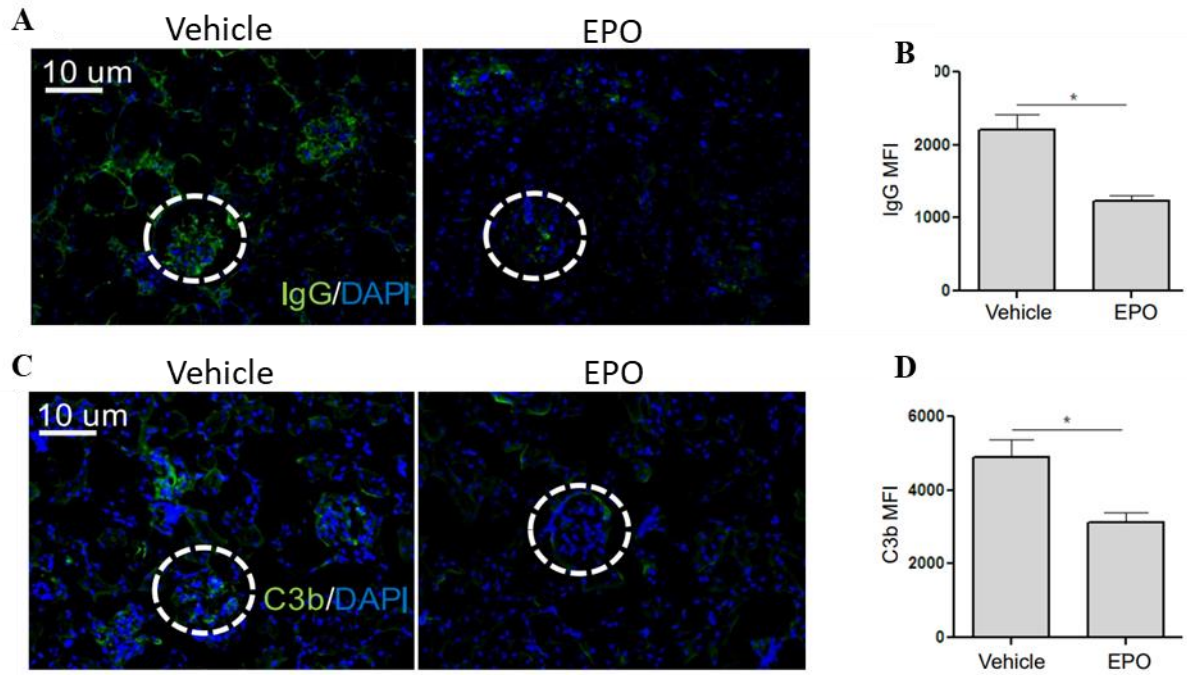


Figure 48. CD8-depleted DBA spleen cells (H2-K^d) were injected into DBA x B6 F1 recipients (H2-K^{b/d}) that were treated daily with EPO (10,000 IU/kg) or vehicle control by intraperitoneal injection until euthanasia on week 6. Representative images of IgG (A) and C3b (C) glomerular deposition in staining of kidney tissues. Original magnification 20x. Differences in IgG (B) and C3b (D) glomerular fluorescent intensity between EPO- and vehicle-treated animals were quantified relative to DAPI using MetaMorph software. At least 20 glomeruli from 3 animals were included in the analysis. Scale bars: 10 μm . Data represent means \pm SE. * $P < 0.05$.

5. CONCLUSION

T cell dependent, antibody isotype switch recombination and affinity maturation are key events to guarantee an effective anti-pathogen immunity. However they also lead to the production of autoreactive and alloreactive IgG in several disease states as well as transplant rejection, multiple autoimmune diseases, and GVHD. Currently, there are still few therapeutic options aimed at reducing pathogenic antibodies to prevent/treat disease (De Silva and Klein, 2015; Stebegg et al., 2018).

Herein, we demonstrate that EPO prevents pathogenic autoantibodies and alloantibodies formation by inhibiting T_{FH} , GC, and class switched B cells. Experiments with EPOR conditional knock-out immunized and/or transplanted mice, indicate that this inhibition occurs *in vivo* through EPO/EPOR interaction on T cells.

Our *in vitro* and *in vivo* experiments with T cell-dependent and T cell-independent stimuli clearly indicate that EPO inhibits B cells by suppressing T_{FH} responses, while it has no major direct inhibitory effect on B cells.

T_{FH} induction is initiated by IL-6/IL-6R and IL-21/IL-21R interaction that leads to STAT3 phosphorylation and transcription of master regulator Bcl-6. Our group has shown that EPO/EPOR interaction leads to STAT5 phosphorylation, which has been shown to compete for pSTAT3 binding site on promoter region of Bcl-6. Importantly, the repression of Bcl6 mediated by STAT5 is dominant over STAT3-mediated induction (Yang et al., 2011; Johnston et al., 2012; Walker et al., 2013)

Our data indicate that EPO inhibitory effects on T_{FH} induction and function are STAT5-dependent. An antagonist of STAT5 phosphorylation abolished EPO effects on T_{FH} induction. These results suggest a novel mechanism accountable for the immune modulating effects of EPO, diverse from the inhibition of IL-2-induced (Purroy et al., 2017) or RORC (Donadei et al., 2019) signaling in Th1 and Th17 cells, respectively.

T_{FR} cells are a subset of thymic regulatory T cells capable of inhibiting T_{FH} cell-mediated B cell responses (Sage and Sharpe, 2016; Maceiras et al., 2017).

To make our data more clinically relevant, we alloimmunized mice, to resemble the situation of hyperimmune patients on a waiting list for organ transplantation. These

patients have reduced chances to find a matched organ donor and higher risk of accelerated graft loss due to preformed alloreactive T_{FH} and GC B cells. In immunized mice, a short treatment with EPO resulted in reduced expansion of T_{FH} and GC B cells and, more importantly, reduced DSA levels after heart transplantation. The findings form the basis for future studies testing the hypothesis that treating hyperimmune patients with EPO increases their chances to find a compatible donor and to prolong graft survival.

Furthermore, in two model of GVHD, we found that EPO treatment reduced T_{FH} and GC B cells and lowered levels of anti-dsDNA autoantibodies. These effects of EPO translated into an amelioration of disease severity.

After solid organ transplantation, the typical maintenance immunosuppressive therapy comprises a calcineurin inhibitor (CNI), a T-cell proliferation inhibitor and steroids. Available evidence indicated that these classic immunosuppressive therapies do not totally block T_{FH}-cell activity (Yan et al., 2017). Therefore, our findings that EPO effectively blocks T_{FH} *in vivo* in mice are important because they form the background for future clinical studies testing the hypothesis that EPO treatment reduces DSA formation in organ transplant recipients.

To ensure rigor and reproducibility of our results, we randomly allocated male and female animals within a litter to experimental groups. Mice in different experimental groups were co-housed, to normalize the microbiome differences.

In the present studies we employed doses of EPO about 20-fold higher than the ones currently used in the clinic to treat anemia. While we previously showed that the EPO immune modulating effects are reached even with standard therapeutic doses (Purroy et al., 2017), we acknowledge that prolonged EPO treatment may be associated with augmented cardiovascular risk. An effective strategy to prevent autoantibody or alloantibody formation while avoiding the side effects of EPO on blood viscosity and platelet function may be represented by the use of the non-erythropoietic agonists of heterodimer EPOR (Brines et al., 2008).

In sum, our results link EPO to T_{FH}-B cell interaction and antibody production. Together with recent evidence that T_{FH} cells likely participate in the pathophysiology of autoantibody and DSA formation in heart and other organ transplantation, as well as in GVHD (Forcade et al., 2016; Knorr et al., 2016), our findings raise the possibility that targeting EPOR signaling (Woodruff et al., 2011) could be a useful therapeutic strategy for prevention and/or treatment of T_{FH} cell-dependent disease processes, including DSA.

6. BIBLIOGRAPHY

- Aachmann-Andersen, N. J., Christensen, S. J., Lisbjerg, K., Oturai, P., Johansson, P. I., Holstein-Rathlou, N. H., et al. (2018). Recombinant erythropoietin acutely decreases renal perfusion and decouples the renin-angiotensin-aldosterone system. *Physiol. Rep.* 6. doi:10.14814/phy2.13573.
- Abraham, I., and Macdonald, K. (2012). Expert Opinion on Drug Safety Clinical safety of biosimilar recombinant human erythropoietins. doi:10.1517/14740338.2012.712681.
- Allen, C. D. C., Ansel, K. M., Low, C., Lesley, R., Tamamura, H., Fujii, N., et al. (2004). Germinal center dark and light zone organization is mediated by CXCR4 and CXCR5. *Nat. Immunol.* 5, 943–952. doi:10.1038/ni1100.
- Allen, C. D. C., Okada, T., Tang, H. L., and Cyster, J. G. (2007). Imaging of germinal center selection events during affinity maturation. *Science (80-)*. 315, 528–531. doi:10.1126/science.1136736.
- Aloulou, M., and Fazilleau, N. (2019). Regulation of B cell responses by distinct populations of CD4 T cells. *Biomed. J.* 42, 243–251. doi:10.1016/j.bj.2019.06.002.
- Avneon, M., Lifshitz, L., Katz, O., Prutchi-Sagiv, S., Gassmann, M., Mittelman, M., et al. (2009). Non-erythroid effects of erythropoietin: Are neutrophils a target? *Leuk. Res.* 33, 1430–1432. doi:10.1016/j.leukres.2009.03.020.
- Bannard, O., Horton, R. M., Allen, C. D. C., An, J., Nagasawa, T., and Cyster, J. G. (2013). Germinal center centroblasts transition to a centrocyte phenotype according to a timed program and depend on the dark zone for effective selection. *Immunity* 39, 912–924. doi:10.1016/j.immuni.2013.08.038.
- Barrio, L., Román-García, S., Díaz-Mora, E., Risco, A., Jiménez-Saiz, R., Carrasco, Y. R., et al. (2020). B Cell Development and T-Dependent Antibody Response Are Regulated by p38 γ and p38 δ . *Front. Cell Dev. Biol.* 8, 189. doi:10.3389/fcell.2020.00189.
- Bazan, J. F. (1990). Haemopoietic receptors and helical cytokines. *Immunol. Today* 11, 350–354. doi:10.1016/0167-5699(90)90139-Z.
- Blanchard, K. L., Fandrey, J., Goldberg, M. A., and Bunn, H. F. (1993). Regulation of the erythropoietin gene. *Stem Cells* 11, 1–7. doi:10.1002/stem.5530110604.
- Boissel, J., Lee, W., Presnells, S. R., Cohens, F. E., and Bunn, H. F. (1993). Erythropoietin Structure-Function Relationships.
- Bonnas, C., Wüstefeld, L., Winkler, D., Kronstein-Wiedemann, R., Dere, E., Specht, K., et al. (2017). EV-3, an endogenous human erythropoietin isoform with distinct functional relevance OPEN. *Science (80-)*. 7(1):3684. doi:10.1038/s41598-017-03167-0.

- Brailsford, J. A., and Danishefsky, S. J. (2012). Probing the stability of nonglycosylated wild-type erythropoietin protein via reiterative alanine ligations. *Proc. Natl. Acad. Sci. U. S. A.* 109, 7196–7201. doi:10.1073/pnas.1202762109.
- Brines, M., and Cerami, A. (2005). Emerging biological roles for erythropoietin in the nervous system. *Nat. Rev. Neurosci.* 6, 484–494. doi:10.1038/nrn1687.
- Brines, M., and Cerami, A. (2006a). Discovering erythropoietin’s extra-hematopoietic functions: Biology and clinical promise. *Kidney Int.* 70, 246–250. doi:10.1038/sj.ki.5001546.
- Brines, M., and Cerami, A. (2006b). Discovering erythropoietin’s extra-hematopoietic functions: Biology and clinical promise. *Kidney Int.* 70, 246–250. doi:10.1038/sj.ki.5001546.
- Brines, M., Grasso, G., Fiordaliso, F., Sfacteria, A., Ghezzi, P., Fratelli, M., et al. (2004). Erythropoietin mediates tissue protection through an erythropoietin and common-subunit heteroreceptor. Available at: www.pnas.org/cgi/doi/10.1073/pnas.0406491101.
- Brines, M., Patel, N. S. A., Villa, P., Brines, C., Mennini, T., De Paola, M., et al. (2008). Nonerythropoietic, tissue-protective peptides derived from the tertiary structure of erythropoietin. *Proc. Natl. Acad. Sci. U. S. A.* 105, 10925–10930. doi:10.1073/pnas.0805594105.
- Brodeur, P. H., and Wortis, H. H. (1980). Regulation of thymus-independent responses: unresponsiveness to a second challenge of TNP-Ficoll is mediated by hapten-specific antibodies. *J. Immunol.* 125, 1499–505. Available at: <http://www.ncbi.nlm.nih.gov/pubmed/6967907>.
- Broxmeyer, H. E. (2013). Erythropoietin: Multiple targets, actions, and modifying influences for biological and clinical consideration. *J. Exp. Med.* 210, 205–208. doi:10.1084/jem.20122760.
- Bunn, H. F. (2013). Erythropoietin. *Cold Spring Harb. Perspect. Med.* 3, 1–20. doi:10.1101/cshperspect.a011619.
- Cano-Romero, F. L., Laguna Goya, R., Utrero-Rico, A., Gómez-Massa, E., Arroyo-Sánchez, D., Suárez-Fernández, P., et al. (2019). Longitudinal profile of circulating T follicular helper lymphocytes parallels anti-HLA sensitization in renal transplant recipients. *Am. J. Transplant.* 19, 89–97. doi:10.1111/ajt.14987.
- Cantarelli, C., Angeletti, A., and Cravedi, P. (2019). Erythropoietin, a multifaceted protein with innate and adaptive immune modulatory activity. *Am. J. Transplant.* 19, 2407–2414. doi:10.1111/ajt.15369.
- Carney, E. F. (2020). The impact of chronic kidney disease on global health. *Nat. Rev. Nephrol.* 16, 251–251. doi:10.1038/s41581-020-0268-7.
- Cassis, P., Gallon, L., Benigni, A., Mister, M., Pezzotta, A., Solini, S., et al. (2012). Erythropoietin, but not the correction of anemia alone, protects from chronic kidney allograft injury. *Kidney Int.* 81, 903–918. doi:10.1038/ki.2011.473.
- Chatterjee, P. K. (2005). Pleiotropic renal actions of erythropoietin. *Lancet* 365, 1890–1892. doi:10.1016/S0140-6736(05)66622-6.

- Cheetham, J. C., Smith, D. M., Aoki, K. H., Stevenson, J. L., Hoeffel, T. J., Syed, R. S., et al. (1998). NMR structure of human erythropoietin and a comparison with its receptor bound conformation. *Nat. Struct. Biol.* 5, 861–866. doi:10.1038/2302.
- Chen, W., Bai, J., Huang, H., Bi, L., Kong, X., Gao, Y., et al. (2017). Low proportion of follicular regulatory T cell in renal transplant patients with chronic antibody-mediated rejection. *Sci. Rep.* 7, 1–10. doi:10.1038/s41598-017-01625-3.
- Chenouard, A., Chesneau, M., Bui Nguyen, L., Le Bot, S., Cadoux, M., Dugast, E., et al. (2017). Renal Operational Tolerance Is Associated With a Defect of Blood Tfh Cells That Exhibit Impaired B Cell Help. *Am. J. Transplant.* 17, 1490–1501. doi:10.1111/ajt.14142.
- Chhabra, M., Alsughayyir, J., Qureshi, M. S., Mallik, M., Ali, J. M., Gamper, I., et al. (2019). Germinal center alloantibody responses mediate progression of chronic allograft injury. *Front. Immunol.* 10, 1–18. doi:10.3389/fimmu.2018.03038.
- Chun, N., Fairchild, R. L., Li, Y., Liu, J., Zhang, M., Baldwin, W. M., et al. (2017). Complement Dependence of Murine Costimulatory Blockade-Resistant Cellular Cardiac Allograft Rejection. *Am. J. Transplant.* 17, 2810–2819. doi:10.1111/ajt.14328.
- Chung, Y., Tanaka, S., Chu, F., and Nurieva, R. (2011a). Follicular regulatory T (Tfr) cells with dual Foxp3 and Bcl6 expression suppress germinal center reactions. *Nat Med* 17, 983–988. doi:10.1038/nm.2426.Follicular.
- Chung, Y., Tanaka, S., Chu, F., Nurieva, R. I., Martinez, G. J., Rawal, S., et al. (2011b). Follicular regulatory T cells expressing Foxp3 and Bcl-6 suppress germinal center reactions. *Nat. Med.* 17, 983–988. doi:10.1038/nm.2426.
- Chung, Y., Tanaka, S., Chu, F., Nurieva, R. I., Martinez, G. J., Rawal, S., et al. (2011c). Follicular regulatory T cells expressing Foxp3 and Bcl-6 suppress germinal center reactions. *Nat. Med.* 17, 983–988. doi:10.1038/nm.2426.
- Coemans, M., Süsal, C., Döhler, B., Anglicheau, D., Giral, M., Bestard, O., et al. (2018). Analyses of the short- and long-term graft survival after kidney transplantation in Europe between 1986 and 2015. *Kidney Int.* 94, 964–973. doi:10.1016/j.kint.2018.05.018.
- Collazo, M. M., Paraiso, K. H. T., Park, M. Y., Hazen, A. L., and Kerr, W. G. (2012). Lineage extrinsic and intrinsic control of immunoregulatory cell numbers by SHIP. *Eur. J. Immunol.* 42, 1785–1795. doi:10.1002/eji.201142092.
- Collazo, M. M., Wood, D., Paraiso, K. H. T., Lund, E., Engelman, R. W., Le, C. T., et al. (2009). SHIP limits immunoregulatory capacity in the T-cell compartment. *Blood* 113, 2934–2944. doi:10.1182/blood-2008-09-181164.
- Conlon, T. M., Saeb-Parsy, K., Cole, J. L., Motallebzadeh, R., Qureshi, M. S., Rehakova, S., et al. (2012). Germinal Center Alloantibody Responses Are Mediated Exclusively by Indirect-Pathway CD4 T Follicular Helper Cells. *J. Immunol.* 188, 2643–2652. doi:10.4049/jimmunol.1102830.
- Cravedi, P., Manrique, J., Hanlon, K. E., Reid-Adam, J., Brody, J., Prathuangasuk, P., et al. (2014). Immunosuppressive effects of erythropoietin on human alloreactive T cells. *J. Am. Soc. Nephrol.* 25, 2003–2015. doi:10.1681/ASN.2013090945.

- Crotty, S. (2014). T follicular helper cell differentiation, function, and roles in disease. doi:10.1016/j.immuni.2014.10.004.
- Cutler, C. S., Koreth, J., and Ritz, J. (2017). Mechanistic approaches for the prevention and treatment of chronic GVHD. *Blood* 129, 22–29. doi:10.1182/blood-2016-08-686659.
- Cuzzocrea, S., Mazzon, E., Di Paola, R., Patel, N. S. A., Genovese, T., Muià, C., et al. (2004). Erythropoietin reduces the development of experimental inflammatory bowel disease. *J. Pharmacol. Exp. Ther.* 311, 1272–1280. doi:10.1124/jpet.104.073197.
- Cuzzocrea, S., Mazzon, E., Paola, R. Di, Genovese, T., Patel, N. S. A., Britti, D., et al. (2005). Erythropoietin reduces the degree of arthritis caused by type II collagen in the mouse. *Arthritis Rheum.* 52, 940–950. doi:10.1002/art.20875.
- Cyster, J. G. (2010). B cell follicles and antigen encounters of the third kind. *Nat. Immunol.* 11, 989–996. doi:10.1038/ni.1946.
- Dame, C., Wolber, E. M., Fahnenstich, H., Hofmann, D., Bartmann, P., and Fandrey, J. (1998). Thrombopoietin (tpo) mrna expression in human fetal and neonatal organs. *Pediatr. Res.* 44, 437. doi:10.1203/00006450-199809000-00140.
- de Graav, G. N., Dieterich, M., Hesselink, D. A., Boer, K., Clahsen-van Groningen, M. C., Kraaijeveld, R., et al. (2014). Follicular T helper cells and humoral reactivity in kidney transplant patients. *Clin. Exp. Immunol.* 180, 329–340. doi:10.1111/cei.12576.
- de Leur, K., Dor, F. J. M. F., Dieterich, M., van der Laan, L. J. W., Hendriks, R. W., and Baan, C. C. (2017). IL-21 receptor antagonist inhibits differentiation of B cells toward plasmablasts upon alloantigen stimulation. *Front. Immunol.* 8, 1–10. doi:10.3389/fimmu.2017.00306.
- De Silva, N. S., and Klein, U. (2015). Dynamics of B cells in germinal centres. *Nat. Rev. Immunol.* 15, 137–148. doi:10.1038/nri3804.
- Deng, R., Hurtz, C., Song, Q., Yue, C., Xiao, G., Yu, H., et al. (2017). Extrafollicular CD4⁺ T-B interactions are sufficient for inducing autoimmune-like chronic graft-versus-host disease. *Nat. Commun.* 8. doi:10.1038/s41467-017-00880-2.
- Ding, Y., Li, J., Yang, P. A., Luo, B., Wu, Q., Zajac, A. J., et al. (2014). Interleukin-21 promotes germinal center reaction by skewing the follicular regulatory T cell to follicular helper T cell balance in autoimmune BXD2 mice. *Arthritis Rheumatol.* 66, 2601–2612. doi:10.1002/art.38735.
- Dominguez-Sola, D., Victora, G. D., Ying, C. Y., Phan, R. T., Saito, M., Nussenzweig, M. C., et al. (2012). The proto-oncogene MYC is required for selection in the germinal center and cyclic reentry. *Nat. Immunol.* 13, 1083–1091. doi:10.1038/ni.2428.
- Donadei, C., Angeletti, A., Cantarelli, C., D’Agati, V. D., La Manna, G., Fiaccadori, E., et al. (2019). Erythropoietin inhibits SGK1-dependent Th17 cell induction and Th17 cell-dependent kidney disease. *JCI Insight* 4, 1–19. doi:10.1172/jci.insight.127428.

- Ebert, B. L., and Bunn, H. F. (1999). Regulation of the erythropoietin gene. *Blood* 94, 1864–1877. doi:10.1182/blood.v94.6.1864.418k37_1864_1877.
- Erbayraktar, S., Yilmaz, O., Gökmen, N., and Brines, M. (2003). Erythropoietin is a multifunctional tissue-protective cytokine. *Curr. Hematol. Rep.* 2, 465–70. Available at: <http://www.ncbi.nlm.nih.gov/pubmed/14561390> [Accessed October 18, 2020].
- Erslev, A. J., and Caro, J. (1986). PHYSIOLOGIC AND MOLECULAR BIOLOGY OF ERYTHROPOIETIN A. J. ERSLEV and J. CARO Cardeza Foundation for Hematologic Research, Thomas Jefferson University, Philadelphia, PA, U.S.A. 3, 159–164.
- Fiordaliso, F., Chimenti, S., Staszewsky, L., Bai, A., Carlo, E., Cuccovillo, I., et al. (2004). A nonerythropoietic derivative of erythropoietin protects the myocardium from ischemia-reperfusion injury. Available at: www.pnas.org/cgi/doi/10.1073/pnas.0409329102.
- Fishbane, S., Singh, B., Kumbhat, S., Wisemandle, W. A., and Martin, N. E. (2018). Article Intravenous Epoetin Alfa-epbx versus Epoetin Alfa for Treatment of Anemia in End-Stage Kidney Disease. *Clin J Am Soc Nephrol* 13, 1204–1214. doi:10.2215/CJN.11631017.
- Forcade, E., Kim, H. T., Cutler, C., Wang, K., Alho, A. C., Nikiforow, S., et al. (2016). Circulating T follicular helper cells with increased function during chronic graft-versus-host disease. *Blood* 127, 2489–2497. doi:10.1182/blood-2015-12-688895.
- Francis Coffey, Boris Alabyev, and T. M. (2009). Initial clonal expansion of germinal center B cells takes place at the perimeter of follicles. 30, 599–609. doi:10.1016/j.immuni.2009.01.011.Initial.
- Garside, P., Ingulli, E., Merica, R. R., Johnson, J. G., Noelle, R. J., and Jenkins, M. K. (1998). Visualization of specific B and T lymphocyte interactions in the lymph node. *Science (80-.)*. 281, 96–99. doi:10.1126/science.281.5373.96.
- Gill, J., Shah, T., Hristea, I., Chavalitdhamrong, D., Anastasi, B., Takemoto, S. K., et al. (2009). Outcomes of simultaneous heart-kidney transplant in the US: A retrospective analysis using OPTN/UNOS data. *Am. J. Transplant.* 9, 844–852. doi:10.1111/j.1600-6143.2009.02588.x.
- Gobe, G. C., Bennett, N. C., West, M., Colditz, P., Brown, L., Vesey, D. A., et al. (2014). Increased progression to kidney fibrosis after erythropoietin is used as a treatment for acute kidney injury. *Am. J. Physiol. - Ren. Physiol.* 306. doi:10.1152/ajprenal.00241.2013.
- Goldwasser, E., Kung, C. K. H., and Eliason, J. (1974). On the mechanism of erythropoietin induced differentiation. XIII. The role of sialic acid in erythropoietin action. *J. Biol. Chem.* 249, 4202–4206. Available at: <https://pubmed.ncbi.nlm.nih.gov/4368980/> [Accessed September 22, 2020].
- Gonzalez, S. F., Degn, S. E., Pitcher, L. A., Woodruff, M., Heesters, B. A., and Carroll, M. C. (2011). Trafficking of B cell antigen in lymph nodes. *Annu. Rev. Immunol.* 29, 215–233. doi:10.1146/annurev-immunol-031210-101255.

- Hebeisen, M., Baitsch, L., Presotto, D., Baumgaertner, P., Romero, P., Michielin, O., et al. (2013). SHP-1 phosphatase activity counteracts increased T cell receptor affinity. *J. Clin. Invest.* 123, 1044–1065. doi:10.1172/JCI65325.
- Heesters, B. A., Myers, R. C., and Carroll, M. C. (2014). Follicular dendritic cells: Dynamic antigen libraries. *Nat. Rev. Immunol.* 14, 495–504. doi:10.1038/nri3689.
- Hirano, I., and Suzuki, N. (2019). The neural crest as the first production site of the erythroid growth factor erythropoietin. *Front. Cell Dev. Biol.* 7, 1–6. doi:10.3389/fcell.2019.00105.
- Ho, M. S. H., Medcalf, R. L., Livesey, S. A., and Traianedes, K. (2015). The dynamics of adult haematopoiesis in the bone and bone marrow environment. *Br. J. Haematol.* 170, 472–486. doi:10.1111/bjh.13445.
- Iwasaki, K., Kitahata, N., Hiramitsu, T., Yamamoto, T., Noda, T., Okada, M., et al. (2018). Increased CD40L+PD-1+ follicular helper T cells (Tfh) as a biomarker for predicting calcineurin inhibitor sensitivity against Tfh-mediated B-cell activation/antibody production after kidney transplantation. *Int. Immunol.* 30, 345–355. doi:10.1093/intimm/dxy039.
- Jacobs, K., Shoemaker, C., Rudersdorf, R., Neill, S. D., Kaufman, R. J., Mufson, A., et al. (1985). Isolation and characterization of genomic and cDNA clones of human erythropoietin. *Nature* 313, 806–810. doi:10.1038/313806a0.
- Jelkmann, W. (1992). Erythropoietin: Structure, control of production, and function. *Physiol. Rev.* 72, 449–489. doi:10.1152/physrev.1992.72.2.449.
- Jelkmann, W. (2011). Regulation of erythropoietin production. *J. Physiol.* 589, 1251–1258. doi:10.1113/jphysiol.2010.195057.
- Johnston, R. J., Choi, Y. S., Diamond, J. A., Yang, J. A., and Crotty, S. (2012). STAT5 is a potent negative regulator of T FH cell differentiation. *J. Exp. Med.* 209, 243–250. doi:10.1084/jem.20111174.
- Juul, S. E., Yachnis, A. T., and Christensen, R. D. (1998). Tissue distribution of erythropoietin and erythropoietin receptor in the developing human fetus. *Early Hum. Dev.* 52, 235–249. doi:10.1016/S0378-3782(98)00030-9.
- Kawabe, T., Matsushima, M., Hashimoto, N., Imaizumi, K., and Hasegawa, Y. (2011). CD40/CD40 ligand interactions in immune responses and pulmonary immunity. *Nagoya J. Med. Sci.* 73, 69–78. doi:10.18999/nagjms.73.3-4.69.
- Kim, E. J., Kwun, J., Gibby, A. C., Hong, J. J., Farris, A. B., Iwakoshi, N. N., et al. (2014). Costimulation blockade alters germinal center responses and prevents antibody-mediated rejection. *Am. J. Transplant.* 14, 59–69. doi:10.1111/ajt.12526.
- Kitamura, H., Isaka, Y., Takabatake, Y., Imamura, R., Suzuki, C., Takahara, S., et al. (2008). Nonerythropoietic derivative of erythropoietin protects against tubulointerstitial injury in a unilateral ureteral obstruction model. *Nephrol. Dial. Transplant.* 23, 1521–1528. doi:10.1093/ndt/gfm842.
- Knorr, D. A., Wang, H., Aurora, M., MacMillan, M. L., Holtan, S. G., Bergerson, R., et al. (2016). Loss of T Follicular Helper Cells in the Peripheral Blood of Patients with Chronic Graft-versus-Host Disease. *Biol. Blood Marrow Transplant.* 22, 825–833. doi:10.1016/j.bbmt.2016.01.003.

- Konvalinka, A., and Tinckam, K. (2015). Utility of HLA antibody testing in kidney transplantation. *J. Am. Soc. Nephrol.* 26, 1489–1502. doi:10.1681/ASN.2014080837.
- La Muraglia, G. M., Wagener, M. E., Ford, M. L., and Badell, I. R. (2019). Circulating T follicular helper cells are a biomarker of humoral alloreactivity and predict donor-specific antibody formation after transplantation. *Am. J. Transplant.* 20, 75–87. doi:10.1111/ajt.15517.
- Ladics, G. S. (2018). “The Sheep Erythrocyte T-Dependent Antibody Response (TDAR),” in *Immunotoxicity Testing: Methods and Protocols*, eds. J. C. DeWitt, C. E. Rockwell, and C. C. Bowman (New York, NY: Springer New York), 83–94. doi:10.1007/978-1-4939-8549-4_6.
- Lam, K. P., Kühn, R., and Rajewsky, K. (1997). In vivo ablation of surface immunoglobulin on mature B cells by inducible gene targeting results in rapid cell death. *Cell* 90, 1073–1083. doi:10.1016/S0092-8674(00)80373-6.
- Le, T. L., Kim, T. H., and Chaplin, D. D. (2008). Intracloonal Competition Inhibits the Formation of High-Affinity Antibody-Secreting Cells. *J. Immunol.* 181, 6027–6037. doi:10.4049/jimmunol.181.9.6027.
- Lin, C. S., Lim, S. K., D’Agati, V., and Costantini, F. (1996). Differential effects of an erythropoietin receptor gene disruption on primitive and definitive erythropoiesis. *Genes Dev.* 10, 154–164. doi:10.1101/gad.10.2.154.
- Lin, F. K., Suggs, S., Lin, C. H., Browne, J. K., Smalling, R., Egrie, J. C., et al. (1985). Cloning and expression of the human erythropoietin gene. *Proc. Natl. Acad. Sci. U. S. A.* 82, 7580–7584. doi:10.1073/pnas.82.22.7580.
- Linterman, M. A., and Hill, D. L. (2016). Can follicular helper T cells be targeted to improve vaccine efficacy? *F1000Research* 5. doi:10.12688/f1000research.7388.1.
- Linterman, M. A., Pierson, W., Lee, S. K., Kallies, A., Kawamoto, S., Rayner, T. F., et al. (2011). Foxp3⁺ follicular regulatory T cells control the germinal center response. *Nat. Med.* 17, 975–982. doi:10.1038/nm.2425.
- Lisowska, K. A., Dębska-Ślizień, A., Bryl, E., Rutkowski, B., and Witkowski, J. M. (2010). Erythropoietin receptor is expressed on human peripheral blood T and B lymphocytes and monocytes and is modulated by recombinant human erythropoietin treatment. *Artif. Organs* 34, 654–662. doi:10.1111/j.1525-1594.2009.00948.x.
- Lisowska, K. A., Dębska-Ślizień, A., Jasiulewicz, A., Jóźwik, A., Rutkowski, B., Bryl, E., et al. (2011). Flow cytometric analysis of STAT5 phosphorylation and CD95 expression in CD4⁺ T lymphocytes treated with recombinant human erythropoietin. *J. Recept. Signal Transduct.* 31, 241–246. doi:10.3109/10799893.2011.578646.
- Lombardero, M., Kovacs, K., and Scheithauer, B. W. (2011). Erythropoietin: A hormone with multiple functions. *Pathobiology* 78, 41–56. doi:10.1159/000322975.

- Louis, K., Macedo, C., Bailly, E., Lau, L., Ramaswami, B., Marrari, M., et al. (2020). Coordinated Circulating T Follicular Helper and Activated B Cell Responses Underlie the Onset of Antibody-Mediated Rejection in Kidney Transplantation. *J. Am. Soc. Nephrol.*, ASN.2020030320. doi:10.1681/ASN.2020030320.
- Luo, B., Gan, W., Liu, Z., Shen, Z., Wang, J., Shi, R., et al. (2016). Erythropoietin Signaling in Macrophages Promotes Dying Cell Clearance and Immune Tolerance. *Immunity* 44, 287–302. doi:10.1016/j.immuni.2016.01.002.
- Luo, W., Hu, L., and Wang, F. (2015). The protective effect of erythropoietin on the retina. *Ophthalmic Res.* 53, 74–81. doi:10.1159/000369885.
- Ma, C. S., Deenick, E. K., Batten, M., and Tangye, S. G. (2012). The origins, function, and regulation of T follicular helper cells. *J. Exp. Med.* 209, 1241–1253. doi:10.1084/jem.20120994.
- MacDonald, K. P. A., Hill, G. R., and Blazar, B. R. (2017). Chronic graft-versus-host disease: Biological insights from preclinical and clinical studies. *Blood* 129, 13–21. doi:10.1182/blood-2016-06-686618.
- Macedo, C., Hadi, K., Walters, J., Elinoff, B., Marrari, M., Zeevi, A., et al. (2019). Impact of Induction Therapy on Circulating T Follicular Helper Cells and Subsequent Donor-Specific Antibody Formation After Kidney Transplant. *Kidney Int. Reports* 4, 455–469. doi:10.1016/j.ekir.2018.11.020.
- Maceiras, A. R., Fonseca, V. R., Agua-Doce, A., and Graca, L. (2017). T follicular regulatory cells in mice and men. *Immunology* 152, 25–35. doi:10.1111/imm.12774.
- MacLennan, I. C. M., Liu, Y. J., Oldfield, S., Zhang, J., and Lane, P. J. L. (1990). The evolution of B-cell clones. *Curr. Top. Microbiol. Immunol.* 159, 37–63. doi:10.1007/978-3-642-75244-5_3.
- Malik, J., Kim, A. R., Tyre, K. A., Cherukuri, A. R., and Palis, J. (2013). Erythropoietin critically regulates the terminal maturation of murine and human primitive erythroblasts. *Haematologica* 98, 1778–1787. doi:10.3324/haematol.2013.087361.
- Marti, H. H., Wenger, R. H., Rivas, L. A., Straumann, U., Oigicaylioglu, M., Volker, H., et al. (1996). Erythropoietin gene expression in human, monkey and murine brain. *Eur. J. Neurosci.* 8, 666–676. doi:10.1111/j.1460-9568.1996.tb01252.x.
- Martinez, F., Kamar, N., Pallet, N., Lang, P., Durrbach, A., Lebranchu, Y., et al. (2010). High Dose Epoetin Beta in the First Weeks Following Renal Transplantation and Delayed Graft Function: Results of the Neo-PDGF Study. *Am. J. Transplant.* 10, 1695–1700. doi:10.1111/j.1600-6143.2010.03142.x.
- Martinez, F., and Pallet, N. (2014). When erythropoietin meddles in immune affairs. *J. Am. Soc. Nephrol.* 25, 1887–1889. doi:10.1681/ASN.2014030240.
- Masuda, S., Okano, M., Yamagishi, K., Nagao, M., Ueda, M., and Sasaki, R. (1994). A novel site of erythropoietin production. Oxygen-dependent production in cultured rat astrocytes. *J. Biol. Chem.* 269, 19488–19493.
- Matas, A. J., Smith, J. M., Skeans, M. A., Lamb, K. E., Gustafson, S. K., Samana, C. J., et al. (2013). OPTN/SRTR 2011 Annual Data Report: Kidney. *Am. J. Transplant.* 13, 11–46. doi:10.1111/ajt.12019.

- Mausberg, A. K., Meyer zu Hörste, G., Dehmel, T., Stettner, M., Lehmann, H. C., Sheikh, K. A., et al. (2011). Erythropoietin ameliorates rat experimental autoimmune neuritis by inducing transforming growth factor-beta in macrophages. *PLoS One* 6. doi:10.1371/journal.pone.0026280.
- McCarron, M. J., and Marie, J. C. (2014). TGF- β prevents T follicular helper cell accumulation and B cell autoreactivity. *J. Clin. Invest.* 124, 4375–4386. doi:10.1172/JCI76179.
- McDonald-Hyman, C., Flynn, R., Panoskaltis-Mortari, A., Peterson, N., MacDonald, K. P. A., Hill, G. R., et al. (2016). Therapeutic regulatory T-cell adoptive transfer ameliorates established murine chronic GVHD in a CXCR5-dependent manner. *Blood* 128, 1013–1017. doi:10.1182/blood-2016-05-715896.
- Mcheyzer-Williams, L. J., Milpied, P. J., Okitsu, S. L., and Mcheyzer-Williams, M. G. (2015). Class-switched memory B cells remodel BCRs within secondary germinal centers. doi:10.1038/ni.3095.
- Mesin, L., Ersching, J., and Vitorica, G. D. (2016). Germinal Center B Cell Dynamics. *Immunity* 45, 471–482. doi:10.1016/j.immuni.2016.09.001.
- Meyer-Hermann, M. E., Maini, P. K., and Iber, D. (2006). An analysis of B cell selection mechanisms in germinal centers. *Math. Med. Biol.* 23, 255–277. doi:10.1093/imammb/dql012.
- Miles, B., and Connick, E. (2018). Control of the germinal center by follicular regulatory t cells during infection. *Front. Immunol.* 9. doi:10.3389/fimmu.2018.02704.
- Müller, J., Sperl, B., Reindll, W., Kiessling, A., and Berg, T. (2008). Discovery of chromone-based inhibitors of the transcription factor STAT5. *ChemBioChem* 9, 723–727. doi:10.1002/cbic.200700701.
- Na, N., Zhao, D., Zhang, J., Yang, S., Xie, D., Wu, J., et al. (2020). Carbamylated Erythropoietin Regulates Immune Responses and Promotes Long-Term Kidney Allograft Survival Through Activation of PI3K/AKT Signaling. *SSRN Electron. J.* doi:10.2139/ssrn.3441801.
- Nairz, M., Schroll, A., Moschen, A. R., Sonnweber, T., Theurl, M., Theurl, I., et al. (2011). Erythropoietin Contrastingly Affects Bacterial Infection and Experimental Colitis by Inhibiting Nuclear Factor- κ B-Inducible Immune Pathways. *Immunity* 34, 61–74. doi:10.1016/j.immuni.2011.01.002.
- Natkunam, Y. (2007). Follicular Lymphoma The Biology of the Germinal Center. *Hematology*.
- Newell, K. A., Asare, A., Kirk, A. D., Gisler, T. D., Bourcier, K., Suthanthiran, M., et al. (2010). Identification of a B cell signature associated with renal transplant tolerance in humans. *J. Clin. Invest.* 120, 1836–1847. doi:10.1172/JCI39933.
- Nguyen, V., Luzina, I., Rus, H., Tegla, C., Chen, C., and Rus, V. (2012). IL-21 Promotes Lupus-like Disease in Chronic Graft-versus-Host Disease through Both CD4 T Cell- and B Cell-Intrinsic Mechanisms. *J. Immunol.* 189, 1081–1093. doi:10.4049/jimmunol.1200318.

- Niu, Q., Kraaijeveld, R., Li, Y., Mendoza Rojas, A., Shi, Y., Wang, L., et al. (2019). An overview of T follicular cells in transplantation: spotlight on their clinical significance. *Expert Rev. Clin. Immunol.* 15, 1249–1262. doi:10.1080/1744666X.2020.1693262.
- Nurieva, R. I., Chung, Y., Hwang, D., Yang, X. O., Kang, H. S., Ma, L., et al. (2008). Generation of T Follicular Helper Cells Is Mediated by Interleukin-21 but Independent of T Helper 1, 2, or 17 Cell Lineages. *Immunity* 29, 138–149. doi:10.1016/j.immuni.2008.05.009.
- Nurieva, R. I., Chung, Y., Martinez, G. J., Yang, X. O., Tanaka, S., Matskevitch, T. D., et al. (2009). Bcl6 mediates the development of T follicular helper cells. *Science* (80-.). 325, 1001–1005. doi:10.1126/science.1176676.
- Okada, T., Miller, M. J., Parker, I., Krummel, M. F., Neighbors, M., Hartley, S. B., et al. (2005). Antigen-engaged B cells undergo chemotaxis toward the T zone and form motile conjugates with helper T cells. *PLoS Biol.* 3, 1047–1061. doi:10.1371/journal.pbio.0030150.
- Palis, J. (2014). Primitive and definitive erythropoiesis in mammals. *Front. Physiol.* 5 JAN. doi:10.3389/fphys.2014.00003.
- Palis, J., and Koniski, A. (2018). “Functional analysis of erythroid progenitors by colony-forming assays,” in *Methods in Molecular Biology* (Humana Press Inc.), 117–132. doi:10.1007/978-1-4939-7428-3_7.
- Parekh, V. V., Prasad, D. V. R., Banerjee, P. P., Joshi, B. N., Kumar, A., and Mishra, G. C. (2003). B Cells Activated by Lipopolysaccharide, But Not By Anti-Ig and Anti-CD40 Antibody, Induce Anergy in CD8 + T Cells: Role of TGF- β 1 . *J. Immunol.* 170, 5897–5911. doi:10.4049/jimmunol.170.12.5897.
- Patterson, H. C. K., Kraus, M., Kim, Y.-M., Ploegh, H., and Rajewsky, K. (2006). The B Cell Receptor Promotes B Cell Activation and Proliferation through a Non-ITAM Tyrosine in the Iga Cytoplasmic Domain. *Immunity* 25, 55–65. doi:10.1016/j.immuni.2006.04.014.
- Peng, B., Kong, G., Yang, C., and Ming, Y. (2020). Erythropoietin and its derivatives: from tissue protection to immune regulation. *Cell Death Dis.* 11. doi:10.1038/s41419-020-2276-8.
- Prémaud, A., Filloux, M., Gatault, P., Thierry, A., Büchler, M., Munteanu, E., et al. (2017). An adjustable predictive score of graft survival in kidney transplant patients and the levels of risk linked to de novo donor-specific anti-HLA antibodies. *PLoS One* 12, 1–16. doi:10.1371/journal.pone.0180236.
- Purroy, C., Fairchild, R. L., Tanaka, T., Baldwin, W. M., Manrique, J., Madsen, J. C., et al. (2017). Erythropoietin receptor-mediated molecular crosstalk promotes T cell immunoregulation and transplant survival. *J. Am. Soc. Nephrol.* 28, 2377–2392. doi:10.1681/ASN.2016101100.
- Qi, H., Cannons, J. L., Klauschen, F., Schwartzberg, P. L., and Germain, R. N. (2008). SAP-controlled T-B cell interactions underlie germinal centre formation. *Nature* 455, 764–769. doi:10.1038/nature07345.

- Qin, L., Waseem, T. C., Sahoo, A., Bieerkehazhi, S., Zhou, H., Galkina, E. V., et al. (2018). Insights into the molecular mechanisms of T follicular helper-mediated immunity and pathology. *Front. Immunol.* 9, 1–21. doi:10.3389/fimmu.2018.01884.
- Raedler, H., Vieyra, M. B., Leisman, S., Lakhani, P., Kwan, W., Yang, M., et al. (2011). Anti-complement component C5 mAb synergizes with CTLA4Ig to inhibit alloreactive T cells and prolong cardiac allograft survival in mice. *Am. J. Transplant.* 11, 1397–1406. doi:10.1111/j.1600-6143.2011.03561.x.
- Rajewsky, K. (1996). Clonal selection and learning in the antibody system. *Nature* 381, 751–758. doi:10.1038/381751a0.
- Rankin, E. B., Wu, C., Khatri, R., Wilson, T. L. S., Andersen, R., Araldi, E., et al. (2012). The HIF signaling pathway in osteoblasts directly modulates erythropoiesis through the production of EPO. *Cell* 149, 63–74. doi:10.1016/j.cell.2012.01.051.
- Robertson, C., and Sadrameli, S. (2013). Erythropoietin in the neurology ICU. *Curr. Treat. Options Neurol.* 15, 104–112. doi:10.1007/s11940-013-0222-0.
- Rodda, L. B., Bannard, O., Ludewig, B., Nagasawa, T., and Cyster, J. G. (2015). Phenotypic and Morphological Properties of Germinal Center Dark Zone Cxcl12 - Expressing Reticular Cells . *J. Immunol.* 195, 4781–4791. doi:10.4049/jimmunol.1501191.
- Sage, P. T., Paterson, A. M., Lovitch, S. B., and Sharpe, A. H. (2014). The coinhibitory receptor CTLA-4 controls B cell responses by modulating T follicular helper, T follicular regulatory, and T regulatory cells. *Immunity* 41, 1026–1039. doi:10.1016/j.immuni.2014.12.005.
- Sage, P. T., and Sharpe, A. H. (2016). T follicular regulatory cells. *Immunol. Rev.* 271, 246–259. doi:10.1111/imr.12411.
- Sage, P. T., and Sharpe, A. H. (2020). The multifaceted functions of follicular regulatory T cells. *Curr. Opin. Immunol.* 67, 68–74. doi:10.1016/j.coi.2020.10.009.
- Sagiv, S. P., Lifshitz, L., Orkin, R., Mittelman, M., and Neumann, D. (2008). Erythropoietin effects on dendritic cells: Potential mediators in its function as an immunomodulator? *Exp. Hematol.* 36, 1682–1690. doi:10.1016/j.exphem.2008.07.010.
- Schmitt, N., Bentebibel, S. E., and Ueno, H. (2014). Phenotype and functions of memory Tfh cells in human blood. *Trends Immunol.* 35, 436–442. doi:10.1016/j.it.2014.06.002.
- Schwaiger, E., Eskandary, F., Kozakowski, N., Bond, G., Kikić, Željko, Yoo, D., et al. (2016). Deceased donor kidney transplantation across donor-specific antibody barriers: Predictors of antibody-mediated rejection. *Nephrol. Dial. Transplant.* 31, 1342–1351. doi:10.1093/ndt/gfw027.
- Schwenger, V., Morath, C., and Zeier, M. (2007). Use of Erythropoietin after solid organ transplantation. *Nephrol. Dial. Transplant.* 22, 47–49. doi:10.1093/ndt/gfm657.

- Shih, H. M., Wu, C. J., and Lin, S. L. (2018). Physiology and pathophysiology of renal erythropoietin-producing cells. *J. Formos. Med. Assoc.* 117, 955–963. doi:10.1016/j.jfma.2018.03.017.
- Sinclair, A., and Elliott (2012). The effect of erythropoietin on normal and neoplastic cells. *Biol. Targets Ther.*, 163. doi:10.2147/btt.s32281.
- Souma, T., Suzuki, N., and Yamamoto, M. (2015). Renal erythropoietin-producing cells in health and disease. *Front. Physiol.* 6, 1–10. doi:10.3389/fphys.2015.00167.
- Stebegg, M., Kumar, S. D., Silva-Cayetano, A., Fonseca, V. R., Linterman, M. A., and Graca, L. (2018). Regulation of the germinal center response. *Front. Immunol.* 9, 2469. doi:10.3389/fimmu.2018.02469.
- Suresh, S., Rajvanshi, P. K., and Noguchi, C. T. (2020). The Many Facets of Erythropoietin Physiologic and Metabolic Response. *Front. Physiol.* 10, 1–20. doi:10.3389/fphys.2019.01534.
- Suzuki, N., Hirano, I., Pan, X., Minegishi, N., and Yamamoto, M. (2013). Erythropoietin production in neuroepithelial and neural crest cells during primitive erythropoiesis. *Nat. Commun.* 4. doi:10.1038/ncomms3902.
- Syed, R. S., Reid, S. W., Li, C., Cheetham, J. C., Aoki, K. H., Liu, B., et al. (1998). Efficiency of signalling through cytokine receptors depends critically on receptor orientation. *Nature* 395, 511–516. doi:10.1038/26773.
- Takahashi, Y., Ohta, H., and Takemori, T. (2001). Fas is required for clonal selection in germinal centers and the subsequent establishment of the memory B cell repertoire. *Immunity* 14, 181–192. doi:10.1016/S1074-7613(01)00100-5.
- Tangye, S. G., Ma, C. S., Brink, R., and Deenick, E. K. (2013). The good, the bad and the ugly-T FH cells in human health and disease. *Nat. Rev. Immunol.* 13, 412–426. doi:10.1038/nri3447.
- Travis D. Hulla, Gilles Benichoub, and J. C. M. (2019). Why some organ allografts are tolerated better than others: new insights for an old question Travis. *Curr Opin Organ Transpl.* 24, 49–57. doi:doi:10.1097/MOT.0000000000000594.
- Trickett, A., and Kwan, Y. L. (2003). T cell stimulation and expansion using anti-CD3/CD28 beads. *J. Immunol. Methods* 275, 251–255. doi:10.1016/S0022-1759(03)00010-3.
- Vaeth, M., Müller, G., Stauss, D., Dietz, L., Klein-Hessling, S., Serfling, E., et al. (2014). Follicular regulatory T cells control humoral autoimmunity via NFAT2-regulated CXCR5 expression. *J. Exp. Med.* 211, 545–561. doi:10.1084/jem.20130604.
- Valujskikh, A., Pantenburg, B., and Heeger, P. S. (2002). Primed allospecific T cells prevent the effects of costimulatory blockade on prolonged cardiac allograft survival in mice. *Am. J. Transplant.* 2, 501–509. doi:10.1034/j.1600-6143.2002.20603.x.
- van Besouw, N. M., Mendoza Rojas, A., and Baan, C. C. (2019). The role of follicular T helper cells in the humoral alloimmune response after clinical organ transplantation. *Hla* 94, 407–414. doi:10.1111/tan.13671.

- van Rijt, G. (2014). *Performance-enhancing strategies for deceased donor kidneys*
Geert van Rijt.
- Victora, G. D., Dominguez-Sola, D., Holmes, A. B., Deroubaix, S., Dalla-Favera, R.,
and Nussenzweig, M. C. (2012). Identification of human germinal center light and
dark zone cells and their relationship to human B-cell lymphomas. *Blood* 120,
2240–2248. doi:10.1182/blood-2012-03-415380.
- Victora, G. D., and Nussenzweig, M. C. (2012). Germinal centers. *Annu. Rev. Immunol.*
30, 429–457. doi:10.1146/annurev-immunol-020711-075032.
- Victora, G. D., Schwickert, T. A., Fooksman, D. R., Kamphorst, A. O., Meyer-
Hermann, M., Dustin, M. L., et al. (2010). Germinal center dynamics revealed by
multiphoton microscopy with a photoactivatable fluorescent reporter. *Cell* 143,
592–605. doi:10.1016/j.cell.2010.10.032.
- Walker, S. R., Nelson, E. A., Yeh, J. E., Pinello, L., Yuan, G.-C., and Frank, D. A.
(2013). STAT5 Outcompetes STAT3 To Regulate the Expression of the Oncogenic
Transcriptional Modulator BCL6. *Mol. Cell. Biol.* 33, 2879–2890.
doi:10.1128/mcb.01620-12.
- Wang, C. J., Heuts, F., Ovcinnikovs, V., Wardzinski, L., Bowers, C., Schmidt, E. M., et
al. (2015). CTLA-4 controls follicular helper T-cell differentiation by regulating
the strength of CD28 engagement. *Proc. Natl. Acad. Sci. U. S. A.* 112, 524–529.
doi:10.1073/pnas.1414576112.
- Wang, Y., Shi, J., Yan, J., Xiao, Z., Hou, X., Lu, P., et al. (2017). Germinal-center
development of memory B cells driven by IL-9 from follicular helper T cells. *Nat.*
Immunol. 18, 921–930. doi:10.1038/ni.3788.
- Westenfelder, C., Biddle, D. L., and Baranowski, R. L. (1999). Human, rat, and mouse
kidney cells express functional erythropoietin receptors. *Kidney Int.* 55, 808–820.
doi:10.1046/j.1523-1755.1999.055003808.x.
- Wing, J. B., Ise, W., Kurosaki, T., and Sakaguchi, S. (2014). Regulatory T cells control
antigen-specific expansion of Tfh cell number and humoral immune responses via
the coreceptor CTLA-4. *Immunity* 41, 1013–1025.
doi:10.1016/j.immuni.2014.12.006.
- Wing, K., Onishi, Y., Prieto-Martin, P., Yamaguchi, T., Miyara, M., Fehervari, Z., et al.
(2008). CTLA-4 control over Foxp3+ regulatory T cell function. *Science* (80-.).
322, 271–275. doi:10.1126/science.1160062.
- Wollenberg, I., Agua-Doce, A., Hernández, A., Almeida, C., Oliveira, V. G., Faro, J., et
al. (2011). Regulation of the Germinal Center Reaction by Foxp3 + Follicular
Regulatory T Cells. *J. Immunol.* 187, 4553–4560. doi:10.4049/jimmunol.1101328.
- Woodruff, T. M., Nandakumar, K. S., and Tedesco, F. (2011). Inhibiting the C5-C5a
receptor axis. *Mol. Immunol.* 48, 1631–1642. doi:10.1016/j.molimm.2011.04.014.
- Wu, H., Chen, Y., Liu, H., Xu, L. L., Teuscher, P., Wang, S., et al. (2016). Follicular
regulatory T cells repress cytokine production by follicular helper T cells and
optimize IgG responses in mice. *Eur. J. Immunol.* 46, 1152–1161.
doi:10.1002/eji.201546094.

- Wu, H., Liu, X., Jaenisch, R., and Lodish, H. F. (1995). Generation of committed erythroid BFU-E and CFU-E progenitors does not require erythropoietin or the erythropoietin receptor. *Cell* 83, 59–67. doi:10.1016/0092-8674(95)90234-1.
- Xie, M. M., and Dent, A. L. (2018). Unexpected Help: Follicular Regulatory T Cells in the Germinal Center. *Front. Immunol.* 9, 1–9. doi:10.3389/fimmu.2018.01536.
- Xin, G., Zander, R., Schauder, D. M., Chen, Y., Weinstein, J. S., Drobyski, W. R., et al. (2018). Single-cell RNA sequencing unveils an IL-10-producing helper subset that sustains humoral immunity during persistent infection. *Nat. Commun.* 9. doi:10.1038/s41467-018-07492-4.
- Yan, L., de Leur, K., Hendriks, R. W., van der Laan, L. J. W., Shi, Y., Wang, L., et al. (2017). T follicular helper cells as a new target for immunosuppressive therapies. *Front. Immunol.* 8, 1–11. doi:10.3389/fimmu.2017.01510.
- Yang, X. P., Ghoreschi, K., Steward-Tharp, S. M., Rodriguez-Canales, J., Zhu, J., Grainger, J. R., et al. (2011). Opposing regulation of the locus encoding IL-17 through direct, reciprocal actions of STAT3 and STAT5. *Nat. Immunol.* 12, 247–254. doi:10.1038/ni.1995.
- Yu, D., Rao, S., Tsai, L. M., Lee, S. K., He, Y., Sutcliffe, E. L., et al. (2009). The Transcriptional Repressor Bcl-6 Directs T Follicular Helper Cell Lineage Commitment. *Immunity* 31, 457–468. doi:10.1016/j.immuni.2009.07.002.
- Yuan, R. R., Maeda, Y., Li, W., Lu, W., Cook, S., and Dowling, P. (2008). Erythropoietin: A potent inducer of peripheral immuno/inflammatory modulation in autoimmune EAE. *PLoS One* 3, 1–11. doi:10.1371/journal.pone.0001924.
- Yusuf, I., Kageyama, R., Monticelli, L., Johnston, R. J., DiToro, D., Hansen, K., et al. (2010). Germinal Center T Follicular Helper Cell IL-4 Production Is Dependent on Signaling Lymphocytic Activation Molecule Receptor (CD150). *J. Immunol.* 185, 190–202. doi:10.4049/jimmunol.0903505.
- Zanjani, E. D., Ascensao, J. L., McGlave, P. B., Banisadre, M., and Ash, R. C. (1981). Studies on the liver to kidney switch of erythropoietin production. *J. Clin. Invest.* 67, 1183–1188. doi:10.1172/JCI110133.
- Zeiser, R., and Blazar, B. R. (2017). Pathophysiology of chronic graft-versus-host disease and therapeutic targets. *N. Engl. J. Med.* 377, 2565–2579. doi:10.1056/NEJMra1703472.
- Zhang, H., Gao, S., Yan, L., Zhu, G., Zhu, Q., Gu, Y., et al. (2018a). EPO Derivative ARA290 Attenuates Early Renal Allograft Injury in Rats by Targeting NF- κ B Pathway. *Transplant. Proc.* 50, 1575–1582. doi:10.1016/j.transproceed.2018.03.015.
- Zhang, J., Zhao, D., Na, N., Li, H., Miao, B., Hong, L., et al. (2018b). Renoprotective effect of erythropoietin via modulation of the STAT6/MAPK/NF- κ B pathway in ischemia/reperfusion injury after renal transplantation. *Int. J. Mol. Med.* 41, 25–32. doi:10.3892/ijmm.2017.3204.
- Zhang, R. (2018). Donor-specific antibodies in kidney transplant recipients. *Clin. J. Am. Soc. Nephrol.* 13, 182–192. doi:10.2215/CJN.00700117.